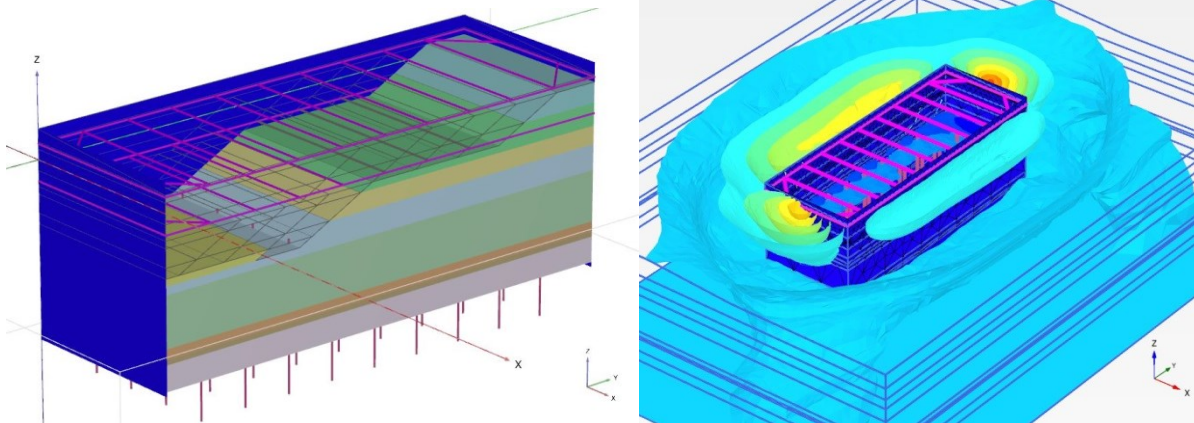


3D FEM analysis for sequential excavation

Master thesis TU Delft

Tianteng Zhou

27 – January – 2015



Contacts

Author

Tianteng Zhou
4224736
Van Hasseltlaan 565,
2625 JJ, Delft
+31 (0) 655795468
timmyzhou88@gmail.com

Graduation committee:**Chairman**

Prof. dr. M.A. Hicks
Section of Geo-Engineering, TU Delft
+31 (0)15 2787433
m.a.hicks@tudelft.nl

Supervisor TU Delft

Dr. P.J. Vardon
Section of Geo-Engineering, TU Delft
+31 (0)15 2781456
P.J.Vardon@tudelft.nl

Supervisor CRUX Engineering BV

Ing. J. A. Zwaan
Senior geotechnical advisor, CRUX Engineering
+31 (20) 4943070
zwaan@cruxbv.nl

External expert

Dr. ir. K.J. Bakker
Section of Hydraulic Engineering, TU Delft
+31 (0)15 278 5075
K.J.Bakker@tudelft.nl

Abstract

This thesis discusses the use of 3D finite element method (FEM) in deep excavations, especially the simulation of sequential excavation method in 3D FEM model. It is an independent research project based on the Spaarndammertunnel project in Amsterdam. This thesis only focused on the excavation part of the tunnel project.

Soil parameters used in models were derived from in situ soil investigation. Cone penetration tests and boreholes were carried out along the tunnel location. The soil data was compared with Amsterdam North-South metro line database as well. The excavation plan, retaining structure and building material were developed from the preliminary design of this project. The data for soil investigation and preliminary design were provided by CRUX Engineering BV.

The research focus was to investigate the advantages and disadvantages of applying 3D FEM modelling for deep excavations. Since the construction of Spaarndammertunnel starts after the completion of this graduation project, no field data was available for verification. Instead, 2D models were made for comparison and verification purpose. The soil and building material parameters were first tested in 2D spring model and 2D FEM model. The deflections of sheet pile walls in both 2D models were at similar level.

The 3D FEM model adopted the model set-up tested and adjusted in 2D FEM model. Parametric study was done in order to investigate how the domain and mesh set-up influence the results in 3D FEM model. Certain geometry (50m * 18m) of excavation section was determined so that the results from 3D FEM model and 2D FEM model were comparable. The excavation method applied in 2D and 3D FEM model was normal staged excavation. The excavation was designed to be dry excavation.

After the comparison between 2D and 3D FEM model, the sequential excavation method was implemented into 3D FEM model. Different excavation rates, excavation directions and lateral support design were tested in order to optimize the sequential excavation model. The responses of sheet pile walls as well as surrounding soil were recorded and compared with results from normal 3D excavation model.

The parametric study of 3D FEM model showed that the geometry of the excavation zone and the mesh set-up has great influence over the response of sheet pile wall. If the excavation section was longer than 50m, the whole domain can be considered as plain strain, so that the results in 2D and 3D FEM models were almost the same. If the section length was lowered from 50m to 30m, the bending of sheet pile wall could be reduced by 20%. This is because the sheet pile wall can benefit from the corner effect in 3D scenario. It is advised to apply 3D FEM model when dimensions and shape of the excavation zone allows the model to maximize the corner effect. The mesh set-up is also crucial to 3D FEM model. Coarse mesh leads to low accuracy results that certain stress points receiving much high stress than it should. Refine mesh requires a lot more time for calculation. For future research, it is still advised to perform field test for verification of 3D FEM models. It is also recommended to test how lateral support like struts and wailing beam influence the performance of sheet pile wall, especially the corners of excavation section.

For the sequential excavation method in this project, the main benefit was to control the settlement of surrounding area. The effect of limiting the deflection and bending moments of sheet pile wall by using sequential excavation was very limited. It is recommended to carry out the sequential excavation when the surrounding area is very sensitive to settlement that control of settlement is of high priorities. But for Spaarndammertunnel, the road near the tunnel is outside the influenced zone even if normal staged excavation is used. The modelling of sequential excavation requires a lot of time and effort, the execution requires even more time and effort. So the disadvantages of applying sequential excavation method in Spaarndammertunnel outweigh the advantages.

Acknowledgements

Hereby I would like to express my gratitude to all the members of my graduation committee, Professor Michael Hicks, Dr Philip Vardon, Ing Johan Zwaan and Dr Klaas Jan Bakker, who guided me throughout the whole graduation project, inspired me to always link the theoretical work with practice of engineering, encouraged me to improve the quality of this thesis to a higher level. It is not just helpful for the very end of my master program, but also inspiring for the start of my career as an engineer.

This graduation project is provided and sponsored by CRUX Engineering BV, where I had a brief but enriching working experience as an intern before the start of the graduation project. I'd like to thank Dr Holger Netzel, Ing Korneel de Jong and Ing Martin op de Kelder in particular, who kindly helped me during my graduation.

I would also like to thank all the friends I met during my time at TU Delft, who made my studying period abroad nothing but an unforgettable experience.

Last but not least, I would like to offer my special thanks to my parents and my girlfriend Chen Si, who offered me motivation, courage and love to face all challenges.

Table of contents

Contacts.....	1
Abstract	2
Acknowledgements	4
Table of contents.....	5
Table of figures.....	9
1. Introduction.....	11
1.1. Research background	11
1.1.1. Design procedure for deep excavation and retaining structure in Netherlands	11
1.1.2. Available analysis models	12
1.2. Problem definition.....	12
1.3. Modelling methodology and thesis structure	13
1.4. Limitations of research	14
2. Spaarndammertunnel project	15
2.1. Project introduction	15
2.2. Soil investigation	17
2.2.1. CPTs and boreholes for Spaarndammertunnel	17
2.2.2. Soil data for Spaarndammertunnel	18
2.3. Excavation pit design.....	21
2.3.1. Cross section of excavation pit.....	21
2.3.2. Building material	21
2.3.3. Excavation process	24
2.3.4. Dewatering	24
2.4. Suggestions for Spaarndammertunnel project	27
3. Literature review on modelling deep excavation.....	29
3.1. Introduction.....	29
2.1. Introduction of analytical model	29
3.2. Spring model.....	29
3.2.1. Introduction of spring model	29
3.2.2. Basic principle.....	30
3.2.3. D-sheet series	31
3.2.4. Advantages and limitations	32

3.3.	Finite element model	33
3.3.1.	General introduction	33
3.3.2.	FEM software for geotechnical problems (PLAXIS)	33
3.3.3.	Soil model	34
3.3.4.	3D application.....	36
3.3.5.	Advantages and limitations	37
4.	2D modelling of excavation.....	38
4.1.	2D model input.....	38
4.2.	Spring model (D-Sheet piling).....	38
4.2.1.	Model cross-section and stages	38
4.2.2.	Soil properties	39
4.2.3.	Calculation and test results	40
4.3.	2D FEM model (PLAXIS 2D).....	44
4.3.1.	Model set-up and calculation stages.....	44
4.3.2.	Mesh set-up.....	45
4.3.3.	Results	46
4.3.4.	Comparison of results between PLAXIS 2D and D-Sheet piling.....	50
4.4.	Conclusion of 2D modelling.....	51
5.	3D modelling of excavation.....	52
5.1	3D Staged excavation model (PLAXIS 3D)	52
5.1.1	General model set up	52
5.2.1	Mesh set up	54
5.2.2	Calculation stages and water levels	55
5.2.3	Results	55
5.2	Parametric study for 3D staged excavation model	61
5.2.1	Study on the size of the excavation pit	61
5.2.2	Study on the mesh set-up	63
5.3	3D sequential excavation model (PLAXIS 3D)	65
5.3.1	Sequential structure	65
5.3.2	Calculation stages.....	66
5.3.3	Results	67
5.4.	Conclusion on 3D modelling.....	70
6.	Optimization for sequential excavation model.....	71
6.1.	Test on lateral support	71

6.1.1.	Model introduction	71
6.1.2.	Model set-up	71
6.1.3.	Test results	72
6.2.	Test on excavation step.....	75
6.2.1.	Model introduction	75
6.2.2.	Model set up.....	75
6.2.3.	Test results	75
6.3.	Test on sequential set up	80
6.3.1.	Model introduction	80
6.3.2.	Model set-up	80
6.3.3.	Test results	81
6.4.	Conclusion of testing for sequential excavation	85
7.	Conclusions and recommendations	86
7.1	Introduction.....	86
7.2	Conclusions of modelling	86
7.3	Advantages and disadvantages of sequential excavation model.....	87
7.4	Recommendations for future research.....	88
	Bibliography.....	90
	Appendix A – CPT data and derivation of soil parameters.....	92
1.	Soil investigation and CPT correlations	92
2.	CPT correlation and soil parameters	92
3.	CPT results	94
4.	Volumetric weight of different soil layers.....	95
	Appendix B – Analytical method for retaining structure design	96
1.	Lateral stresses in soil.....	96
2.	Rankine earth pressure theory.....	97
3.	Coulomb earth pressure theory	99
4.	Other earth pressure theories.....	101
5.	Sheet pile wall design	102
6.	Blum’s method	104
	Appendix C.....	107
1.	Calculation steps for D-Sheet piling	107
2.	Calculation steps for PLAXIS 2D.....	110
3.	Calculation steps for 3D staged excavation model in PLAXIS 3D	114

Table of figures

<i>Figure 1-1 Design procedure for deep excavation and retaining structure</i>	11
<i>Figure 1-2 Demonstration of sequential excavation</i>	12
<i>Figure 1-3 modelling sequence</i>	13
<i>Figure 2-1 the overview of Spaarndammertunnel</i>	15
<i>Figure 2-2 the construction sequence of cut-and-cover tunnel (source: fhwa.dot.gov)</i>	16
<i>Figure 2-3 Tunnel elements and retaining wall</i>	16
<i>Figure 2-4 the position of the tunnel and the N-S metro line</i>	17
<i>Figure 2-5 The CPT and borehole map</i>	18
<i>Figure 2-6 Cross-section of the excavation pit model</i>	21
<i>Figure 2-7 the cross section of sheet pile element, Z type on the left and U type on the right</i>	22
<i>Figure 2-8 Definition of positive normal force (N), shear force (Q) and bending moment (M) for a plate based on local system of axes</i>	23
<i>Figure 2-9 the well point method and configuration of an individual well point</i>	25
<i>Figure 2-10 Scenarios of dewatering positions</i>	26
<i>Figure 2-11 Damage expectation for sheet pile wall in Amsterdam due to installation (Source: CUR166 4th edition)</i>	28
<i>Figure 3-1 Schematic of a long beam on elastic foundation</i>	30
<i>Figure 3-2 the beam on elastic foundation method: (a) springs placed at both sides of the continuous beam, (b) at rest earth pressure before excavation, (c) distribution of earth pressures on both sides of the retaining wall before wall movement, and (d) distribution of earth pressures on both sides of the wall after wall movement</i>	31
<i>Figure 3-3 Change of earth pressure coefficient in D-sheet piling</i>	32
<i>Figure 3-4 the example of plane strain and axisymmetric model (source: PLAXIS 2D reference manual)</i>	34
<i>Figure 3-5 Position of nodes and stress points in soil elements (source: PLAXIS 2D reference manual)</i>	34
<i>Figure 3-6 General types of Geo-Engineering computing</i>	35
<i>Figure 3-7 Applications of different soil models</i>	36
<i>Figure 3-8 3D soil elements with 10-node tetrahedrons (source: PLAXIS 3D reference manual)</i>	37
<i>Figure 4-1 cross-section of full excavation on left and right side of excavation pit</i>	38
<i>Figure 4-2 Stage overview for D-Sheet piling</i>	39
<i>Figure 4-3 Soil materials input in D-Sheet piling</i>	40
<i>Figure 4-4 Soil properties in D-Sheet piling</i>	40
<i>Figure 4-5 Summary of max displacement and forces on left side</i>	41
<i>Figure 4-6 Summary of max displacement and forces on right side</i>	41
<i>Figure 4-7 Charts of Moments, Forces and Displacements on left side</i>	42
<i>Figure 4-8 Charts of Moments, Forces and Displacements on right side</i>	42
<i>Figure 4-9 Cross-section and soil profile for PLAXIS 2D model</i>	44
<i>Figure 4-10 Calculation stages for PLAXIS 2D model</i>	44
<i>Figure 4-11 Water condition for the excavation phase</i>	45
<i>Figure 4-12 Mesh overview for PLAXIS 2D model</i>	46
<i>Figure 4-13 Deformed mesh in the last calculation stage</i>	46

Figure 4-14 Ground water head in the last phase	47
Figure 4-15 Lateral displacement on both sides of excavation pit	48
Figure 4-16 Bending moment on both sides of excavation pit	49
Figure 5-1 Soil profile in PLAXIS 3D model.....	52
Figure 5-2 structure set up in PLAXIS 3D model	53
Figure 5-3 Input properties for piles, struts and wailing beams.....	54
Figure 5-4 Overview of mesh set up in PLAXIS 3D model	54
Figure 5-5 Sequence of water level set up.....	55
Figure 5-6 Overview of lateral displacement (left) and bending moment M_{11} (right) for the last phase	55
Figure 5-7 Maximum deformation on both sides of excavation pit	56
Figure 5-8 Maximum bending moments on both sides of excavation pit	56
Figure 5-9 Comparison of bending moment for the sheet pile wall between PLAXIS 2D and 3D.....	57
Figure 5-10 Cross-section of water head for the last phase at half of domain	58
Figure 5-11 Overview of vertical displacement of soil at the last phase	59
Figure 5-12 Comparison of vertical displacement for soil in 2D (up) and 3D (down) models	59
Figure 5-13 Corner effect for 3D modelling	61
Figure 5-14 Models overview for different testing pit length: 30m, 50m, 70m	62
Figure 5-15 Bottom view of the mesh in excavation zone (green area highlights the excavation pit, red dots are piles)	63
Figure 5-16 Side view of bending moment distribution for different mesh quality.....	64
Figure 5-17 Common method to refine mesh locally	64
Figure 5-18 Side view for structures of staged excavation model and sequential excavation model... ..	65
Figure 5-19 Several calculation steps for sequential model	66
Figure 5-20 Overview of lateral deformation and bending moment for sequential excavation model	67
Figure 5-21 Maximum deformation and bending moment on both sides of excavation pit.....	68
Figure 5-22 Comparison of vertical movement of soil.....	69
Figure 6-1 Comparison of construction stage in sequential model and staged excavation model.....	71
Figure 6-2 Maximum lateral displacements of the sheet pile wall at mid-point.....	73
Figure 6-3 Maximum bending moments of the sheet pile wall at mid-point	74
Figure 6-4 the plot for lateral displacements for 25m excavation step	75
Figure 6-5 Maximum lateral displacements on left side of the excavation pit	76
Figure 6-6 Bending moments distribution without using smoothing function for 15m model	77
Figure 6-7 Bending moments results after smoothing function	78
Figure 6-8 Bending moments results without smoothing	79
Figure 6-9 Structure of test sequential model	80
Figure 6-10 Calculation sequence for the test sequential model	81
Figure 6-11 The lateral displacements distribution for the sheet pile wall on left side.....	82
Figure 6-12 Lateral displacements for test sequential model	82
Figure 6-13 Comparison of maximum bending moments with smoothing function.....	83
Figure 6-14 Comparison of maximum bending moments without smoothing function	83
Figure 6-15 Bending moments of test model at calculation stage6.....	84
Figure 7-1 Example of more complex excavation zone	88

1. Introduction

Deep excavation and retaining structure are traditional Geo-engineering topics. It requires good understanding of behaviour of soils and engineering experience of structure design. Experimental, mathematical and numerical models are developed to simulate soil and structure reactions due to the excavation. This graduation project is an independent research project based on in situ soil investigation and preliminary design of Spaarndammertunnel project in Amsterdam. The preliminary design, including the cross-section, element dimensions and material properties, has been provided by CRUX Engineering BV. This graduation project will only analyse the excavation of building pit for the tunnel. The research focus is to use numerical models to investigate excavation process and its influence over the soil and retain structure. Both two dimension and three dimension numerical analysis are performed.

In this chapter, the research background is introduced. Then the research problems are defined. It is followed by the modelling methodology and thesis outline. At last the limitations are listed.

1.1. Research background

1.1.1. Design procedure for deep excavation and retaining structure in Netherlands

There are a lot of calculation models available for designing and optimizing retaining structures. But due to the time and financial budget, not all calculation models are adopted in practice. The following procedure is proved to be well balanced among safety, efficiency and accuracy, thus becomes a standard designing procedure in Netherlands. The standard designing procedure and details in each design step are shown in *Figure 1-1*. This design sequence is concluded based on TU Delft Geo-engineering master course CIE4363 Foundation and deep excavation.

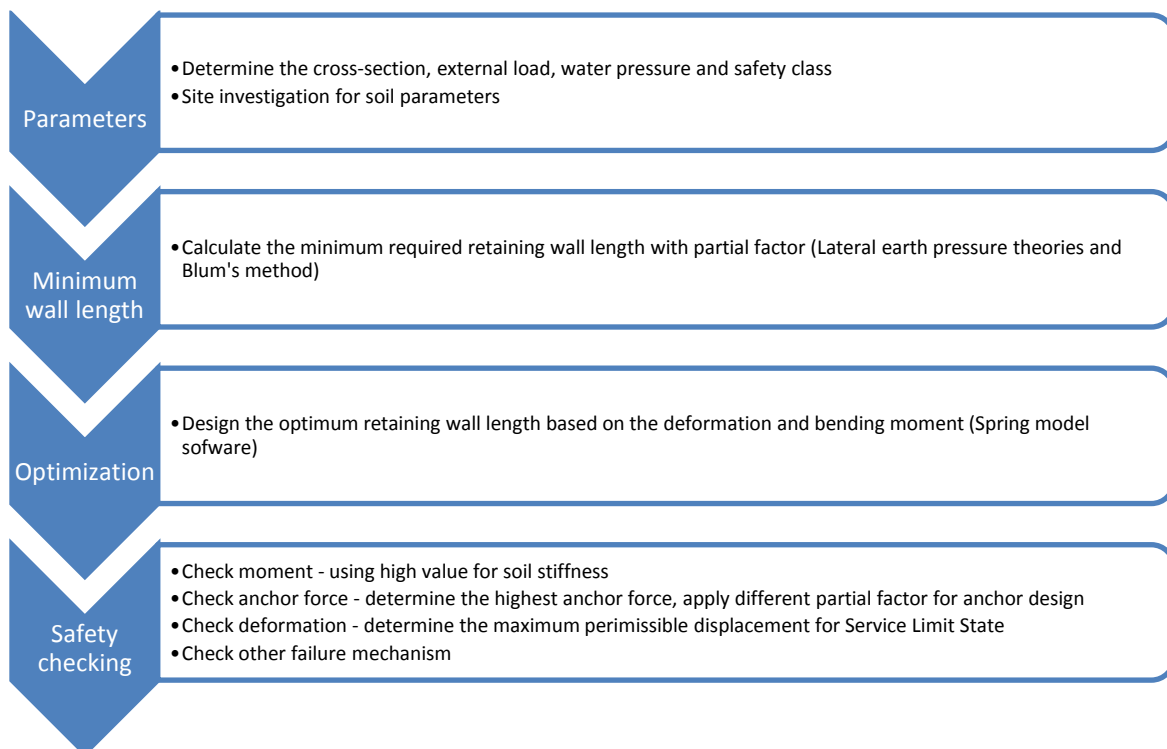


Figure 1-1 Design procedure for deep excavation and retaining structure

1.1.2. Available analysis models

As mentioned in section 1.1.1, there are numerous calculation models available for deep excavation and retaining structure design. The most essential and popular ones are:

- Analytical model (e.g. Blum 1931)
- Spring model (e.g. D-sheet piling)
- Finite Element Method (e.g. PLAXIS)

In general the analytical model and spring model are relatively easy to use compared to FEM model, but provides acceptably accurate results. Thus these two models are widely used to perform first estimation and preliminary design. All three calculation models are used during the preliminary design of Spaarndammertunnel project. Therefore all three models will be introduced and elaborated in this thesis. But for preliminary design, only 2D FEM model was made to optimize the retaining wall design.

1.2. Problem definition

Most geo-technical issues are currently modelled and analysed in 2D software, since it is easier for setting up the model and faster for calculation, compared to 3D modelling. For most projects, the results from 2D analysis are accurate enough to ensure safety and efficiency. In 2D models, the whole investigating domain normally considered as plain strain or axisymmetric, only the cross-section is analysed. However, there are situations that the excavation domain is hard or impossible to simulate in 2D model. Meanwhile normal PCs nowadays are capable of handling the calculation for 3D FEM models. It is worth investigating in what conditions that worth applying 3D modelling, and how the project can benefit from 3D modelling.

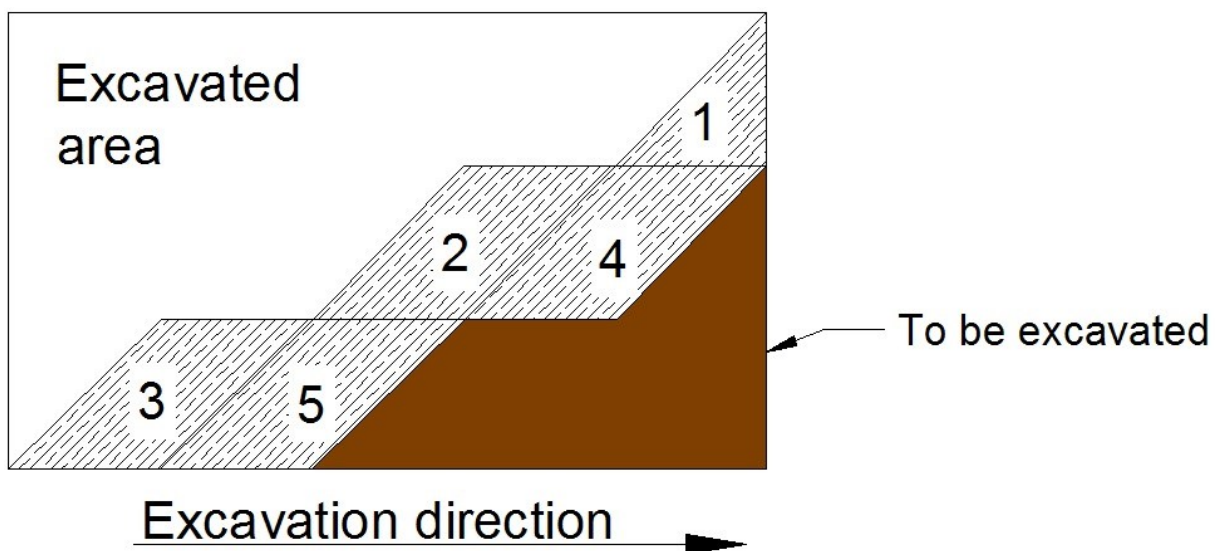


Figure 1-2 Demonstration of sequential excavation

The sequential excavation model, also known as New Austrian Tunneling Method (NATM), is a popular method of modern tunnel design and construction. It is one of the scenarios that are impossible to analyse in 2D models. The excavation zone is divided into segments first. The segments are then excavated sequentially with supports. Figure 1-2 is the side view of one excavation section. The excavation is assumed to go from left to right. The white area on top left of the domain is already

excavated. The brown area on bottom right is the remaining area to be excavated. The shaded area with numbers is excavation zone that sequential excavation model is applied. The numbers in segments are the order of excavation sequence. The reason why sequential model is impossible to simulate in 2D model is that the geometry changes along the longitudinal direction of excavation zone; cross-section for the lateral support differs from each other. Since this graduation project is based on a real tunnel project, it is beneficial to test how Spaarndammertunnel project can benefit from sequential excavation model.

1.3. Modelling methodology and thesis structure

For this graduation project, the design procedure demonstrated in *Figure 1-1* was already done in the preliminary design of Spaarndammertunnel project. The project will focus on testing the design and the sequential excavation method in 3D FEM models. In order to investigate the problems defined in above while applying the engineering conditions and preliminary design of Spaarndammertunnel project, a sequence of 2D and 3D numerical models is developed. The order of modelling approached in this thesis is shown in *Figure 1-3*. The software used for the spring model is D-Sheet Piling, a sheet pile wall design program developed by Dutch institute Deltares. Both 2D and 3D FEM models are set up and tested in PLAXIS, a widely used FEM program for geotechnical problems analysis in Netherlands.

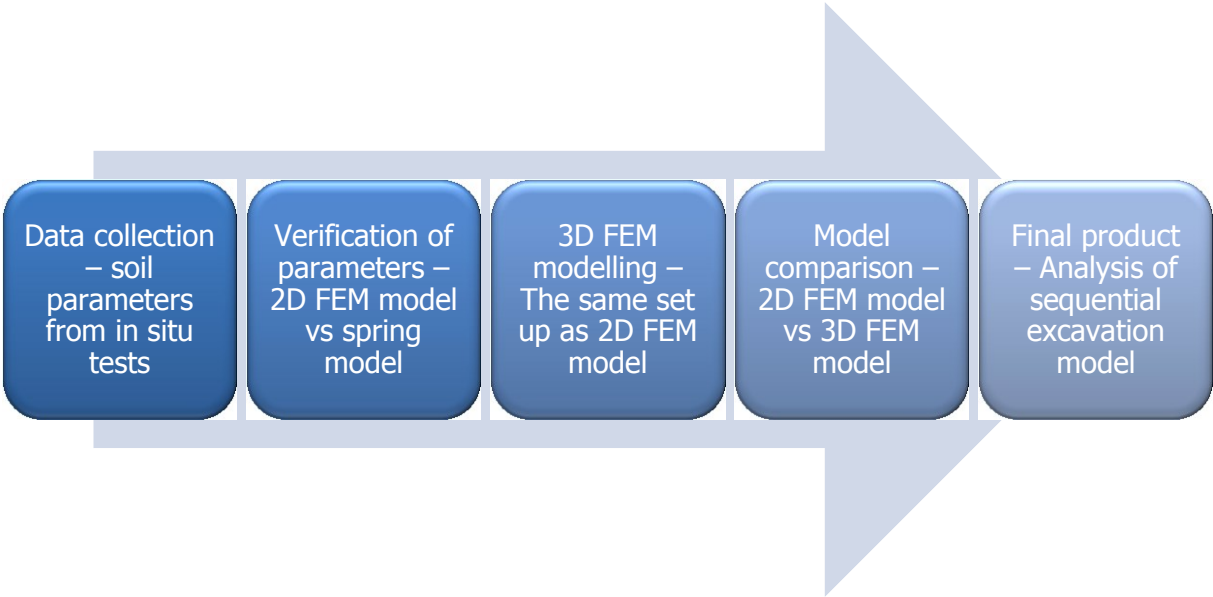


Figure 1-3 modelling sequence

The first part is to determine the soil parameters based on in situ soil tests. Cone penetration tests and soil sampling were done for Spaarndammertunnel. The soil parameters are compared to Amsterdam North-South line database and empirical data from CRUX Engineering BV. The detailed soil data is shown in Section 2.2, the soil investigation of Spaarndammertunnel project. The procedure of how the soil data is correlated into parameters in software is elaborated in Chapter 3.

After the soil parameters are determined, they are tested in both D-Sheet piling and PLAXIS 2D. The D-sheet piling software is used to estimate the order of magnitude of deflection. The theory that the

spring model applies is explained in Section 2.3.2. The testing procedure and parameters used in spring model are demonstrated in Section 4.1.1. The general principles, applications and limitations of FEM method used for geo-engineering are explained in Section 2.3.3. The results from D-Sheet piling are compared with 2D FEM model, in order to check the 2D FEM model is properly constructed. The parameters for soil and retaining structure are thoroughly tested in this stage, so that the 3D models can run smoothly, and the results are comparable.

Subsequent model is the 3D FEM model based on the same test set up used in 2D models. A parametric study regarding the size of the building pit and mesh set-up is also done in this stage. Since the 2D model is built for a plane strain situation, the retaining wall is treated as an infinite long structure; it is not influenced by the corner effect. But in 3D modelling as well as reality, the length, width and L/W ratio have great influence on how the retaining wall behaves. The results from 3D FEM models are then compared with 2D FEM model. The model set-up and test results are presented in Section 4.4.

The final part of modelling is the 3D sequential excavation modelling. The excavation domain is the same as the one used in normal 3D FEM model. The sequential excavation model is then tested with different lateral support set-up, different excavation rates and different sequential set-up. The sequential model set-up and comparison with normal 3D FEM model are introduced in Chapter 5. The test scenarios are shown in Chapter 6.

The outline of this thesis is as follow:

- Chapter 1 – Introduction
- Chapter 2 – Spaarndammertunnel project
- Chapter 3 – Literature review on modelling deep excavation
- Chapter 4 – 2D modelling of excavation
- Chapter 5 – 3D modelling of excavation
- Chapter 6 – Optimization for sequential excavation
- Chapter 7 – Conclusion and recommendation

1.4. Limitations of research

This graduation project is only focused on testing and optimizing the 3D FEM models for excavation including the sequential excavation model. The modelling of long term safety for the tunnel is not within the scope of research. The optimization of the current building pit design, including the choice of material dimensions and properties, is not part of the investigation. However, suggestions regarding the design and execution are provided in the conclusion part according to the results from numerical models.

The construction of Spaarndammertunnel project starts at early 2015, while all the modelling of this thesis was done in 2014. So the testing results only come from numerical models with no verification from field testing.

2. Spaarndammertunnel project

2.1. Project introduction

The Spaarndammertunnel locates at the North West side of Amsterdam Central Station and parallel to the Tasmanstraat and Spaandammerdijk. The tunnel is designed to be a concrete cut-and-cover tunnel with a total length of approximately 800 metres. The municipality of Amsterdam wants to improve quality of life in the neighbourhood of Spaarndammerbuurt and Houthaven. As a part of the project, a park on top of the tunnel is to be constructed as a green connection between the Spaarndammerbuurt neighbourhood and the newly developed “Houthavens” plan (Bartels, 2014). The position and surrounding area of the project site is shown in *Figure 2-1*. The figure is a print screen from Google earth with tunnel position highlighted in red. The street and district names are displayed in the figure as well.

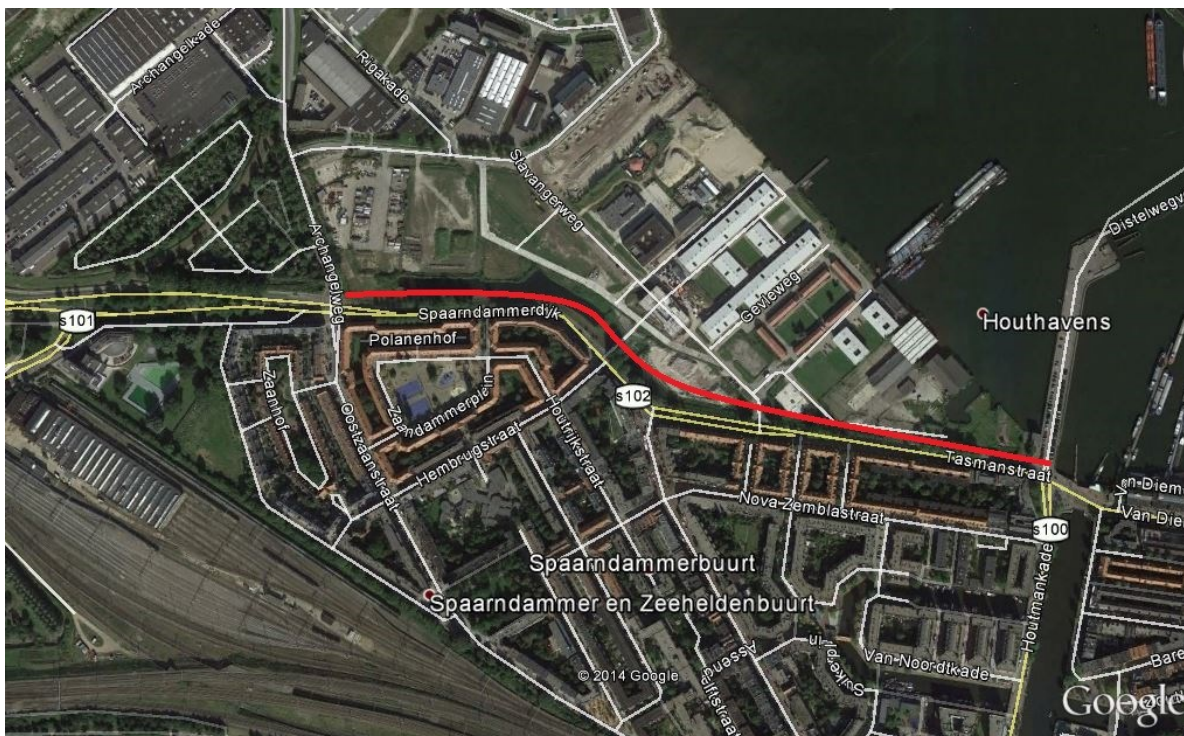


Figure 2-1 the overview of Spaarndammertunnel

As mentioned above, this project applies the cut-and-cover tunnelling technology. It is a tunnel construction method for shallow tunnels where the excavation from the surface is possible, economical, and acceptable in relation to soil and surroundings. It has been used for many years, building underground transportation facilities, such as subways, railways, and metro systems. In a traditional construction sequence of cut and cover tunnel, a trench is excavated first and then the tunnel elements are constructed and placed in the pit. After the construction of tunnel is complete, the top of the tunnel is covered with backfill material. The cross-sections of general construction sequence for cut-and-cover tunnelling are illustrated in *Figure 2-2*. This tunnelling method involves the installation of walls (temporary/permanent) to support the sides of the excavation, a bracing system, and control of ground water and possible underpinning of adjacent structures. For depths of 10 m to 12 m, cut and cover is usually more economical and more practical than mined or bored

tunnelling. Shallow cut-and cover-tunnels have several other advantages, such as easy access from street level, a conventional construction method well understood by contractors.

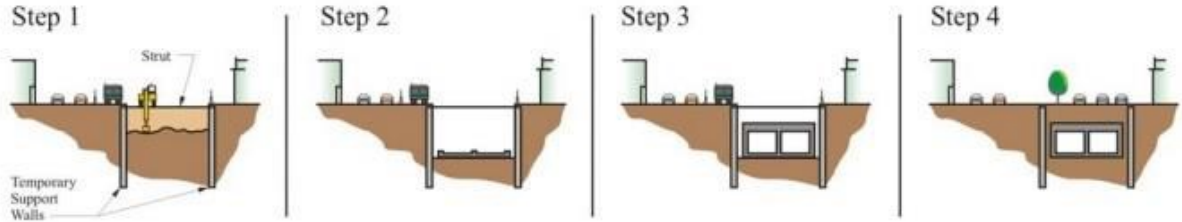


Figure 2-2 the construction sequence of cut-and-cover tunnel (source: fhwa.dot.gov)

The preliminary design, including the cross-section, element dimensions and material properties, has been provided by CRUX Engineering BV. Sheet pile walls together with two layers of struts would be used as a retaining structure for the building pit. The tunnel elements together with retaining wall are illustrated in Figure 2-3. The tunnel element shown in Figure 2-3 demonstrates the service station in tunnel with extra safety aisle aside and pump station beneath. Detailed design and in situ site characterisation of the Spaarndammertunnel will be introduced in Chapter 3. This master thesis will only focus on the simulation of the excavation process based on the preliminary design and the soil profile of the Spaarndammertunnel project.

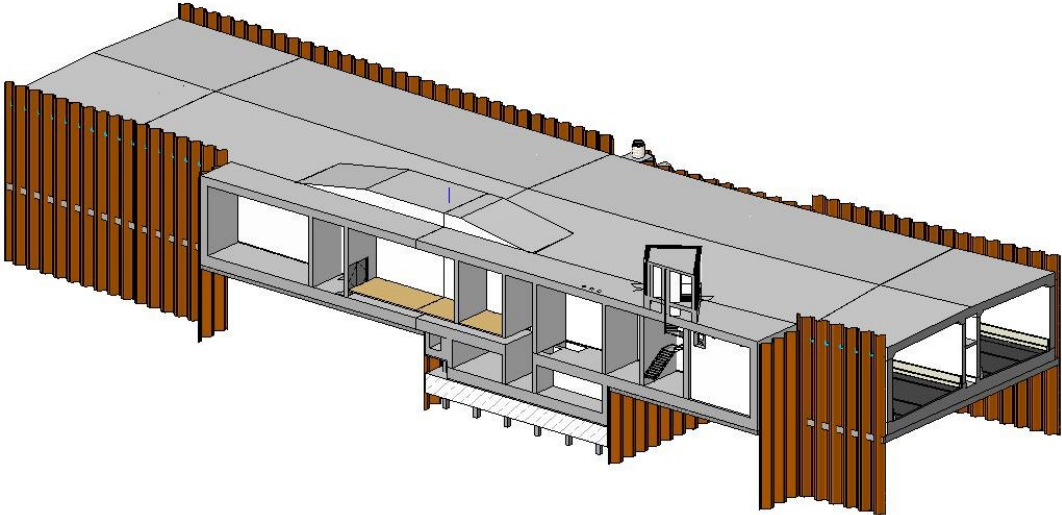


Figure 2-3 Tunnel elements and retaining wall

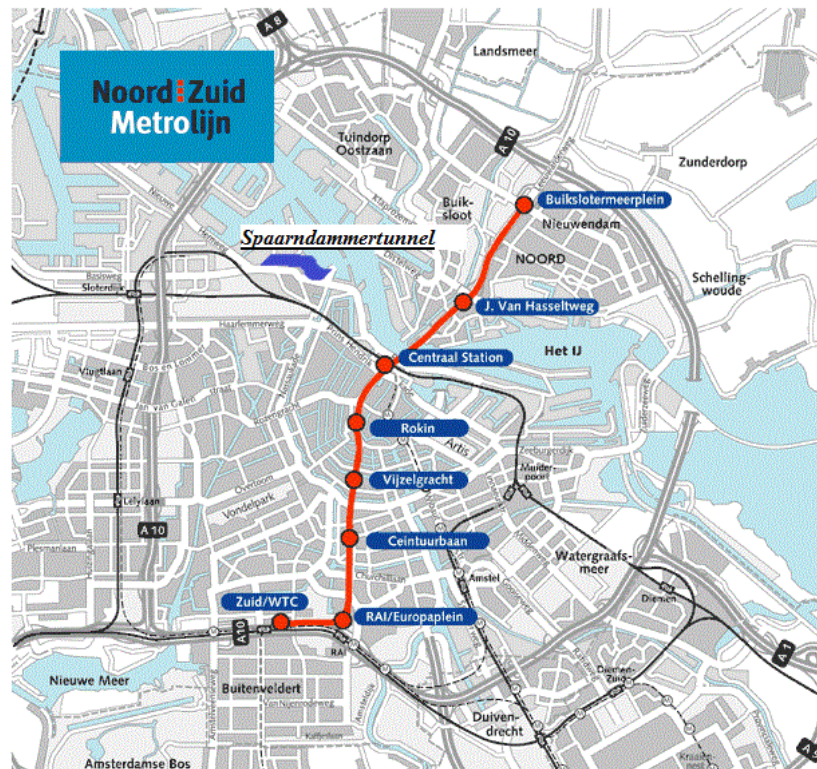


Figure 2-4 the position of the tunnel and the N-S metro line

The Figure 2-4 shows the location of Spaarndammertunnel and the North-South line in Amsterdam city map. The Spaarndammertunnel is highlighted in purple and the N-S line is in red. It is clear to see that this tunnel is very close to the N-S line and the city centre of Amsterdam. It is located in a crowded residential area, where buildings are adjacent to the excavation pit and sensitive to ground settlement. And the Spaarndammerdijk is a very busy road that next to the excavation put. Thus the project needs careful design and execution. The control of deformations of sheet piles and pile foundation, which supports lateral earth pressure and vertical loading respectively, are of first priorities.

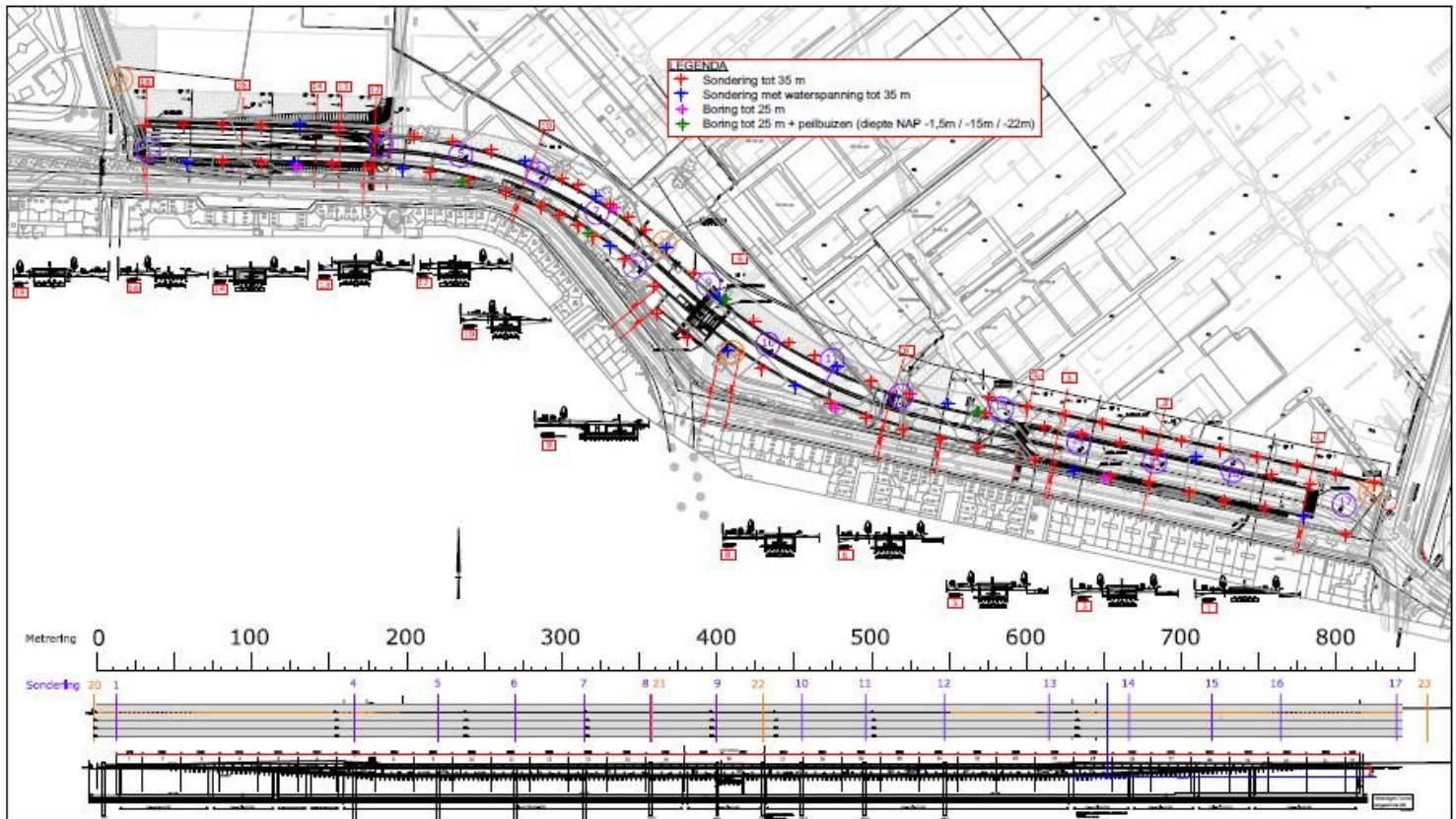
2.2. Soil investigation

Due to the weak soil layers (Estuary peat, Holland peat, Base peat and etc.) in Amsterdam, pile foundation is needed to support the tunnel elements. Piles are installed under the bottom slab before the excavation according to the preliminary design. The current soil parameters are acquired based on the Amsterdam North-South line database. The North-South line is a new metro line that will form an important transport artery through the central districts to connect suburbs north of the River IJ. Due to the importance and the complexity of the project, thorough soil investigation has been done for the surrounding area. Those soil profiles formed the North-South line database. The local soil condition might differ from the general data. As the soil investigation is carried out in situ, the soil profile is examined, compared and validated. The process of soil investigation and data interpretation are presented in Appendix A.

2.2.1. CPTs and boreholes for Spaarndammertunnel

In order to construct the tunnel safely in city centre, site investigation with 84 CPTs and 8 boreholes was done before the design stage. CPT stands for cone penetration test, is a popular in situ method

for soil investigation in Netherlands. A CPT device consists in a cylindrical probe with a cone-shaped tip with different sensors that allow a real time continuous measurement of cone tip resistance, sleeve friction by pushing it into the ground at a speed of 2 cm/s. From the CPT parameters, geotechnical data including soil strength can be derived. Some of them are equipped with a geophone in order to be able to perform shear wave velocity measurements. The data is normally read by a field computer that displays it real-time and stores it at regular depth intervals.



Measurements can be taken at any intervals desired, being 2.5 cm the interval.

Figure 2-5 The CPT and borehole map

Commercial CPT is done by a truck pushing a “cone” into the ground. The weight of the truck is partially supported by both the tip of the cone and the sleeve of the cone. The “tip resistance” is determined by the force required to push the tip of the cone and the “sleeve friction” is determined by the force required to push the sleeve through the soil. The “friction ratio” is the ratio between sleeve friction and tip resistance, measured as a percentage. Soil type and thereby resistance to liquefaction can be inferred from these measurements. The positions of CPTs and boreholes for Spaarndammertunnel are shown in Figure 2-5. Red and blue cross along the tunnel highlight the positions of CPT. All CPT are done all the way to 35 metres deep. Pink and green cross show the locations of boreholes. The soil samples taken from boreholes were sent to laboratory tests.

2.2.2. Soil data for Spaarndammertunnel

The Table 2-1 and Table 2-2 display part of the general soil data from in situ investigation and Amsterdam database respectively. The soil parameters shown in Table 2-1 are generalized from the interpretation of CPT data. The names of soil layers are kept in Dutch in coordination with original

literature. The soils are defined individually in *Table 2-2*. Note that the first categories in two tables are different as the one in database is the dry volumetric weight.

Soil		Bottom depth	γ	γ_{sat}	c'	ϕ'	Kh1 *	Kh2 *	Kh3 *
[-]		[m NAP]	[kN/m ³]	[kN/m ³]	[kPa]	[°]	[kN/m ³]	[kN/m ³]	[kN/m ³]
1A	Ophooglaag (zand)	0.5	17	19	0	28	4800	2400	1200
7A	Geul humeuse klei	-0.5	13.6	13.6	6	21	3200	1500	650
8	Hollandveen	-3.5	10.2	10.2	5	17	1600	800	400
9	Oude Zeeklei	-5.5	16.2	16.2	7	25	3600	1750	700
10B	Wadzand	-6.5	15.8	17.8	2	27	6600	3300	1650
11	Hydrobiaklei	-12.5	15.2	15.2	8	27	4000	2000	800
12	Basisveen	-14	11.7	11.7	6	18	2000	800	500
13	1 ^e Zandlaag	-14.25	18	20	0	32	22000	11000	5500
14	Alleröd	-18	18.5	18.5	3	28	14800	7400	3700
17	2 ^e Zandlaag	-20	18	20	0	32	37000	18500	9250

Table 2-1 General representative soil profile and soil parameters for Spaarndammertunnel

Nr.	Soil	Definition	γ_{dry}	γ_{sat}	c'	ϕ'	k_v	c_v	v	K_0
			[kN/m ³]	[kN/m ³]	[kPa]	[°]	[m/s]	[m ² /s]	[-]	[-]
01A	Ophooglaag (zand)	Land fill	15.0	18.4		30	1.0E-05			
07A	Geul humeuse klei	Clay	7.0	13.9	10	23	5.7E-10	1.0E-06	0.35	0.55
08	Hollandveen	Peat	2.5	10.5	5	19	1.0E-08	1.0E-10	0.35	0.65
09	Oude Zeeklei	Clay	11.0	16.5	7	26	1.5E-09	6.0E-07	0.33	0.50
10B	Wadzand	Sand	15.8	17.8		4	5.0E-07			
11	Hydrobiaklei	Clay	9.0	15.2	8	27	1.0E-09		0.30	0.59
12	Basisveen	Peat	4.2	11.7	6	21	1.0E-08	2.0E-08	0.35	0.65
13	1e Zandlaag	Sand	16.8	19.8		33	1.5E-04		0.25	0.40
14	Alleröd	Loam, sand	14.4	18.5	3	28	3.0E-05		0.30	0.40
17	2e Zandlaag	Sand	15.9	19.0		33	1.0E-04		0.25	0.40

Table 2-2 General soil data from N-S line database

Judging by the saturated volumetric weight and strength (c' and ϕ') values in these two tables, the soils found at site are very similar to the generalized database. It is worth noting that the soil parameters listed in database are generally on the conservative side. This may be because of high requirement for settlement control in North-South line project. As the metro line goes through the heart Amsterdam, where old houses with wooden piles locate, the standard for settlement tolerance is extremely strict. The soil parameters derived from CPT data are compared with soil samples taken from boreholes as well. The comparison of saturated volumetric weight in Lab test and generalized values is shown in *Table 2-3*. According to *Table 2-3*, the difference of soil weight between derived values and lab test results is within 10%. According to the comparison of soil properties among CPT data, Lab tests, and Amsterdam database, the deviation of values are acceptable. This means that there no major errors in soil investigation. The values listed for *Table 2-1* are later used for numerical models. The detailed CPT data and soil properties are shown in Appendix A.

Ysat		Delta	Deviation
[kN/m ³]		[kN/m ³]	%
LAB	CPT		
	19		
13.3	13.6	-0.3	-3%
9.5	10.2	-0.7	-7%
16.8	16.2	0.6	4%
18.3	17.8	0.5	3%
15.7	15.2	0.5	3%
12.9	11.7	1.2	9%
	20		
19.0	18.5	0.5	3%
	20		

Table 2-3 Comparison of volumetric weight for Lab test and generalized value

2.3. Excavation pit design

2.3.1. Cross section of excavation pit

The ground level on left side of the cross-section is 2.9m NAP, and on right side is 1.7m NAP. There are two layers of struts that locate at 1.5m NAP and -2m NAP. The sheet pile walls drive all the way to -17m NAP on both side of excavation pit. The bottom of full excavation is at -6.7m NAP, and is later filled with a 0.7m thick concrete floor. There are four piles a row, which locate from -6.3m NAP to -21m NAP. The width of the model is 80m and the depth of the model is 27.9m, so that the boundary would not influence the deformation results. The cross-section of the excavation zone is shown in *Figure 2-6*. All the models used in this thesis are set based on this cross section.

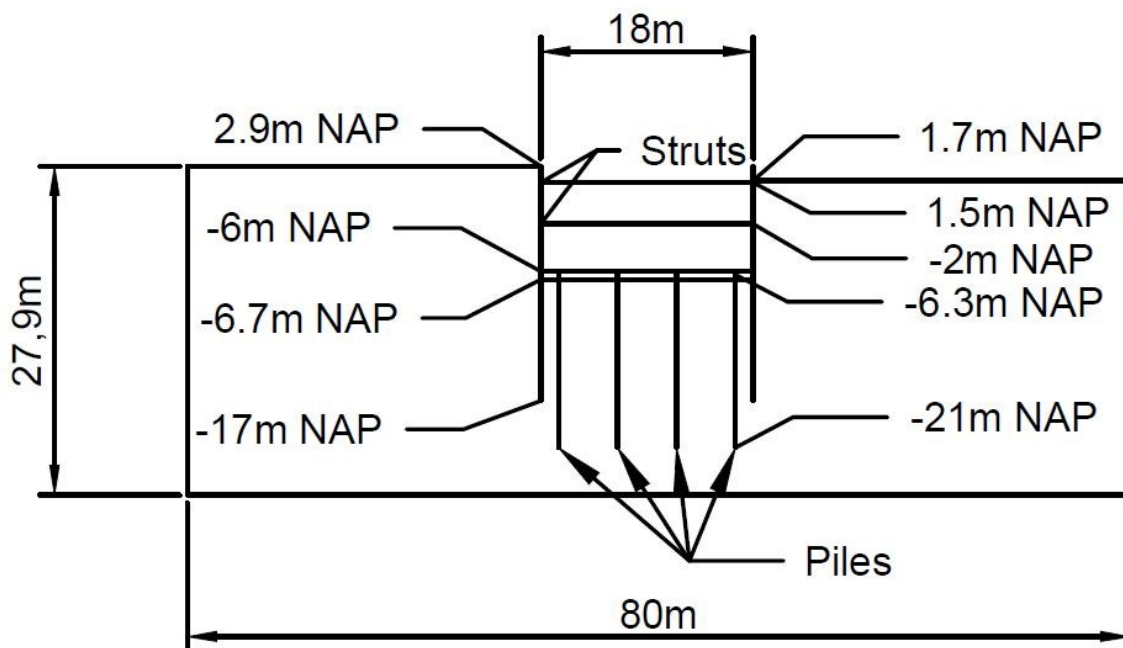


Figure 2-6 Cross-section of the excavation pit model

2.3.2. Building material

The building material for the retaining structure is determined in the preliminary design. As stated in Chapter 1, the focus of this thesis is to test and optimize the numerical model instead of optimize the material selection. All materials are derived from preliminary report directly.

There are two types of sheet pile wall in terms of section profile, Z type and U type namely. The cross sections of both types are shown in *Figure 2-7*. The sheet pile wall used for this project is the light weight AZ 26 – 700. AZ piles are normally supplied in pairs which save time in handling and pitching. In all models mentioned in this thesis, the sheet pile wall is designed to be a temporary retaining structure. The dimensions and properties of AZ-26 sheet pile wall are shown in *Table 2-4*.

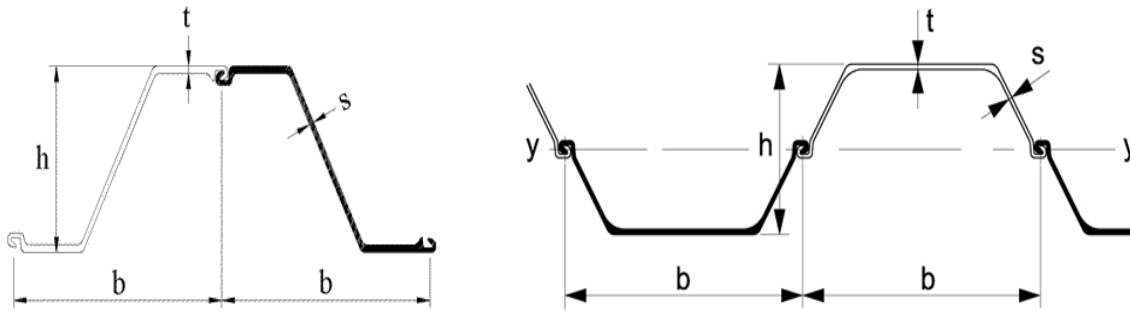


Figure 2-7 the cross section of sheet pile element, Z type on the left and U type on the right

Section	S = Single pile D = Double pile	Sectional area cm ²	Mass kg/m	Moment of inertia cm ⁴	Elastic section modulus cm ³	Radius of gyration cm	Coating area* m ² /m
AZ 26-700	Per S	131.0	102.9	41800	1815	17.86	0.97
	Per D	262.1	205.7	83610	3635	17.86	1.93
	Per m of wall	187.2	146.9	59720	2600	17.86	1.38

Section	Width	Height	Thickness	Sectional area	Mass	Moment of inertia	Elastic section modulus	Static moment	Plastic section modulus	Class*		
	b mm	h mm	t mm	s mm	cm ² /m	kg/m of single pile	kg/m ² of wall	cm ⁴ /m	cm ³ /m	S 240 GP S 270 GP S 320 GP S 355 GP S 390 GP S 430 GP S 460 AP		
AZ 26-700	700	460	12.2	12.2	187	102.9	147	59720	2600	1535	3070	2 2 2 2 2 2 2

Table 2-4 Dimensions and properties of AZ 26-700

	Bending moment capacity	Moment of inertia	Section modulus	Min. tensile strength	Min. yield strength	Min. elongation at failure
	kNm/m	cm ⁴ /m	cm ³ /m	N/mm ²	N/mm ²	%
S 240 GP	624	59720	2600	340	240	26
S 270 GP	702	59720	2600	410	270	24
S 320 GP	832	59720	2600	440	320	23
S 355 GP	923	59720	2600	480	355	22
S 390 GP	1014	59720	2600	490	390	20
S 430 GP	1118	59720	2600	510	430	19

Table 2-5 Bending moment capacity for AZ 26-700 Sheet pile wall

The bending moment capacity of sheet piles is determined by the steel properties and the section modulus from the sheet piles dimensions. The bending moment capacities for AZ 26-700 are listed in Table 2-5. In practice, steel grades S 270 GP and S 355 GP are generally used. The choice of steel grade depends on structural aspects, the method of driving selected, the embedment depth and the ground conditions.

The struts used for lateral support are hollow steel bars. The out diameter for the strut is 610mm and the thickness is 20mm. The physical properties for the strut are shown in Table 2-6.

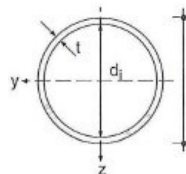
		G	G_E	A	d_1	A_L	$I_y = I_z$	$W_{y,el} = W_{z,el}$	$W_{y,pl} = W_{z,pl}$	$i_y = i_z$	I_t	classificatie ⁽¹⁾	profieffactor	
		kg/m	kg/m	mm ² × 10 ²	mm	m ² /m	mm ⁴ × 10 ⁴	mm ³ × 10 ³	mm ³ × 10 ³	mm	mm ⁴ × 10 ⁴	buiging of druk	[A _L /A]m ⁻¹	
												S275	S355	
		610 × 20	291	297	370,7	570,0	1,916 161490	5295	6965	229	322979	1	1	52

Table 2-6 Physical properties for the strut

The wailing beam is used to distribute the loads induced by the excavation to the surrounding soil. It is attached to struts so that the lateral force coming from struts can be re-distributed instead of giving a large focused force directly on the sheet pile wall. On the other hand, the sheet pile wall is good at resisting bending moment for the direction (M_{11}), but not capable of handling negative N_2 . In case of a rectangular excavation zone, earth pressure coming from two ends will induce dramatically deformation of sheet pile walls. The wailing beam also acts as a longitudinal support against normal force for sheet pile wall. The directions for forces mentioned above are illustrated in *Figure 2-8*. Unfortunately, the preliminary design is based on 2D cross-sections of the excavation pit. It is simulated as a plane strain situation with no wailing beam. For the PLAXIS 3D models, a relatively stiff beam HEB-300 is used. The parameters in PLAXIS material input are shown in *Table 2-7*.

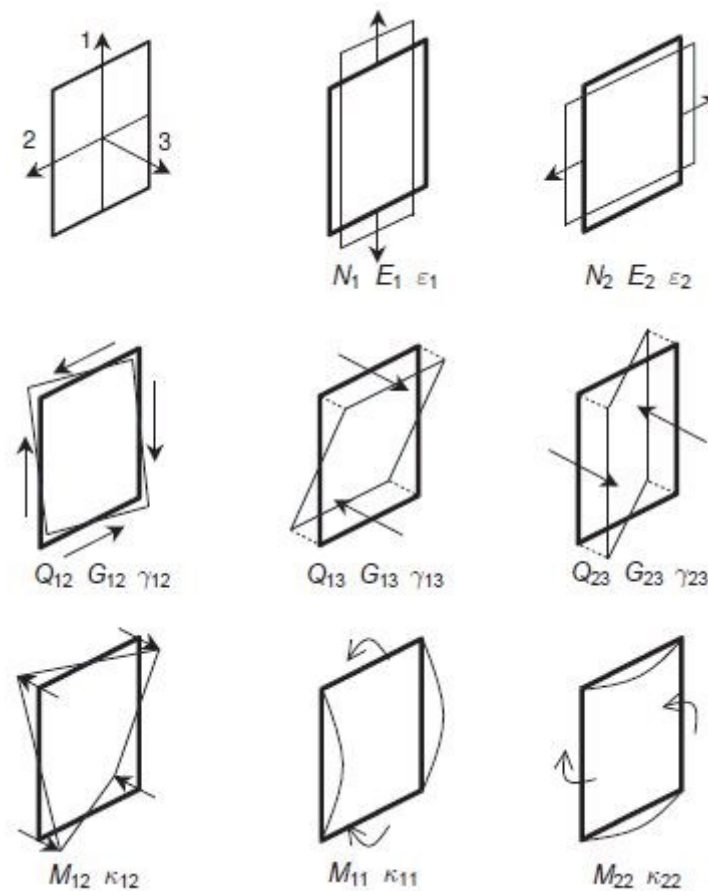


Figure 2-8 Definition of positive normal force (N), shear force (Q) and bending moment (M) for a plate based on local system of axes

Parameter	A	E	I_2	I_3	I_{23}
Value	0.015	$2.1 \cdot 10^8$	$2.517 \cdot 10^{-4}$	$8.563 \cdot 10^{-5}$	0
Unit	M^2	kPa	M^4	M^4	M^4

Table 2-7 Material properties for the waling beam in PLAXIS 3D

2.3.3. Excavation process

The actual excavation is not started yet. It is still the designing and optimizing stage for the project. Thus the design has made a lot of changes over time. Both the staged and sequential excavation models used in this thesis are based on the preliminary design, which are done in sections.

The preliminary design was that the excavations will be done in sections, and each section is an individual building pit with sheet pile walls wrapping around. After the tunnel elements are installed, the sheet pile walls and supporting struts will be removed and shifted forward.

As for each excavation section, the first step is to flatten the surface and install the pile foundation, which serves as foundation of tunnel elements later. The pile tips are at -6.3m NAP. And the length of the piles is 15m that the bottom of the piles is at -21.3m NAP. Then the sheet pile walls are driven into the ground, filters are installed to lower the water level locally to -7.2m NAP (0.5m below the bottom of the building pit) in the building pit, so that the excavation can start. The dewatering of the excavation will be explained in section 3.3.3. The first part of excavation will continue to 1m NAP level, half meter below the high struts (1.5m NAP). Followed by the first excavation, the high struts together with the waling beams are installed to provide lateral support for the retaining structure. The second part of the excavation goes from 1m NAP to -2.5m NAP (0.5m below the low struts). The low struts and waling beams are then installed at -2m NAP. After two layers of struts are installed, the excavation will continue all the way to -6.7m NAP (0.4m below the pile tips). The last meter of excavation should be done with extra care, since the pile tips may be damaged during the excavation process. In order to provide a rigid and dry working environment, and also provide lateral support to the whole retaining structure, a concrete layer is constructed from -6.7m NAP to -6m NAP. The pile tips are thus rigidly connected to the concrete layer. After the concrete layer is hardened, the low struts are removed. In the 2D and 3D staged excavation model, the struts are deactivated at this phase. But in the sequential model and the reality, the struts are shifted forward together with the excavation process.

However, the latest design is that the whole tunnel will be excavated in one piece. There are no sheet pile walls to seal off the front and back of the building pit. The excavation will be executed sequentially from one end to the other like a trench. And on one side, the sheet pile wall will be served as permanent structure after the tunnel is built.

As it is stated in Chapter 1, the modelling will be based on the preliminary design. So the building pit

2.3.4. Dewatering

Dewatering is a method of lowering the groundwater level in sand or gravel layer rather than clay. The permeability of clay is very low. And the properties of clay soil, shear strength and compressibility for instance, change significantly due to the dewatering. Thus dewatering in clay layer is often referring to soil improvement. However, the water flow in sandy and gravelly soils is rather rapid. For excavation of soil, the water may leak into excavation zone and ultimately lead to loosening of soils, sand boiling or uplift failure.

The goal of dewatering is to create a dry excavation environment, prevent leakage of water or sand, avoid sand boiling or uplift failures, and forestall the floating of basement. As for this thesis, dewatering is part of excavation process, but the influence of dewatering is not considered in the numeric model. Thus the execution of dewatering in real case will be introduced in this section without quantified analysis. A full dewatering plan in an excavation includes several steps:

- 1) Choose a dewatering method
- 2) Determine the hydraulic parameters
- 3) Analyse the results of pumping tests
- 4) Estimate the amount of water to be pumped out
- 5) Calculate the numbers of pumping wells needed
- 6) Compute the settlement of influence zones

The dewatering method chosen for this project is the well point method. Each collecting point is connected to the pumping pipe inside a small diameter well. The collecting points are often arranged in a line or in a rectangle that is 0.8-2.0 metre away from each other. The pumping pipe is then connected to a common collecting pipe on top, which is pumped out using vacuum pump. The vacuum well point method and the configuration each well point are illustrated in *Figure 2-9*.

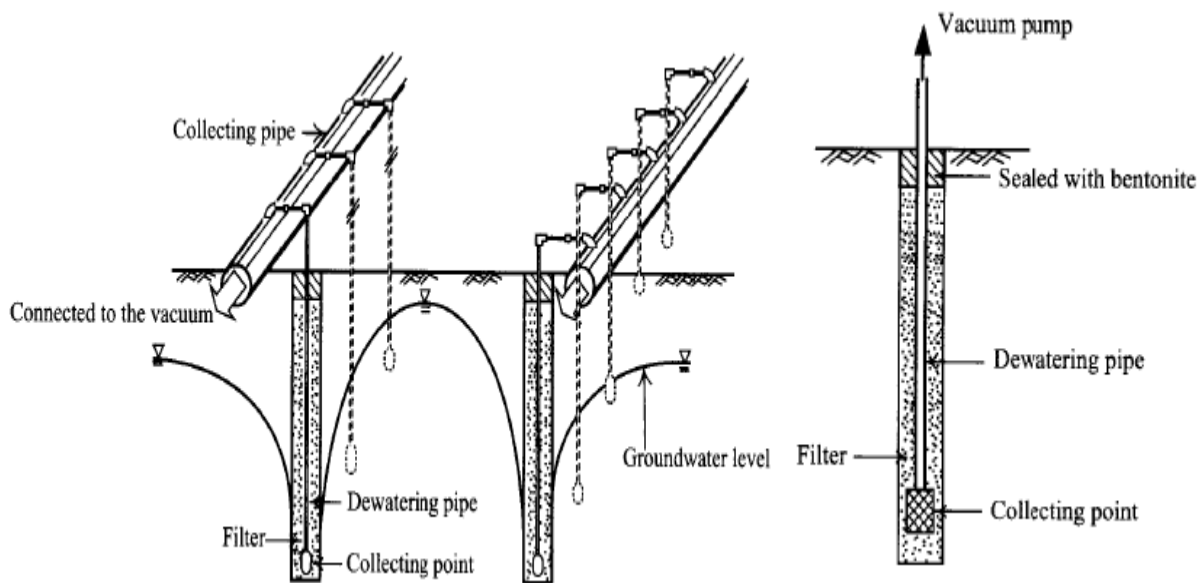


Figure 2-9 the well point method and configuration of an individual well point

There are several ways of arranging collecting points in terms of influence of dewatering positions. *Figure 2-10* demonstrates most common scenarios: (a) dewatering within excavation zone above an impermeable layer, (b) dewatering outside of the excavation zone and above an impermeable layer, (c) dewatering in a sandy/gravelly layer below the excavation zone, (d) dewatering in a sandy layer within the excavation zone, and € dewatering in a sandy layer below the wall bottom. The scenario applied in the numerical model is the same as (a). For each excavation stage, the water level in excavation zone is always 0.5 metre lower than the bottom of the excavation pit.

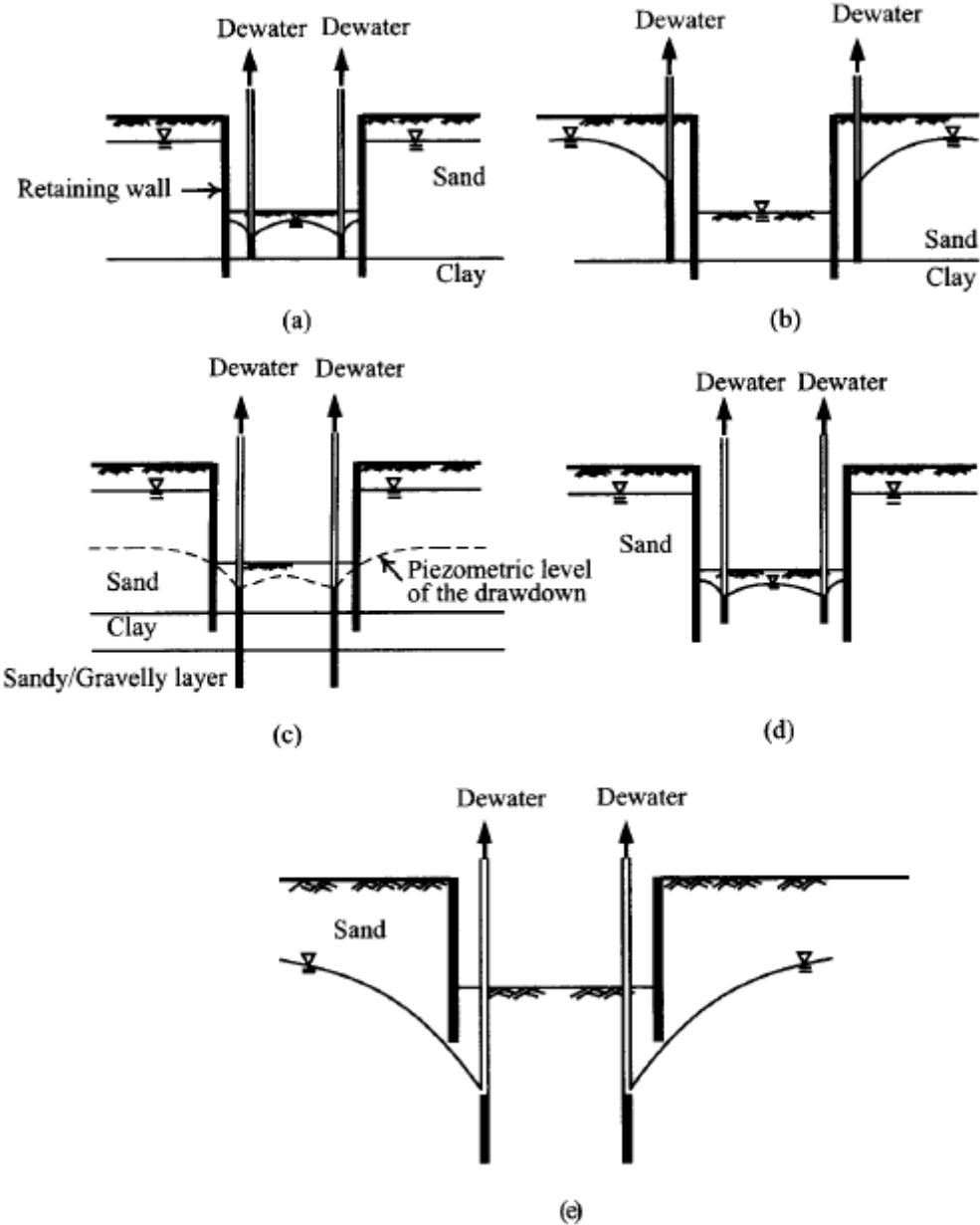
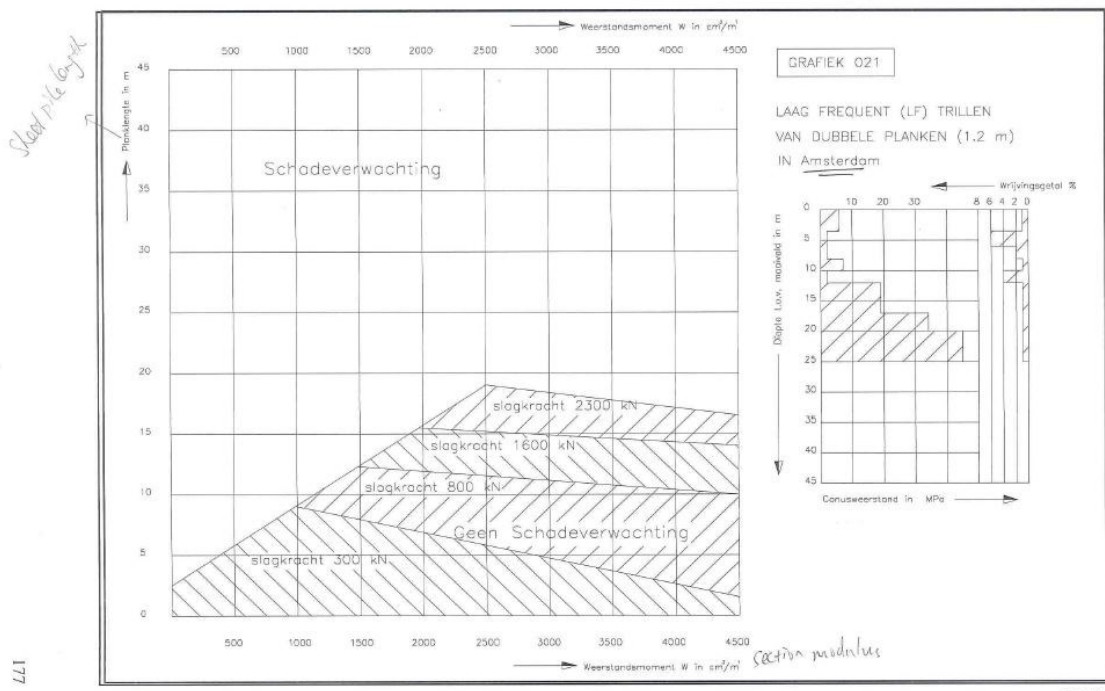


Figure 2-10 Scenarios of dewatering positions

2.4. Suggestions for Spaarndammertunnel project

As it is stated in the introduction chapter, the whole graduation project is based on the preliminary design of the Spaarndammertunnel. Over the year 2014, the design of this tunnel has been improved. However, it is still worth noting that some areas of the preliminary design can be improved according to the numerical simulation of the excavation process.

As mentioned in Section 2.3.2 the building material for retaining structures, the sheet pile wall chosen for project are light weight, which may cause problems for installation. According to Dutch code CUR166 for sheet pile wall design, the combination of sheet pile length and the section modulus is the edge of being damaged during installation. This is probably because of the bottom end of the sheet pile wall is into the deep sand layer, which is very stiff and likely to cause damage. *Figure 2-11* shows the damage expectation for sheet pile wall installation in high and low frequency scenarios. The judging criteria on two axes are depth and section modulus of the sheet pile wall. Based on these two inputs, it is easy to find the estimated required force for installation. The shaded area in the bottom half means that the sheet pile wall is unlikely to be damaged during the installation. While the white half on the top half means that it is prone to be damaged. According to the figure, the sheet pile wall goes deeper than 20m (into the deep sand layer) is likely to be damaged, no matter what section modulus is. In fact, the installation of sheet piles often requires stronger material than resistance of bending during excavation.



CUR-publicatie 166 4^e druk, deel I

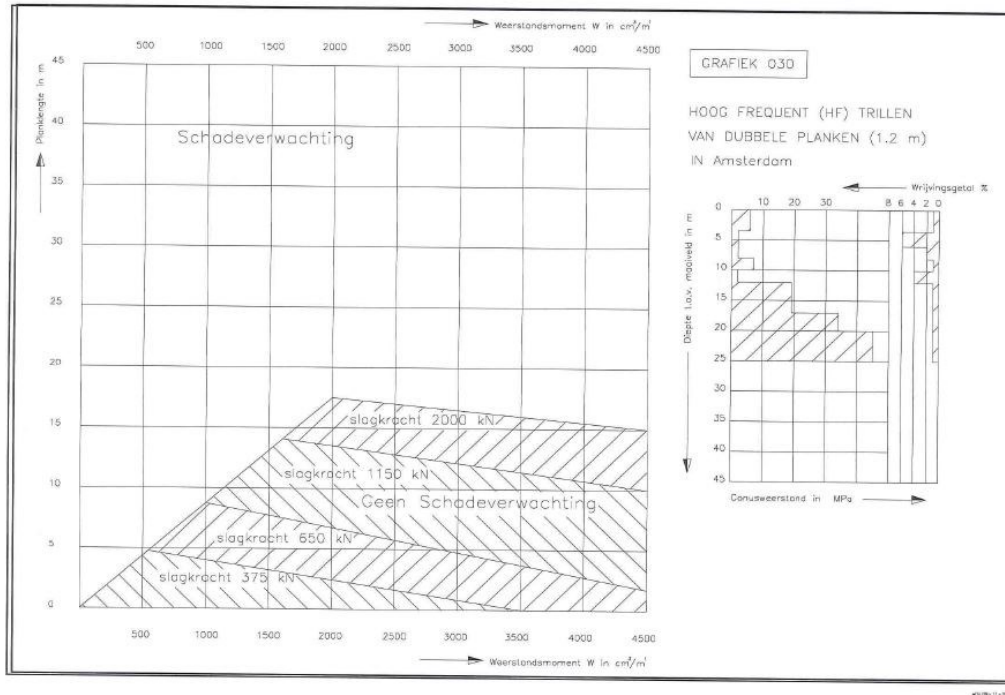


Figure 2-11 Damage expectation for sheet pile wall in Amsterdam due to installation (Source: CUR166 4th edition)

One of the special features for this project is the asymmetrical domain. The surface level on left side is at 2.9m NAP while the right side is 1.7m NAP. The high struts are at 1.5m NAP. They are optimized accordingly with the sheet pile wall on the high surface side. They are almost at the top of the low surface side. Since the excavation zone is rather wide, the struts might be optimized as inclined towards the lower side to optimize the use of the sheet pile wall on low surface side. But the earth pressure on left side is higher and probably leads to higher bending moments in sheet pile wall. Since the same grade of sheet pile wall would be used for both sides. As long as the left side is not failing, it should be fine on the other side.

The preliminary design is based on 2D numerical calculations, the design for lateral support including the struts and wailing beam was vague. The struts positions in the corners of the excavation sections were not specified. For safety concern as well as construction convenience, the design can be improved with detailed struts set-up for the corners of excavation sections.

3. Literature review on modelling deep excavation

3.1. Introduction

This chapter serves as a theoretical review for the modelling and analysis of deep excavation. Problems of deep excavation, no matter if stability analysis, stress analysis or deformation analysis, entail the distribution of earth pressure (Ou, 2006). Thus the key point of designing an earth retaining structure and its excavation process is to determine the lateral earth pressure and the corresponding response of the retaining structure.

As mentioned in Chapter 1, currently there are three major way to perform the lateral earth pressure analysis and earth retaining structure design:

- Analytical model
- Spring model
- Finite element model

In this chapter, the theory application of spring model and finite element method is elaborated. The application and software used in this thesis are introduced. The analytical model mentioned previously is not used in this thesis. So the theory of analytical model together with basic earth pressure theory is further elaborated in Appendix B.

2.1. Introduction of analytical model

The analytical model is based on some classical theories that determine the stresses on a retaining structure for the cases of active and passive earth pressure. The most famous and widely used theories among which are Rankine and Coulomb earth pressure theories. By applying these theories, the lateral earth pressure can be calculated, thus the minimum length of the sheet pile wall needed to achieve equilibrium can be determined. The retaining wall will certainly fail when the length of the sheet pile wall length is shorter than the minimum length. If the length of the wall is longer than minimum required length, the Blum's method can be used to analyse the bending moments and deformation, so that design could be optimized. These theories give a quick first estimation that can be done by hand calculation.

3.2. Spring model

3.2.1. Introduction of spring model

For a deep excavation process, the soil pressure and deformation change accordingly to the force acting on the retaining structure, the stiffness of retaining wall and so on. The forces are also related to the soil, water condition and excavation plan. It is a coupled process as the excavation induces unbalanced force against retaining structure and causes change in stress state and deformations, and these changes in return affect the unbalanced force. Compared to analytical models, numerical models can simulate and solve more complex conditions, as the computer can easily take over the calculation process. Therefore, the numerical methods can provide more accurate and realistic results. As for geotechnical problems, most commonly used numerical methods are the beam on elastic foundation method (spring method) and finite element method. The finite element model normally requires a lot of computation time and fast computer. Thus the spring method is more

favourable for practical design. One of the most widely used geo-technical software for retaining wall design in Netherlands, D-Sheet piling, is based on this beam on elastic foundation theory. In this section, the spring model is introduced.

3.2.2. Basic principle

The soil structure interaction, as one of the focus in foundation engineering, is often simulated by applying a series of springs. And the Winkler's model is the most widely used to formulate this simulation.

This theory focuses on the bending of a beam resting on an elastic foundation as shown in *Figure 3-1*. Assume that the reaction offered by the support at any point is directly proportional to the displacement of that point along the vertical direction, and is in a direction opposite to the displacement. Thus, if H is the vertical displacement of a point in the beam, q_y is the support reaction per unit width of the beam, then the above assumption that the reaction force is proportional to the displacement mathematically translates into requiring

$$q_y = K_s * H \quad (1)$$

In which K_s is the modulus of subgrade reaction, indicates the constant of proportionality of those springs. The advantage of Winkler's model is that all elements are assumed to be working individually with no interactions, so that the analysis is simplified.

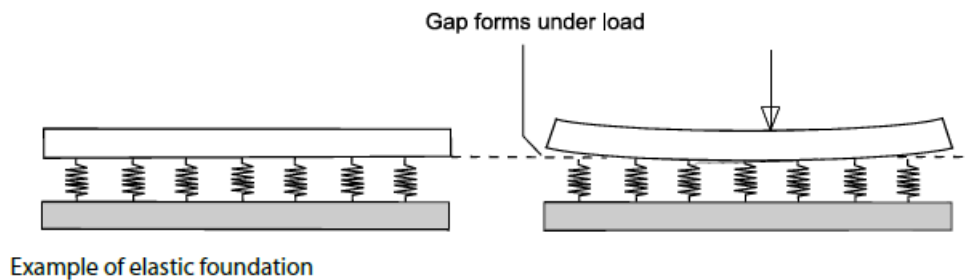


Figure 3-1 Schematic of a long beam on elastic foundation

As it is illustrated in *Figure 3-2*, the retaining structure is simulated as a vertical beam on elastic foundation with springs on both sides of retaining wall. The springs are taken to be the at-rest pressure (K_0 -condition) before the excavation start. During the excavation, the removal of soil on one side induces unbalanced force and results in the deflection of retaining wall. Due to the deformation of the wall, the distribution of earth pressure is changed. The earth pressure behind the retaining wall is decreased to $p_0 - k_h * \delta$. In which k_h is the horizontal coefficient of subgrade reaction, δ is the horizontal displacement of the retaining wall. While on the other side of the wall, the earth pressure increased to $p_0 + k_h * \delta$ due to the bending of the wall. When springs develop up to the passive condition, the soil on the passive side ceases increasing and remains the passive earth pressure. This is called the plastic state as demonstrated in *Figure 3-2* (d). When the reaction forces of soil springs are smaller than the passive earth pressure at a point, it is called the elastic state.

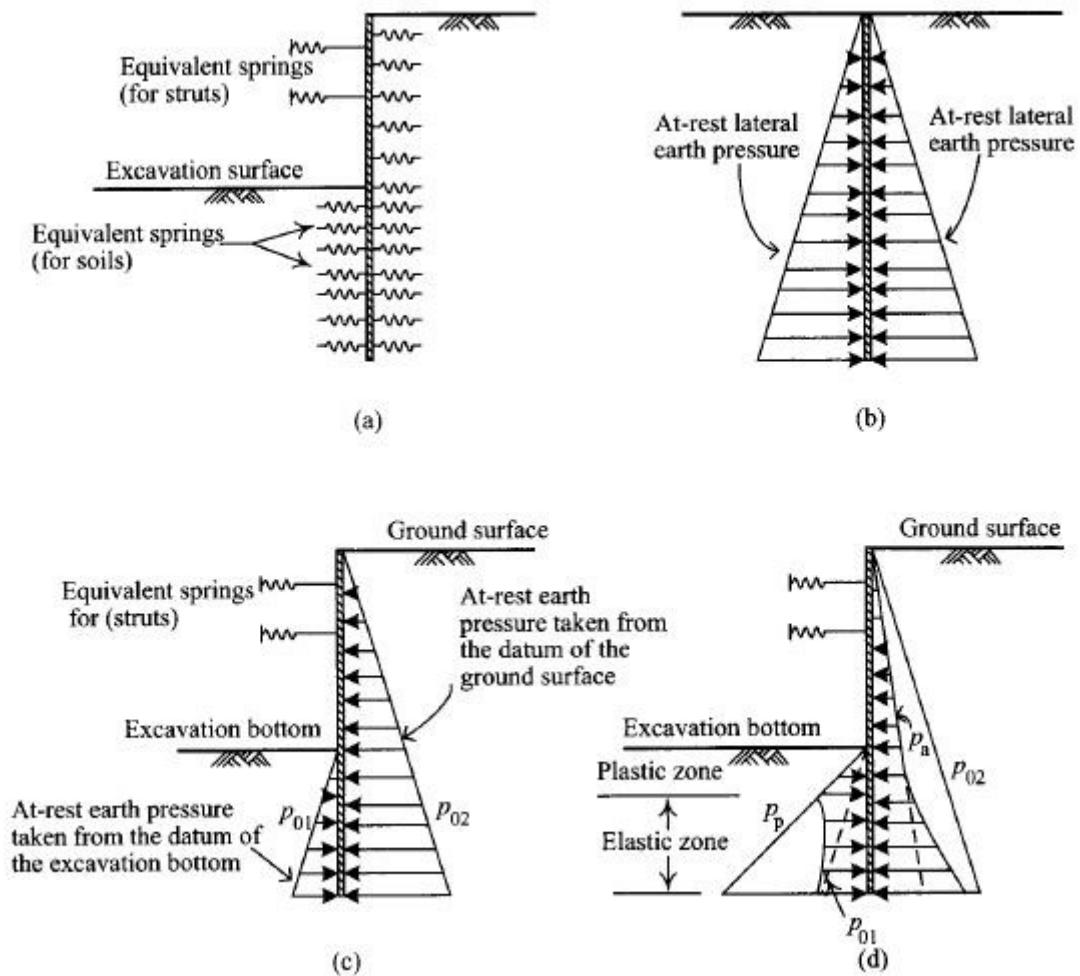


Figure 3-2 the beam on elastic foundation method: (a) springs placed at both sides of the continuous beam, (b) at rest earth pressure before excavation, (c) distribution of earth pressures on both sides of the retaining wall before wall movement, and (d) distribution of earth pressures on both sides of the wall after wall movement.

3.2.3. D-sheet series

One of the software used for 2D modelling in this thesis, D-sheet piling also applies the beam on elastic foundation theory. D-sheet piling is a part of the Deltares systems, a series of geo and hydro technical software developed by the Dutch institute Deltares. It is a popular tool to design the retaining structure, especially the sheet pile wall. Unlike earlier models, it uses uncoupled soil springs to represent the soil structure interaction. The program adopts the Euler-Bernoulli beam theory, which assumes the cross-section of the beam remains straight and perpendicular to the beam axle. It is a simplified model that offers reasonable approximation for engineering problems. But it tends to slightly overestimate the natural frequencies, especially for non-slender beams. (Han, S.M., et al. 1999)

The behaviour of the beam element is approximated by a differential equation below (D-Sheet piling Manual v9.2):

$$bEI \frac{d^4w}{dx^4} + N \frac{d^2w}{dx^2} = bf(x, w) \tag{2}$$

In which w is the horizontal displacement of the beam; f is the total pressure on the beam per meter; EI is the stiffness of the beam; x is the coordinate along the axle of the beam; N is the normal force within the beam; b is the acting width of the beam.

D-sheet piling solves equation (2) by applying finite element methods. The beam is divided into several elements connecting to each other. For the lateral earth pressure, the program applies slip surface theories. As it is mentioned in the Chapter 2.3.1, the shape of the slip surface has a large influence on the lateral stress calculation. In terms of lateral earth pressure coefficient, *Culmann* and *Müller-Breslau* theories are applied for straight slip surface, while the *Kötter* theory is applied for curved slip surface. The program uses an elasto-plastic model to simulate soil behaviour, thus the stiffness differs between initial loading and loading/ reloading situation. The strength and stiffness can also be altered for different phases. The earth pressure efficient changes accordingly with the displacement of the retaining wall.

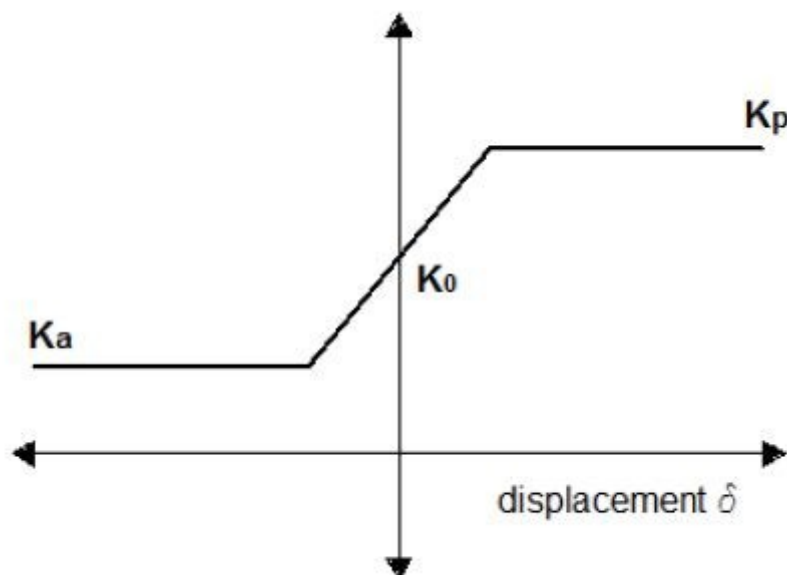


Figure 3-3 Change of earth pressure coefficient in D-sheet piling

3.2.4. Advantages and limitations

Compared to the analytical method introduced in section 2.3.1, the spring model simulates the soil structure interaction accordingly with the deflection of the retaining structure. Therefore it provides more realistic simulation. And the model is easily adopted by computer program, which makes the calculation done in a very short period of time.

Compared to finite element method that is going to be introduced in next section, the spring model uses a rather simple model that requires fewer parameters and the calculation time is a lot shorter than the FEM model. These advantages make the spring model the most popular model in the practical retaining structure design, especially when the structure is not very complex.

The spring model also has its limitations. It is an analysis method based on the plane strain condition. But in reality, the excavation on the short side of the building pit will be affected by the corner effect, and result in smaller deformation compared to plane strain condition. This can be better approached by 3D finite element method. Besides, it is hard to determine the appropriate spring stiffness constants of the soil, as these constants are not fundamental properties of soil. And the spring model isn't suitable to estimate the surface settlement behind the retaining structure, which is crucial if the excavation is taken place in city centre.

3.3. Finite element model

3.3.1. General introduction

The finite element method is the dominant discretization technique that subdivides the mathematical model into non-overlapping disjoint components of simple geometry called elements. The response of each is expressed in terms of a finite number of degrees of freedom at a set of nodal points. It is then approximated by connecting and assembling all elements. Unlike finite difference models, finite elements do not overlap in space.

The common FEM solution procedure is:

- 1) Divide the system into elements with nodes(discretization/meshing);
- 2) Assemble all elements at nodes to approximate the whole system (forming element matrices);
- 3) Solve the system for specific problem by applying governing equations accordingly;
- 4) Calculate desired quantities at selected elements

As stated in the previous sections for the analytical model and spring model, the excavation of soil induces coupled interaction between soil pressure and retaining structure. Theoretically speaking, the finite element method is capable of simulating the change of soil pressure, structure deformation, groundwater pressure and etc. However, finite element method is merely a tool that simulates the problem numerically. It is still down to the proper geotechnical theories applied that solve the problem. Moreover, modern commercial FE software provides rather robust solutions. It requires analysts' knowledge and experience to make sure the model is built up correctly and properly translated when the result presents. Due to the complexity of the FEM and the any small neglect is likely to lead to wrong results; the results of FEM should be checked by other methods.

3.3.2. FEM software for geotechnical problems (PLAXIS)

PLAXIS is special purpose finite element software designed for deformation and stability analysis. It is widely used for analysing geotechnical problems. Especially the PLAXIS 2D, it gives a more realistic approximation for soil structure interaction compared to analytical model and spring model, without sacrificing too much calculation time.

In order to approximate the real case in a two dimensional domain, PLAXIS 2D uses either a plane strain or axisymmetric model. A plane strain model is used for geometries with a uniform cross section and corresponding stress state and loading scheme over a certain length perpendicular to the cross section. An axisymmetric model is used for a circular structure with a uniform radial cross section and loading scheme around the central axis, where the deformation and stress state are

engineering computing can be divided into two groups: (a) those whose goal is to assess bearing capacity and slope or wall stability which are related to the ultimate limit state analysis (ULS), and (b) those which are related to the limit state analysis (SLS), such as deep excavations or tunnel excavations in urban areas. In general, as long as assessment of ULS for bearing capacity or slope stability is foreseen, the analysis may be limited to basic linear models such as the Mohr-Coulomb model (but this is not a rule). On the other hand, a precise deformation analysis requires the application of advanced constitutive models which approximate the stress-strain relation more accurately than simple linear-elastic, perfectly plastic model, and in effect, the form of displacement fields can be modelled more realistically (Rafal Obrazud, 2010).

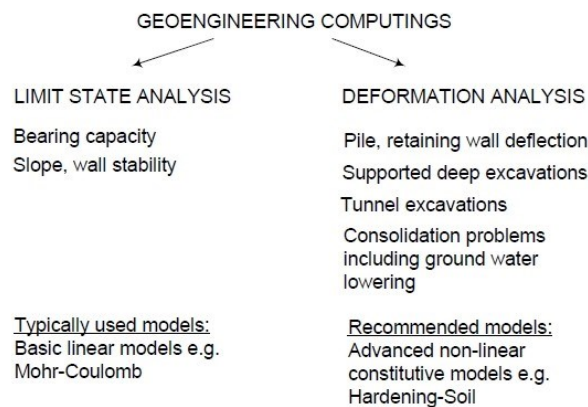


Figure 3-6 General types of Geo-Engineering computing

For this graduation project, the main focus is excavation. Sand, clay and peat are all included in the model. The thesis only consider the excavation period, thus time effect is not important in the model. Then there is no need to use creep model to simulate the secondary settlement. According to the application of soil models suggested by Plaxis material models manual, the most suitable soil models are Hardening Soil and Hardening Soil with small strain stiffness (PLAXIS, 2011) The application of soil models are shown in *Figure 3-7*. For modelling this excavation project, both Hardening Soil and HS Small Strain soil models will be used, in order to check the difference of the settlement for the embankment and surrounding buildings behind the sheet pile wall.

As for the material type, Drained, Undrained A and Undrained B refer to a plastic, dynamics and phi/c reduction analysis respectively. In this case, only the drained behaviour will be investigated, as the excavation pit is drained before the excavation commence.

Considering different types of applications (consider also type of soil!)

Model	Foundation	Excavation	Tunnel	Embankment	Slope	Dam	Offshore	Other
Linear Elastic model			C					
Mohr-Coulomb model	C	C	C	C	C	C	C	C
Hardening Soil model	B	B	B	B	B	B	B	B
HS small model	A	A	A	A	A	A	A	A
Soft Soil Creep model	B	B	B	A	A	B	B	B
Soft Soil model	B	B	B	A	A	B	B	B
Jointed Rock model	B	B	B	B	B	B	B	B
Modified Cam-Clay model	B	B	B	B	B	B	B	B
NGI-ADP model	B	B	B	A	A	B	A	B
Hoek-Brown model	B	B	B	B	B	B	B	B

A : The best standard model in PLAXIS for this application

B : Reasonable modelling

C : First order (crude) approximation

Considering different types of soils

Model	Concrete	Rock	Gravel	Sand	Silt	OC clay	NC clay	Peat (org)
Linear Elastic model	C	C						
Mohr-Coulomb model	A	B	C	C	C	C	C	C
Hardening Soil model			B	B	B	B	B	
HS small model			A	A	A	A	B	
Soft Soil Creep model							A*	A*
Soft Soil model							A*	A*
Jointed Rock model		A**						
Modified Cam-Clay model							B	B
NGI-ADP model							A*	A*
Hoek-Brown model		A**						

A : The best standard model in PLAXIS for this application

B : Reasonable modelling

C : First order (crude) approximation

* : Soft Soil Creep model in case time-dependent behaviour is important; NGI-ADP model for short-term analysis, in case only undrained strength is known

** : Jointed Rock model in case of anisotropy and stratification; Hoek-Brown model for rock in general

Figure 3-7 Applications of different soil models

3.3.4. 3D application

Although there are many geotechnical problems that can be approximated to either plane strain or axisymmetric conditions, some remain very three dimensional. Such problems will therefore require full three dimensional numerical analysis. In wither plane strain or axisymmetric model, it is implied that displacements in one particular direction are zero, which is a simplification of real case. However, in real geotechnical problems usually three components of displacement must be taken into account. Especially when the whole domain has an irregular shape rather a square or circle, the corner effect has huge influence of how the structure behaves.

For PLAXIS 3D, the basic soil elements of the 3D finite element mesh are the 10-node tetrahedral elements (*Figure 3-8*). In addition to the soil elements, special types of elements are used to model structural behaviour. For beams, 3-node line elements are used, which are compatible with the 3-node edges of a soil element. In addition, 6-node plate and geo-grid elements are used to simulate the behaviour of plates and geo-grids respectively.

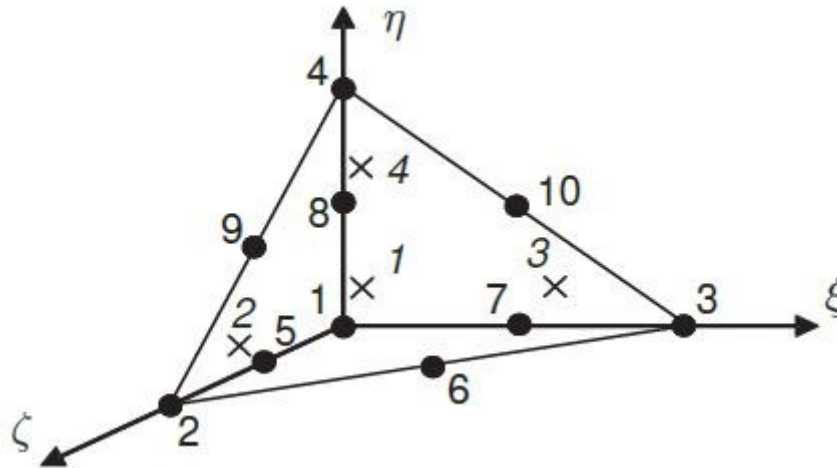


Figure 3-8 3D soil elements with 10-node tetrahedrons (source: PLAXIS 3D reference manual)

The major difference between 2D and 3D FE model is stated as below:

1. Full 3D finite element analysis does not involve any major developments to the theory presented for 2D plane strain and axisymmetric analyses. The main differences are that the full 3D geometry must be discretised and that there are now three, as opposed to two, displacement degrees of freedom at each node.
2. Full 3D finite element analyses require large amounts of computer resources, both memory and time. With present day computers only very simple nonlinear 3D problems can be analysed.
3. It is not advisable to use linear displacement elements in order to reduce the computer resources required, because these elements are not able to accurately reproduce limit loads. For geotechnical problems higher order (at least quadratic) displacement elements should be used.

3.3.5. Advantages and limitations

As mentioned in previous sections, a major advantage of finite element method is that the model has more realistic approximation for the change of deformation of soil and structure, as well as the change of stress state accordingly. For a complete theoretical solution the following four conditions should be satisfied: Equilibrium; Compatibility; Material constitutive behaviour; Boundary conditions. The analytical model is not able to fulfil all these conditions at the same time. And it does not provide information on movements or structural forces under working load conditions. Simple numerical methods, such as the beam-spring approach, can provide information on local stability and on wall movements and structural forces under working load conditions. But they do not provide information on overall stability or on movements in the adjacent soil and the effects on adjacent structures or services. Full numerical analysis, for instance the FEM, can provide information on all design requirements.

However, the finite element method especially the three dimensional model requires large amounts of computing resources and an experienced operator. It is becoming widely used for the analysis of geotechnical structures and this trend is likely to increase as the cost of computing continues to decrease. (Potts,D 1999)

4. 2D modelling of excavation

In this chapter, the model set-up, input parameters and calculation steps are introduced. The focus of this chapter is to test the input parameters and model set-up by comparing the results in D-Sheet piling and PLAXIS 2D. The test results were also used later as comparison with results from 3D models.

4.1. 2D model input

There are many commercial programs in the market that is specially designed for Geotechnical problems. The most popular ones in Netherlands are D-series and Plaxis, which are explained in Chapter 3. As mentioned in Chapter 3, it is better to use two different programs to verify the result for the finite element model in case the monitoring data is not available. For the 2D modelling part, both of these two programs are used to verify the test results for the deflection and bending moment for sheet pile walls.

4.2. Spring model (D-Sheet piling)

4.2.1. Model cross-section and stages

In D-Sheet piling, it is impossible to simulate the asymmetrical cross-section for this project. Thus, left and right side of the excavation zone are computed individually in two different files. The unbalanced force caused by the height difference is implemented by adding an additional force at the struts. In reality, the unbalanced lateral force induced by height difference is transferred by struts. The cross-section of the excavation zone for both sides of sheet pile walls are shown in *Figure 4-1*.

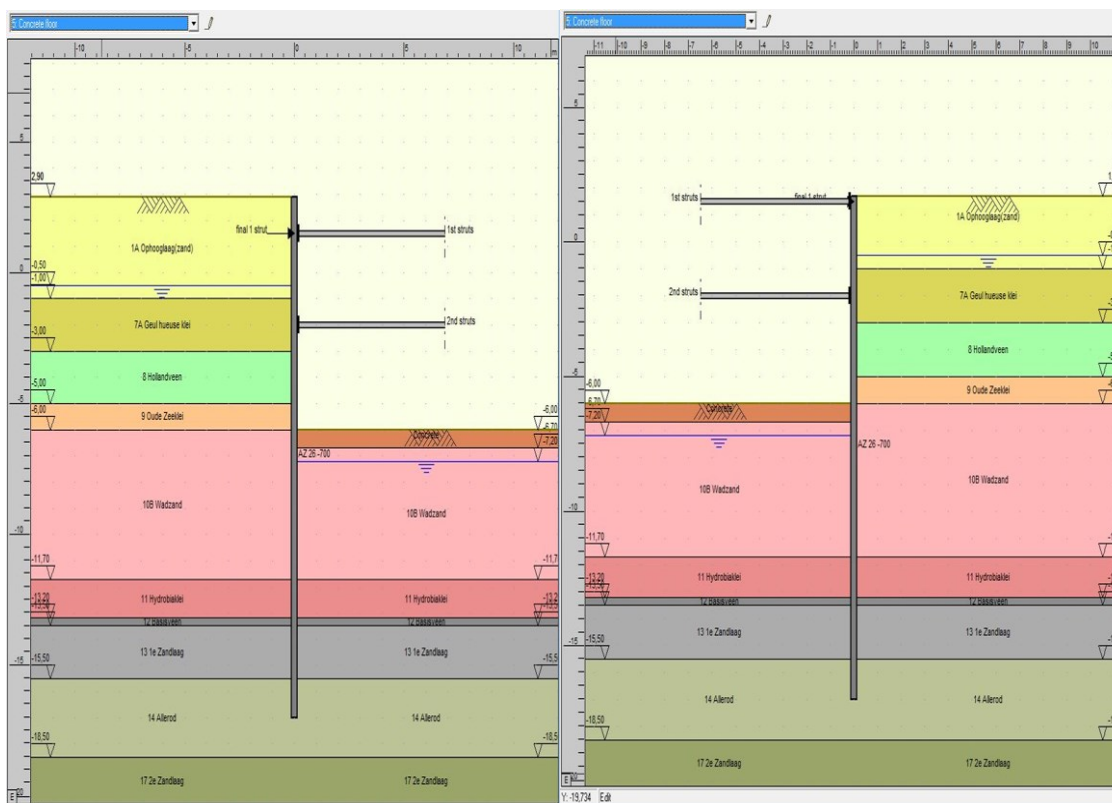


Figure 4-1 cross-section of full excavation on left and right side of excavation pit

The entire model consists of six stages: initial, excavation to 1st struts, excavation to 2nd struts, full excavation, construct concrete floor and removal of 2nd struts. The whole sequence of spring model is shown in Appendix C. The stage overview is shown in Figure 4-2.

	Stage 1	Stage 2	Stage 3	Stage 4	Stage 5	Stage 6
Name	Initial stage	Install of 1st struts	Excavation to 2nd strut level	Full excavation	Concrete floor	Removal of strut
Passive side	D-Sheet Piling determined	D-Sheet Piling determined	D-Sheet Piling determined	D-Sheet Piling determined	D-Sheet Piling determined	D-Sheet Piling determined
Methods						
Left	Ka, Ko, Kp	Ka, Ko, Kp	Ka, Ko, Kp	Ka, Ko, Kp	Ka, Ko, Kp	Ka, Ko, Kp
Right	Ka, Ko, Kp	Ka, Ko, Kp	Ka, Ko, Kp	Ka, Ko, Kp	Ka, Ko, Kp	Ka, Ko, Kp
Water levels						
Left	Initial	Initial	Initial	Initial	Initial	Initial
Right	Initial	Initial	Dewater full	Dewater full	Dewater full	Dewater full
Surfaces						
Left	Initial	Initial	Initial	Initial	Initial	Initial
Right	Initial	1st strut	2nd strut	Full excavation	Concrete	Concrete
Soil profiles						
Left	Initial	Initial	Initial	Excavation let	Excavation let	Excavation let
Right	Initial	Initial	Initial	Excavation right	Concrete	Concrete
Anchors						
Pre-tensioning forces [kN/m']						
Struts						
1st struts						
2nd struts						
Pre-compressions [kN/m']						
1st struts						
2nd struts						
Spring supports						
Rigid supports						
Uniform loads						
Surcharges left						
Surcharges right						
Horizontal Forces						
1 ex 1 strut						
2 ex 1 strut						
2 ex 2 strut						
full ex 1 strut						
full ex 2 strut						
final 1 strut						
Moments						
Normal Forces						

Figure 4-2 Stage overview for D-Sheet piling

The settings regarding the struts, the surface level and the pore pressure are displayed in Figure 4-2. In D-Sheet piling, the excavation of soil is simulated as different surface level. For this project, the surface level named 1st struts and 2nd struts are the excavation to the depth that is half metre below the 1st and 2nd struts respectively. Full excavation as the name tells, means excavate all the way to the bottom of the building pit. At last the concrete level is the surface level after the construction of concrete layer.

The water level simulates the drainage in the building pit. The water level in this project is designed to be half metre lower than the bottom of the building pit. The pore pressure change in soils due to dewatering cannot be automatically interpolated in D-Sheet piling. So the pore pressure has to be calculated by hand and added to the model with different soil profile.

In order to simulate the asymmetric domain for this project, additional force has to be added to the struts. There are two major ways to add this force. One is to add springs at the struts to simulate the extra lateral force. The deformation of springs on both sides of excavation pit requires testing until the lateral forces on both sides reach equilibrium. Another way is to add lateral force directly at the struts level. But the force needs to be calculated either by hand or another computer program. In this project, the second method was used. The extra force was checked in PLAXIS 2D and then added to D-Sheet piling files.

4.2.2. Soil properties

The soil profile was derived from the in-situ soil investigation introduced in Chapter 2. According to the manual, the earth pressure coefficient for clay and peat is Muller-Breslau (straight slip surfaces), and Kotter (curved slip surfaces) for sand layer. The pore pressures are added manually when the

water level is lowered within the excavation zone. An example of soil material input is shown in *Figure 4-3*. The physical properties of soils used in D-Sheet piling model are shown in *Figure 4-4*.

Figure 4-3 Soil materials input in D-Sheet piling

Layer name	Level [m]	Unit weight		Cohesion [kN/m ²]	Friction angle phi [deg]	Delta friction angle [deg]
		Unsat [kN/m ³]	Sat [kN/m ³]			
1A Ophooglaag...	2,90	17,00	19,00	0,00	28,00	9,30
7A Geul hueus...	-1,00	13,60	13,60	6,00	21,00	14,00
8 Hollandveen	-3,00	10,20	10,20	5,00	17,00	0,00
9 Oude Zeeklei	-5,00	16,20	16,20	7,00	25,00	16,70
10B Wadzand	-6,00	15,80	17,80	2,00	27,00	9,00
11 Hydrobiaklei	-11,70	15,20	15,20	8,00	27,00	18,00
12 Basisveen	-13,20	11,70	11,70	6,00	18,00	0,00
13 1e Zandlaag	-13,50	18,00	20,00	0,00	32,00	16,00
14 Allerod	-15,50	18,50	18,50	3,00	28,00	9,30
17 2e Zandlaag	-18,50	18,00	20,00	0,00	32,00	16,00

Figure 4-4 Soil properties in D-Sheet piling

4.2.3. Calculation and test results

For the calculation in D-Sheet piling, the program provides several options in corresponds to different codes applied and different situation needed (optimization of sheet pile length, stability check, verify sheet piling and etc.). This model only uses the standard calculation, since the design of sheet pile wall is already determined and the focus of the thesis is on finite element model. The D-Sheet piling can automatically generate a calculation report, which summarises the displacement and forces per stage.

Stage no.	Stage name	Displacement [mm]	Moment [kNm]	Shear force [kN]	Mob. perc. moment [%]	Mob. perc. resistance [%]	Vertical balance
1	Initial stage	0,0	0,0	0,0	0,0	14,8	---
2	Install of 1st struts	5,4	-24,3	-18,6	0,0	17,1	---
3	Excavation to 2...	21,8	231,6	96,1	26,1	29,0	---
4	Full excavation	66,7	451,4	302,7	0,0	81,7	---
5	Concrete floor	66,7	451,4	303,2	0,0	10,1	---
6	Removal of strut	64,0	340,9	-188,6	9,4	10,7	---
Max		66,7	451,4	303,2	26,1	81,7	---

Figure 4-5 Summary of max displacement and forces on left side

Stage no.	Stage name	Displacement [mm]	Moment [kNm]	Shear force [kN]	Mob. perc. moment [%]	Mob. perc. resistance [%]	Vertical balance
1	Initial stage	0,0	0,0	0,0	0,0	14,4	---
2	Install of 1st struts	0,9	-11,8	-11,8	0,0	14,6	---
3	Excavation to 2...	-9,6	-79,2	41,5	23,6	25,7	---
4	Full excavation	-47,5	-380,8	-254,5	0,0	75,5	---
5	Concrete floor	-47,1	-341,6	-191,9	0,0	10,4	---
6	Removal of strut	-45,3	-332,4	161,3	9,1	10,6	---
Max		-47,5	-380,8	-254,5	23,6	75,5	---

Figure 4-6 Summary of max displacement and forces on right side

The summaries of maxima per stage are shown in *Figure 4-5* and *Figure 4-6*. Judging by the excavation depth, the maximum deflections and maximum bending moments of sheet pile walls on both sides of the excavation pits are acceptable. In reality, the deflection of sheet pile wall is directly related to the settlement of surrounding area. So the tolerance for the bending of sheet pile is often determined by the surrounding area. But as a rule of thumb, 70mm is about the deflection that is expected according to the dimension of this sheet pile wall.

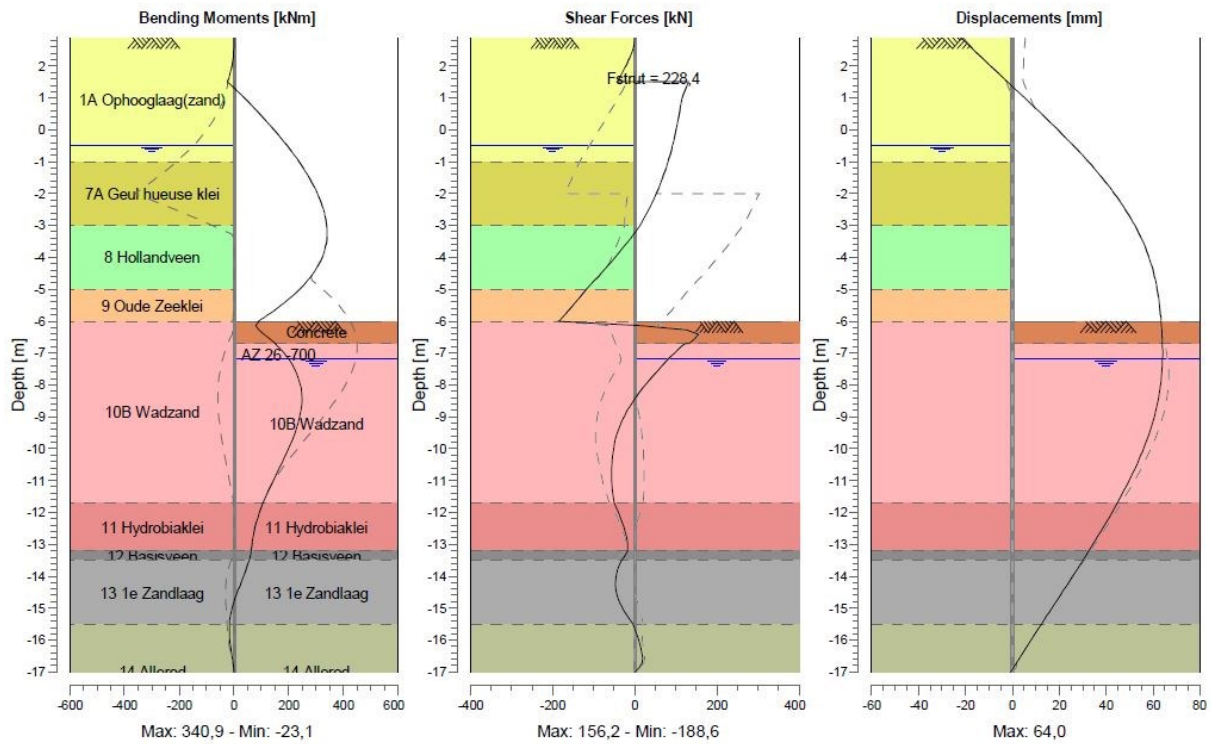


Figure 4-7 Charts of Moments, Forces and Displacements on left side

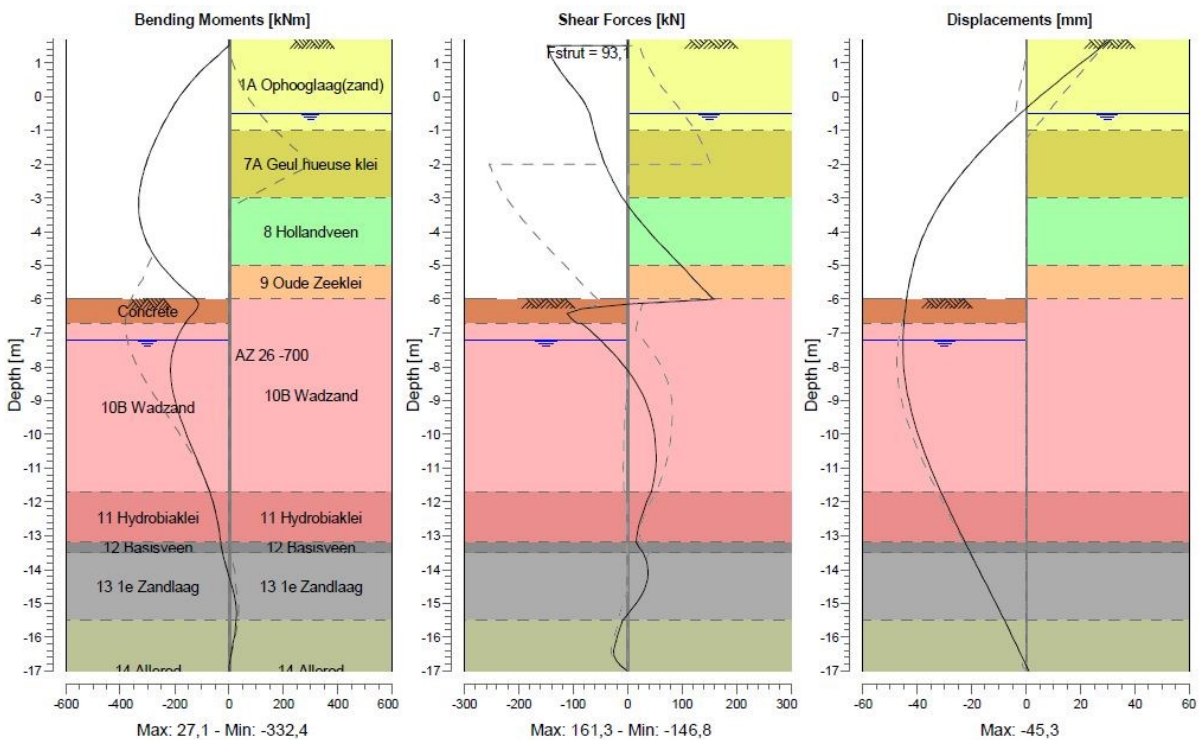


Figure 4-8 Charts of Moments, Forces and Displacements on right side

The stress and displacement distribution on the last stages are presented in details in *Figure 4-7* and *Figure 4-8*. The sheet pile wall is being pushed inward into the building pit due to the excavation in the building pit. The struts and concrete floor provide lateral support on sheet pile wall to balance the soil pressure and reduce the deflection. The maximum deflections are near the bottom of the

building pit. The maximum deflection on right side is partly because the surface level on right side is lower than left side, but also because extra lateral force is added at struts. The sheet pile wall on the right side especially the top side is being pushed into the soil due to height difference at surface level.

In general, the maximum bending moments took place in between the 1st strut and the bottom of building pit. According to the maximum bending moments in *Figure 4-7* and *Figure 4-8*, the excavation design was well optimized as the maximum bending moments in both sides of retaining wall are very close. As introduced in Section 2.3.2, the building material for excavation pit, the maximum bending moments AZ-26 can handle is ranging from 600 to 1100 kNm/m. Thus the bending moment results shown in D-Sheet piling calculation is acceptable.

4.3. 2D FEM model (PLAXIS 2D)

4.3.1. Model set-up and calculation stages

One of the advantages of PLAXIS model is that the program is capable of simulating the asymmetrical model in one piece. It provides more realistic response on real time soil structure interaction. The cross-section is based on the excavation pit design introduced in section 3.3.1. The soil profile is the same as the one used in D-Sheet piling program, so that the results are comparable. The cross-section and soil profile are illustrated in *Figure 4-9*.

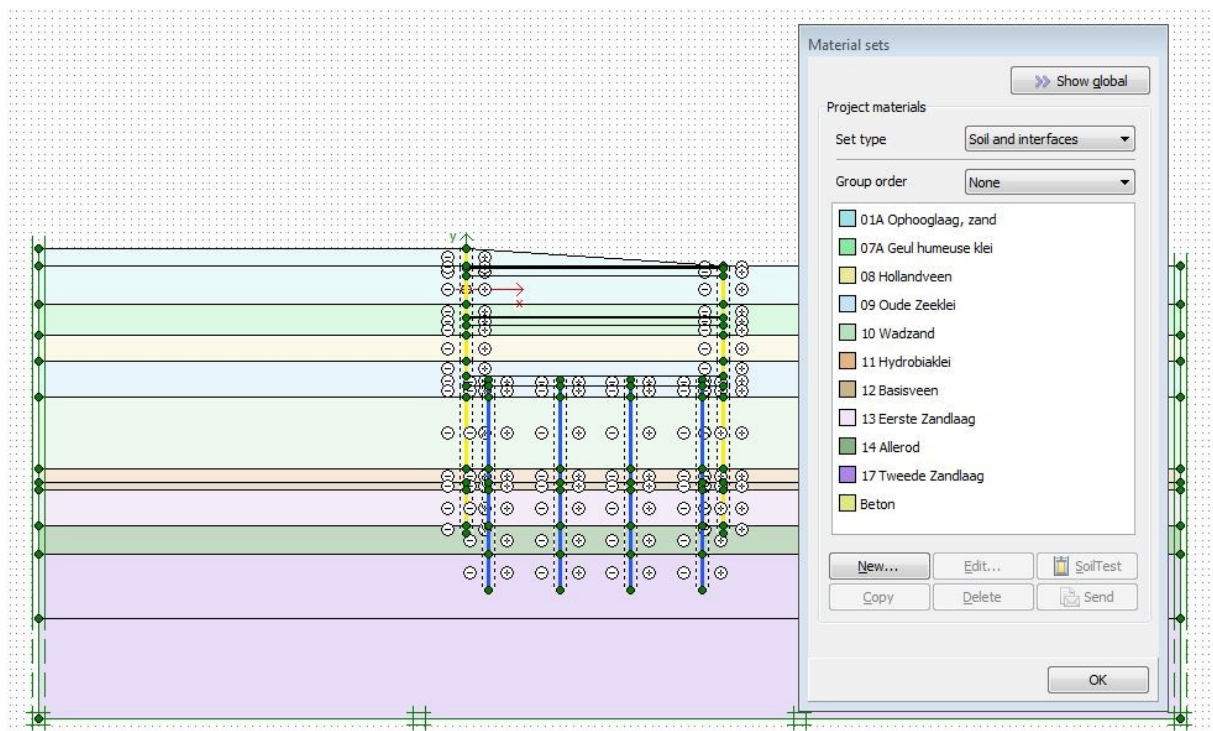


Figure 4-9 Cross-section and soil profile for PLAXIS 2D model

As for the calculation stages, it's the same six stages as used in D-Sheet piling. But the pore pressure can be interpolated in clay layers in PLAXIS model. Thus there is no need to calculate the pore pressure manually. The calculation stages are highlighted in *Figure 4-10*. The water conditions are set individually at each stage. In top sand layers, the phreatic level is -0.5m NAP. The water table for deep sand layers is -2m NAP. For the clay layers, the permeability is very low so that these layers are considered impermeable. The water condition is interpolated from adjacent layers.

Identification	Phase no.	Start from	Calculation	Loading input	Pore pressure	Time	Stage	Water	First	Last
✓ Initial	0	N/A	K0 procedure	Unassigned	Phreatic	0,00 day	L 0	W 0	1	1
✓ Sheet pile wall a...	2	0	Plastic	Staged construction	Phreatic	0,00 day	L 2	W 2	2	7
✓ 1st struts	4	2	Plastic	Staged construction	Phreatic	0,00 day	L 4	W 4	8	13
✓ 2nd struts	5	4	Plastic	Staged construction	Phreatic	0,00 day	L 5	W 5	14	27
✓ Full excavation	6	5	Plastic	Staged construction	Phreatic	0,00 day	L 6	W 6	28	49
✓ Concrete floor	7	6	Plastic	Staged construction	Phreatic	0,00 day	L 7	W 7	50	52
✓ Remove 2nd struts	8	7	Plastic	Staged construction	Phreatic	0,00 day	L 8	W 8	53	57

Figure 4-10 Calculation stages for PLAXIS 2D model

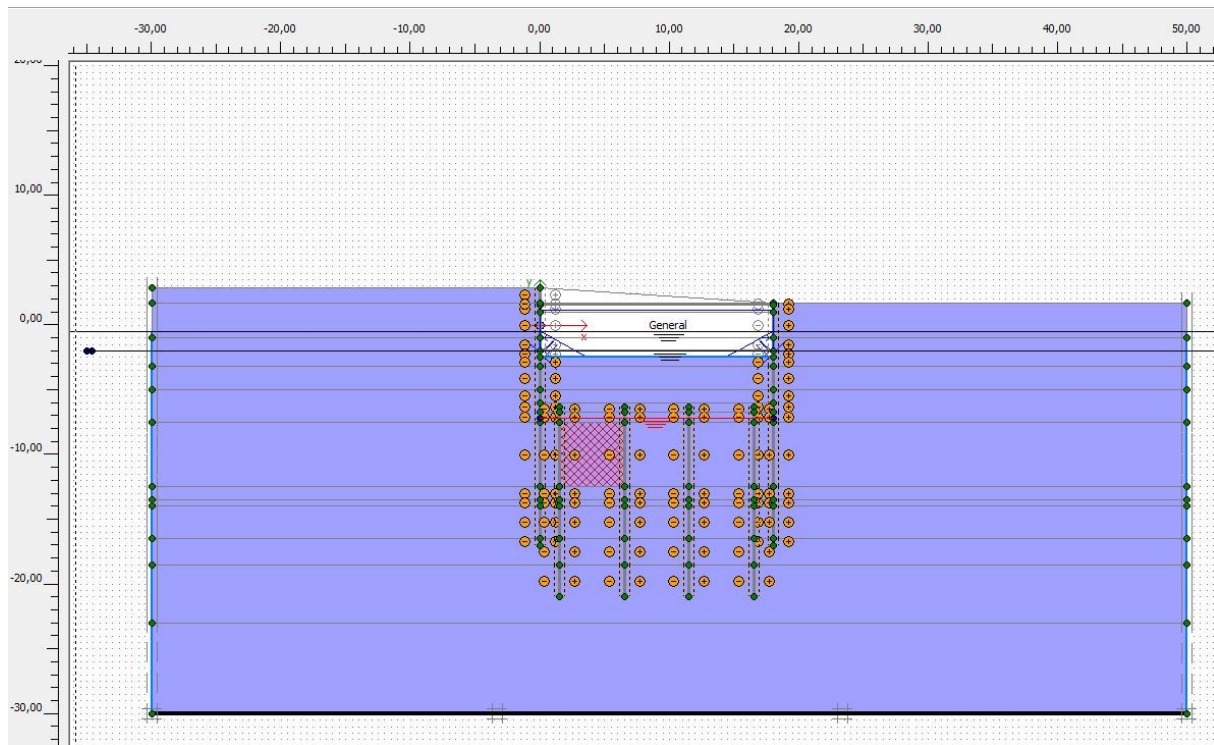


Figure 4-11 Water condition for the excavation phase

The water condition set up is shown in *Figure 4-11*. This is taken when the excavation is at the 2nd struts level. The water level in the building pit is already drained till half metre below the bottom of the building pit. The two black horizontal lines across the whole domain represent the general water level for top soil layers and deep sand layers respectively. The interfaces in the building pit were deactivated due to the excavation. The red line near the top of the piles represents the water level inside the building pit. It is highlighted in red because the sand cluster shaded in red is selected. This function makes it very easy to check the water level for any soil layer.

4.3.2. Mesh set-up

One different set up in PLAXIS model compared to D-Sheet piling is that the mesh for finite elements can be optimized locally. Optimization of mesh in finite elements means that the area worth investigating receives more elements, and area requires less focus gets fewer elements. The area to be investigated would be approximated properly without sacrificing too much calculation time. The mesh for this excavation model is shown in *Figure 4-12*.

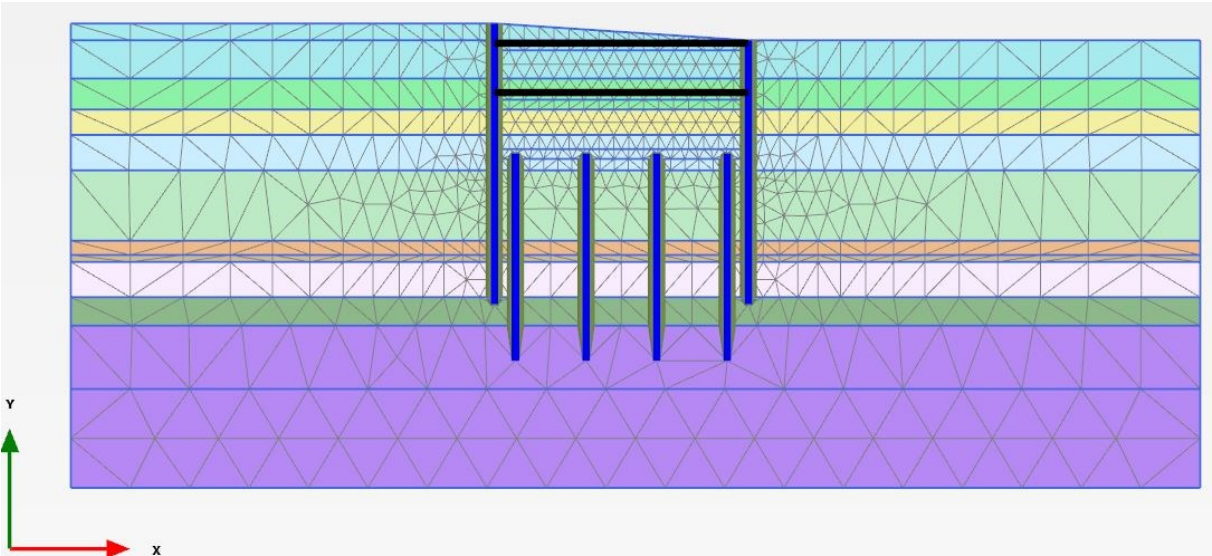


Figure 4-12 Mesh overview for PLAXIS 2D model

4.3.3. Results

The deformed mesh in the last calculation stage is shown in Figure 4-13. The scale of deformation is exaggerated by 50 times to highlight the area that deforms most, because the maximum deflection of sheet pile wall is around 70mm over the height of almost 10m. According to this figure, the whole structure is pushed towards right side due to the height difference of surface level. The maximum deflection and bending moments are further examined.

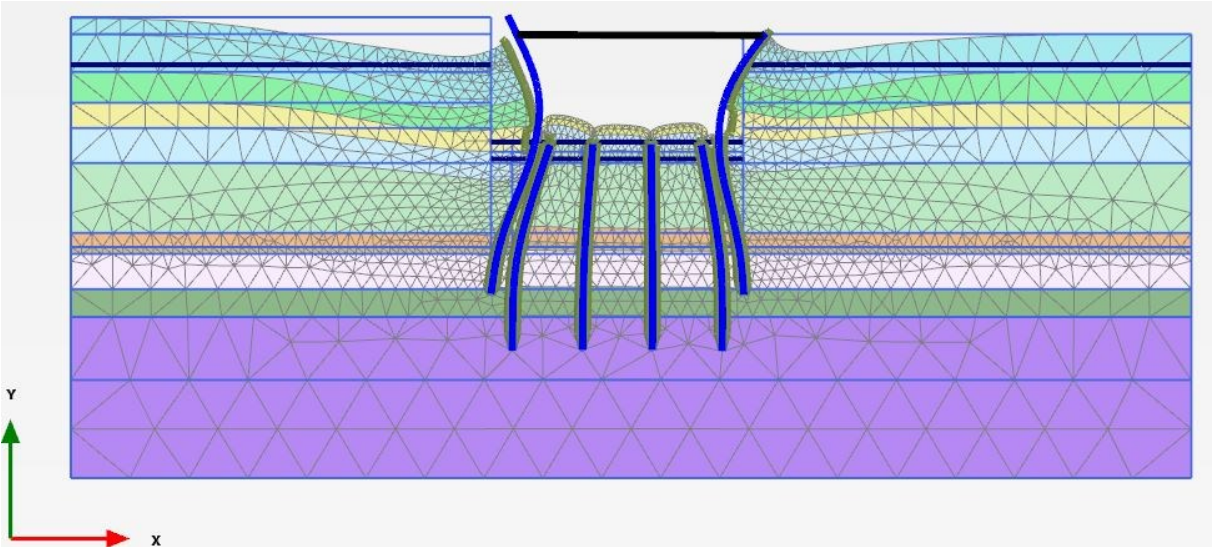


Figure 4-13 Deformed mesh in the last calculation stage

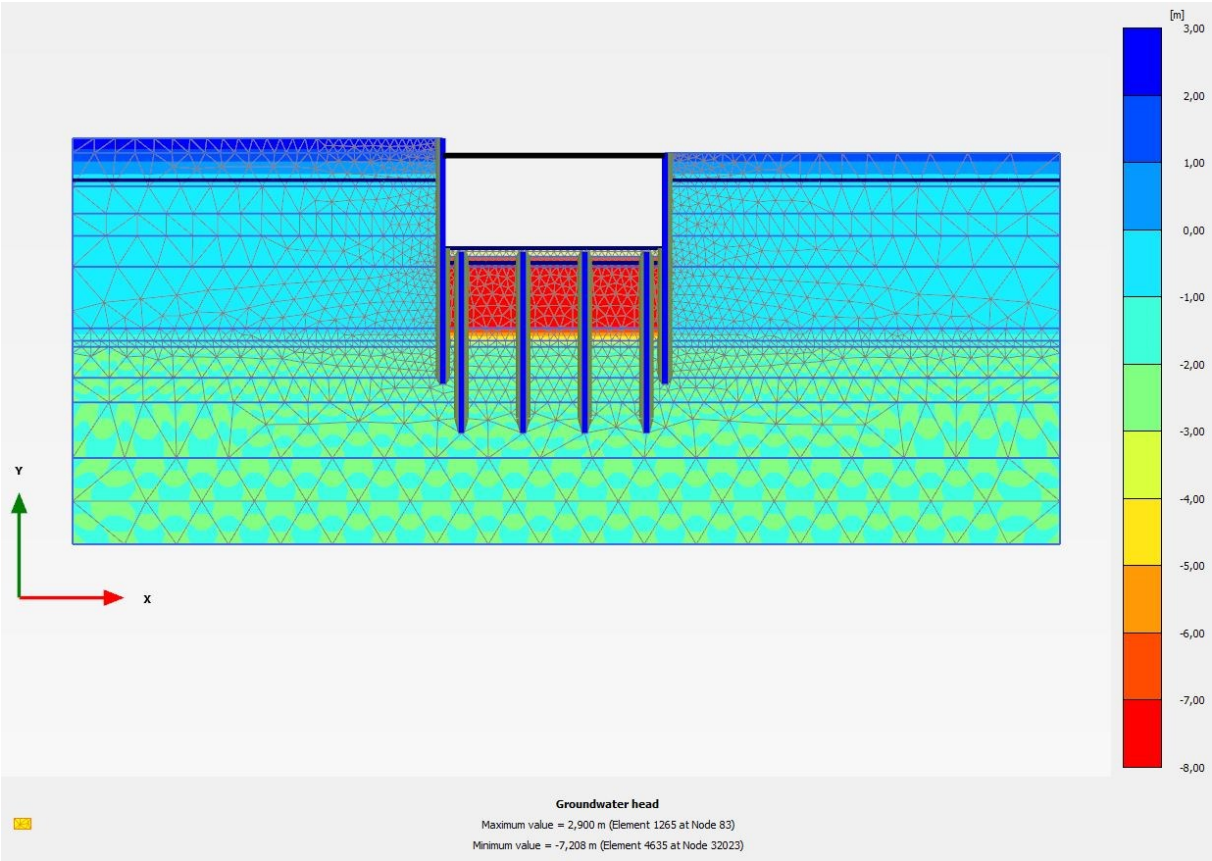


Figure 4-14 Ground water head in the last phase

The ground water head in the last phase is shown in Figure 4-14. According to the figure, the ground water set up in all clusters is correct. The soil in the building pit is in red because the water in the pit was drained till -7.2m NAP. It is also clear the read that the minimum value shown below the graph corresponds with the drainage setting. The soil around the sheet pile walls is generally in light blue, as the general ground water level is -0.5m NAP. The change of colour on top soil layers represents the gradient of water level. The colour in deep soil layer is different, because the water level in deep sand layer is -2.0m NAP instead of -0.5m NAP.

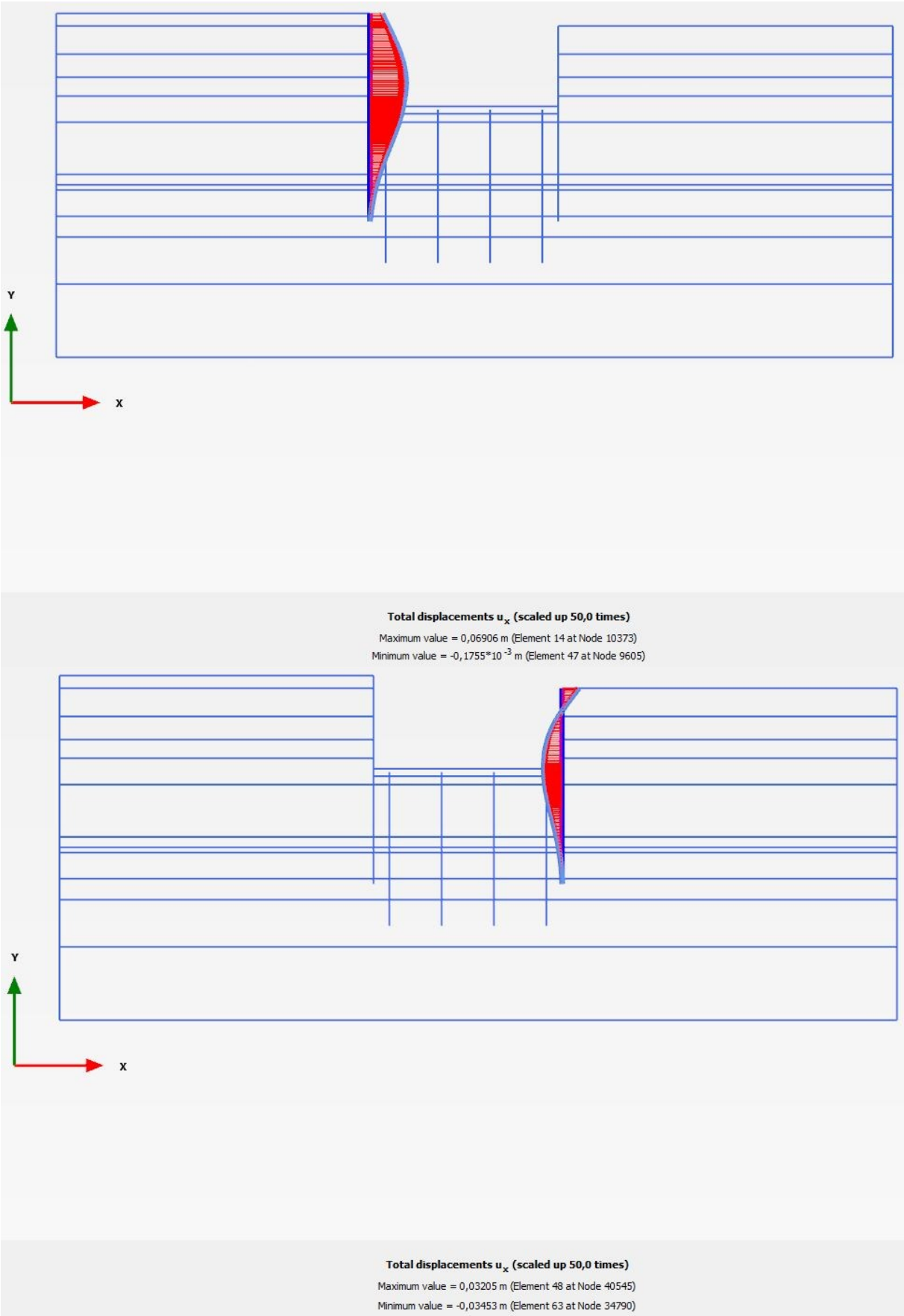


Figure 4-15 Lateral displacement on both sides of excavation pit

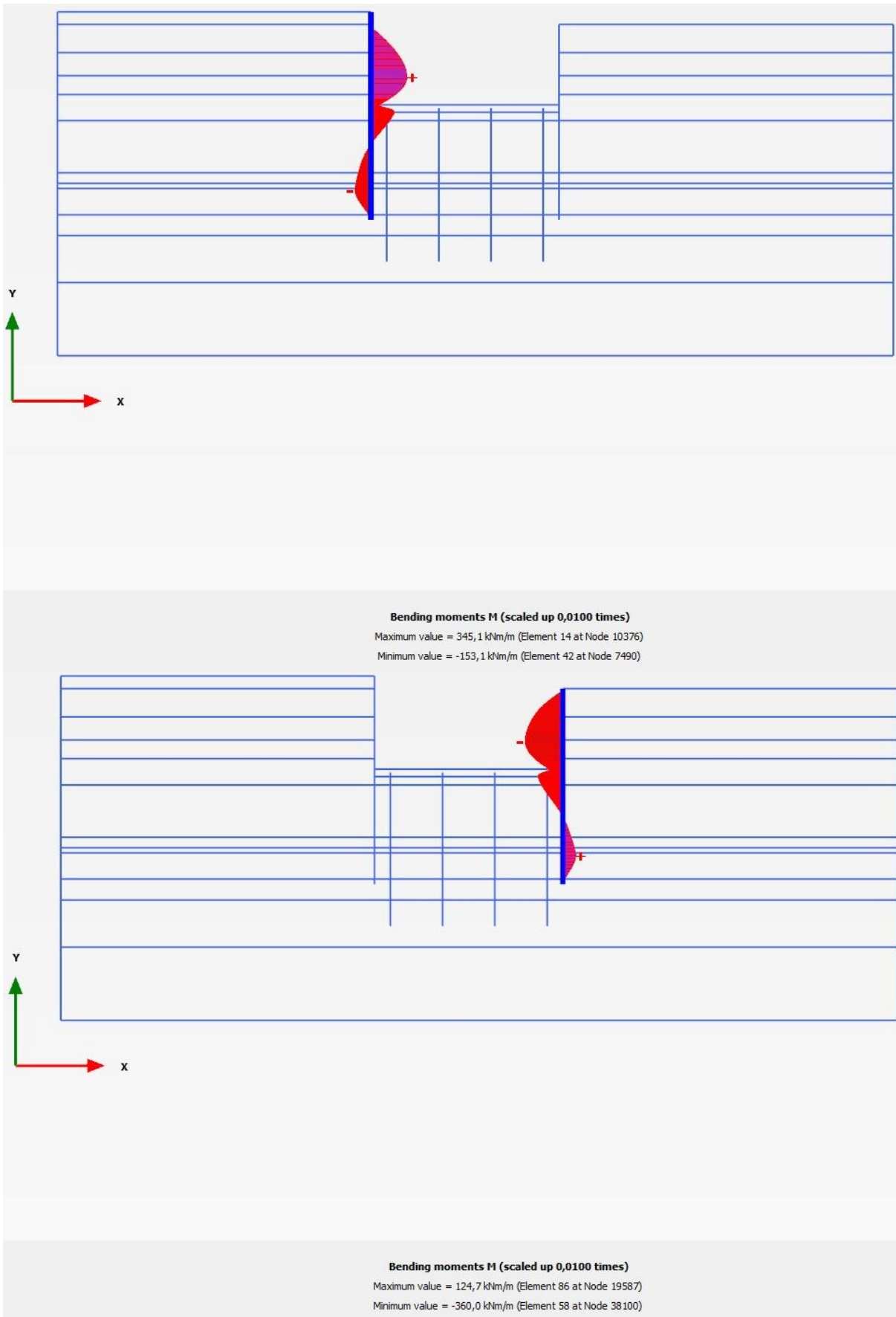


Figure 4-16 Bending moment on both sides of excavation pit

The charts of lateral displacements and bending moments for both sides of sheet pile wall are presented in *Figure 4-15* and *Figure 4-16*. The difference of maximum deflection is caused by the height difference, as it was explained in D-Sheet piling section. As it was observed in *Figure 4-13*, the whole retaining structure on both sides are pushed towards right side. This is the reason why the deflection outline is different.

4.3.4. Comparison of results between PLAXIS 2D and D-Sheet piling

The most important and comparable engineering values for comparing this excavation simulation in these two different software are the displacements and bending moments for the retaining structure after all excavation process. The maximum displacements and bending moments from PLAXIS 2D and D-Sheet piling are highlighted in *Table 4-1*. According to *Table 4-1*, the displacement and bending moments for sheet pile wall on the left side of the excavation pit are almost the same. However, the displacements and bending moments on right side are bit different. It is probably because of the horizontal line loads added at the struts that are not accurate enough. Because of the asymmetrical cross-section, the load from the left has to transfer to the right through the struts. The horizontal forces thus affect the final result on displacements as well as bending moments.

	Displacement (mm)		Bending moment (kNm)	
	Left	Right	Left	Right
PLAXIS 2D	69,1	34,5	345,1	360,0
D-Sheet piling	64,0	45,3	340,9	332,4

Table 4-1 Comparison for maxima in last excavation stage

The *Figure 4-7* and *Figure 4-8* in D-Sheet piling section, and *Figure 4-15* and *Figure 4-16* in PLAXIS 2D section show the results of deflections and bending moments in detail. Judging by these figures, the outlines are very similar in different 2D programs. But one thing worth noting that, although the maximum bending moments in two programs are almost the same, the outline at lower part of the sheet pile walls and maximum negative values are quite different. The bending moment for low part of sheet pile wall is overlooked in spring model.

The main advantage of applying PLAXIS 2D rather than D-Sheet piling is that PLAXIS can model the reaction from soil as well as the structure, while D-Sheet piling is only capable of analysing the retaining structure itself. This is especially important when the project locates in city centre, where the settlement of surrounding area needs to be as low as possible.

However, the model in PLAXIS 2D is more difficult to make because the required parameters are way more than D-Sheet piling. Thus the requirement for soil investigation is higher. PLAXIS model gives a more comprehensive outcome, but also requires more engineering experience to analyse the results.

In general the results from two different programs correspond with each other. Thus the parameters and model set up from PLAXIS 2D are accurate and stable enough to apply to PLAXIS 3D model. The results from PLAXIS 3D will be compared with the results from 2D.

4.4. Conclusion of 2D modelling

In terms of the bending of sheet pile wall, the results from both D-Sheet piling and PLAXIS 2D are at similar level. The main difference was caused by the asymmetrical domain of investigation. In PLAXIS 2D, the software is capable of simulating the asymmetrical domain automatically. But in D-Sheet piling, the lateral force caused by difference of surface level and interpolation of water pressure has to be calculated and added by the analysts. In this case, the lateral force added at struts could be further adjusted to simulate response of sheet pile wall more accurately.

As for applications in deep excavation design, D-Sheet piling is more preferable because the soil parameters required are easier to get compared to PLAXIS, which results in lower cost. With careful testing and adjusting, the interpolation of water level in clay layer and asymmetrical domain can also be solved in D-Sheet piling. The biggest disadvantage for spring model is that the model only simulates the soil structure interaction. It is not able to analyse the deformation of soil itself. In reality, the settlement control for surrounding area can be crucial to the whole project, when the excavation takes place very close to buildings and roads.

For the recommendation of using 2D modelling, it depends on the location and priorities of the project itself. If the project locates in an open area with good local expertise, D-Sheet piling based on the spring model is more preferable due to the relatively low cost for designing. But if the project locates in downtown area, the control of settlement is of high priority. Thorough soil investigation has to be done to eliminate the risk from heterogeneity in soil profile. Thus PLAXIS 2D based on FEM analysis is recommended.

5. 3D modelling of excavation

The 3D modelling section consists of two major parts, namely the standard staged excavation model based on the previous 2D model, and the sequential excavation model. All the models use the same soil profile, structural cross-section and building material, so that the results for deformation and forces are comparable among different models.

5.1 3D Staged excavation model (PLAXIS 3D)

5.1.1 General model set up

The standard staged excavation model is widely used for 3D FEM analysis. As it gives a more realistic simulation of the excavation process, taking into account the 3D effect, without sacrificing too much on the calculation time. This staged excavation model uses the same soil profile and calculation stages so that it is comparable to the 2D models. It is also used as a control group compared to optimized sequential excavation models.

The soil profile is implemented by adding four bore logs in the domain, so that the soil profile as well as the height difference is the same as 2D PLAXIS model. The soil properties used in 3D model are the same as 2D. The soil profile set up is shown in *Figure 5-1*. As it is shown in the figure, the whole domain is assumed to be homogeneous. Although there are different CPT data available, implementing all CPTs in the model will slow down the calculation drastically. And the space between each CPT is still assumed to be changing linearly, which underestimates the risk of sudden change of non-homogeneous layers. Since the size of the excavation pit is not stated in preliminary design, it is estimated to be 50m * 18m by engineering practice. On each direction, there is a 30m non-excavation zone, so that the excavation zone is not influenced by the boundary. The size of the excavation pit is further tested in parametric testing, introduced in next section.

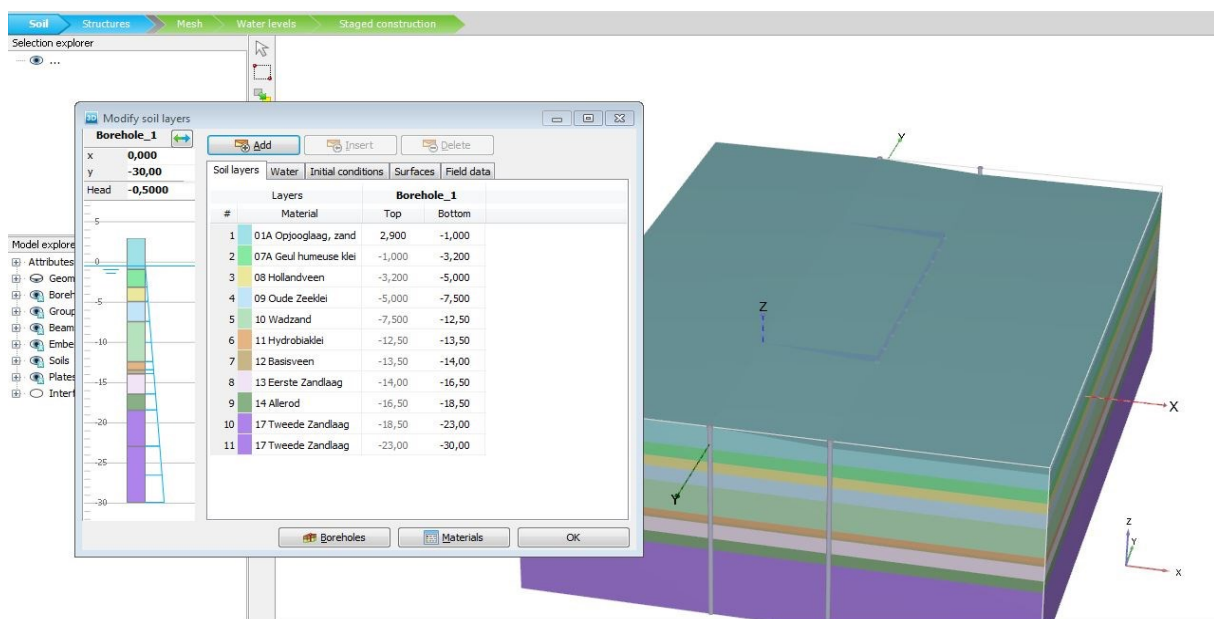


Figure 5-1 Soil profile in PLAXIS 3D model

The excavation zone and all the building elements are added in the structure section in PLAXIS 3D. First the surfaces are created at designed locations, including the sheet pile walls, certain excavation

depth and concrete surface. The sheet pile walls are simulated by creating plates for surfaces. The supporting structure (struts and wailing beams) are approximated with beam elements in PLAXIS 3D. This is one of the significant differences between 2D and 3D FE models. In 2D model, it is assumed as plane strain situation. Instead of beam element, all struts are simulated as node-to-node anchors, wailing beams are not implemented in 2D model. In the latest PLAXIS 2D classic version, it is possible to add embedded pile as well. But the version available at TU Delft does not have this function. So the piles are approximated by plates in 2D model. The structures of the model are shown in *Figure 5-2*. The interfaces between plates and soil and horizontal surfaces created for excavation stages are not shown in this figure.

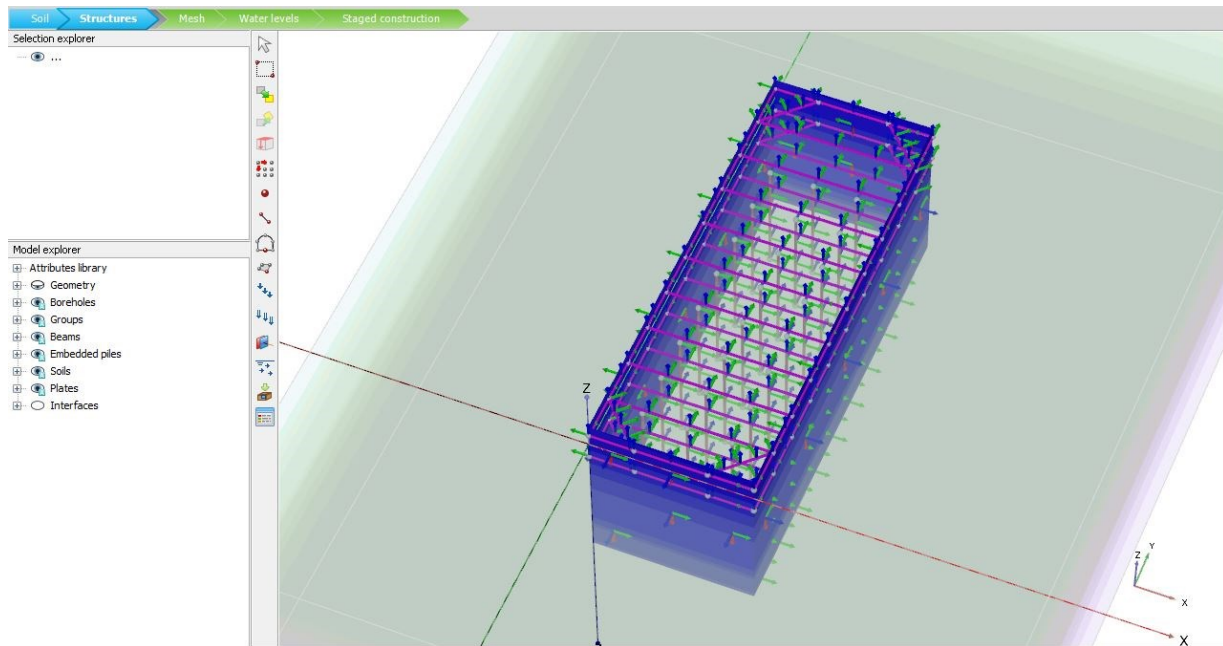


Figure 5-2 structure set up in PLAXIS 3D model

The distance between the struts is 5m. The distance between pile rows is also 5m. This is set according to the preliminary design of Spaarndammertunnel project. But other values for distance between struts were also tested in 3D models. The distance tested were 5m, 8m and 10m. The relationship between the struts distance and the deflection of sheet pile wall is shown in *Table 5-1*. The influence of struts distance is not further explored as it is not the focus of modelling.

Distance between struts	Maximum deflection
5m	69mm
8m	97mm
10m	13mm

Table 5-1 Relationship between the struts distance and the deflection of sheet pile wall

The physical properties of struts and wailing beams are introduced in Chapter 2. The properties of piles, struts and wailing beams are presented in *Figure 5-3*.

Embedded pile - Pile			Beam - Struts 610*20			Beam - Wailing HEB300		
Property	Unit	Value	Property	Unit	Value	Property	Unit	Value
Material set			Material set			Material set		
Identification		Pile	Identification		Struts 610*20	Identification		Wailing HEB300
Comments			Comments			Comments		
Colour		RGB 199, 82, 143	Colour		RGB 220, 0, 251	Colour		RGB 234, 12, 239
Properties			Properties			Properties		
E	kN/m^2	33,80E6	A	m^2	0,03707	A	m^2	0,01500
γ	kN/m^3	24,00	γ	kN/m^3	78,50	γ	kN/m^3	78,50
Pile type		Predefined	Linear		<input checked="" type="checkbox"/>	Linear		<input checked="" type="checkbox"/>
Predefined pile type		Massive circular pile	E	kN/m^2	210,0E6	E	kN/m^2	210,0E6
Diameter	m	0,5080	I_3	m^4	1,615E-3	I_3	m^4	0,08563E-3
A	m^2	0,2027	I_2	m^4	1,615E-3	I_2	m^4	0,2517E-3
I_3	m^4	3,269E-3	Rayleigh α		0,000	Rayleigh α		0,000
I_2	m^4	3,269E-3	Rayleigh β		0,000	Rayleigh β		0,000
Multi-linear skin resistance								
T _{top, max}	kN/m	0,000						
T _{bot, max}	kN/m	0,000						
T _{max}	kN/m	500,0						
Base resistance								
F _{max}	kN	10,00E3						

Figure 5-3 Input properties for piles, struts and wailing beams

5.2.1 Mesh set up

The refinement of the mesh affects the calculation results greatly in FE method. On the other hand, the refinement of the mesh is also closely related to calculation time. A good balance between accuracy and efficiency is the key to the mesh set up. In PLAXIS 3D, mesh is generated automatically with global refinement. But the refinement for elements and soil layers can be changed locally. The refinement used for this model is medium, with locally increased refinement on plates. The overview of mesh set-up is illustrated in Figure 5-4. There is also an individual section discuss the parametrical study on the mesh refinement in section 5.2.2.

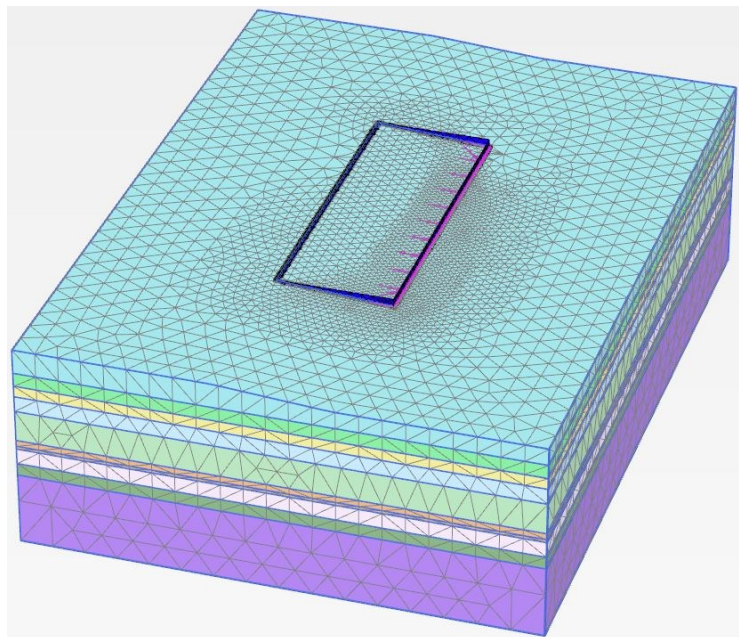


Figure 5-4 Overview of mesh set up in PLAXIS 3D model

5.2.2 Calculation stages and water levels

As mentioned in previous sections, the calculation stages in this 3D staged excavation model are the same as the 2D models: Initial, excavation to 1st struts, excavation to 2nd struts, full excavation, construct concrete floor and removal of 2nd struts. The set up for water levels is similar to PLAXIS 2D. The water levels in excavation zone are set locally in each cluster. Once the excavation reaches 1st strut level, the water level in excavation pit is lowered to -7.2m NAP (0.5m lower than the bottom of the excavation pit). The sequence of water level set up for clusters in excavation is illustrated in *Figure 5-5*. The initial phase, excavation to 1st struts and last phase are shown. The clusters in dark blue are with general water level. The ones in yellow are the clayey layers that the water pressure is interpolated. And the ones in light blue have the local water level (-7.2m NAP in this model). The horizontal blue plates represent different depth of water levels (-0.5m, -2m and -7.3m NAP).

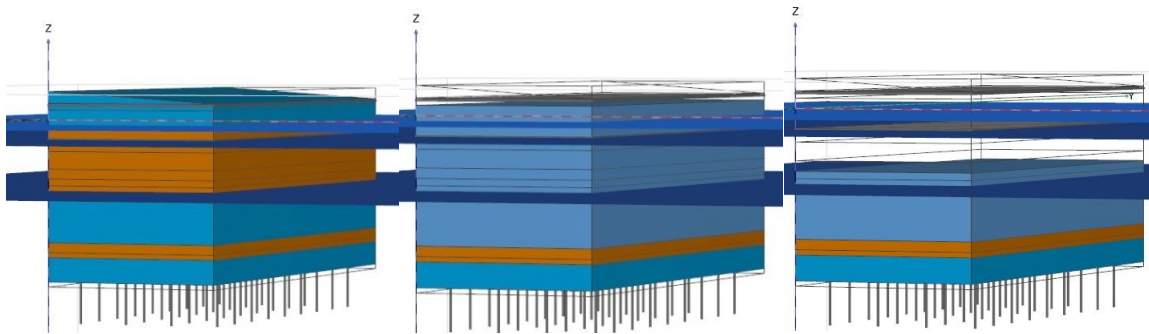


Figure 5-5 Sequence of water level set up

5.2.3 Results

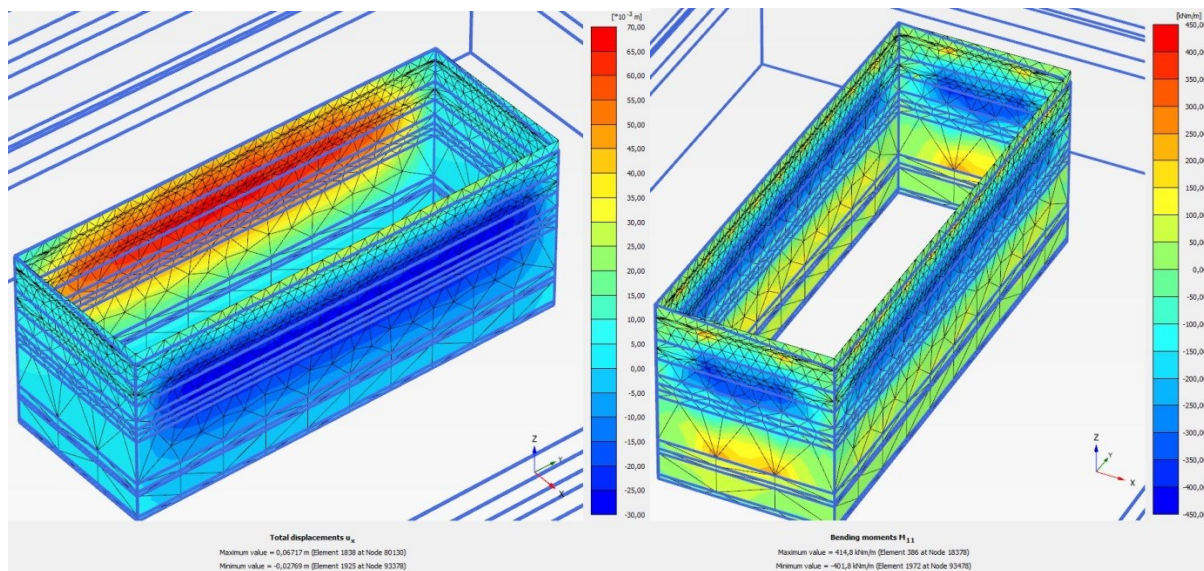


Figure 5-6 Overview of lateral displacement (left) and bending moment M_{11} (right) for the last phase

According to *Figure 5-6*, the maximum lateral deformation and bending moment take place near the middle part of the model. This corresponds with the hypothesis that the corners affect the arching of the retaining walls. The deformation figure also shows clearly that the places where struts exist have lower lateral deformation. Based on *Figure 5-6*, it is reasonable to focus on certain cross-section near the half of the whole excavation pit.

The maximum lateral displacements and bending moments on both sides of sheet pile walls are shown in *Figure 5-7* and *Figure 5-8*. The comparison of results on deformations and bending moments for PLAXIS 2D and 3D model is shown in *Table 5-2*.

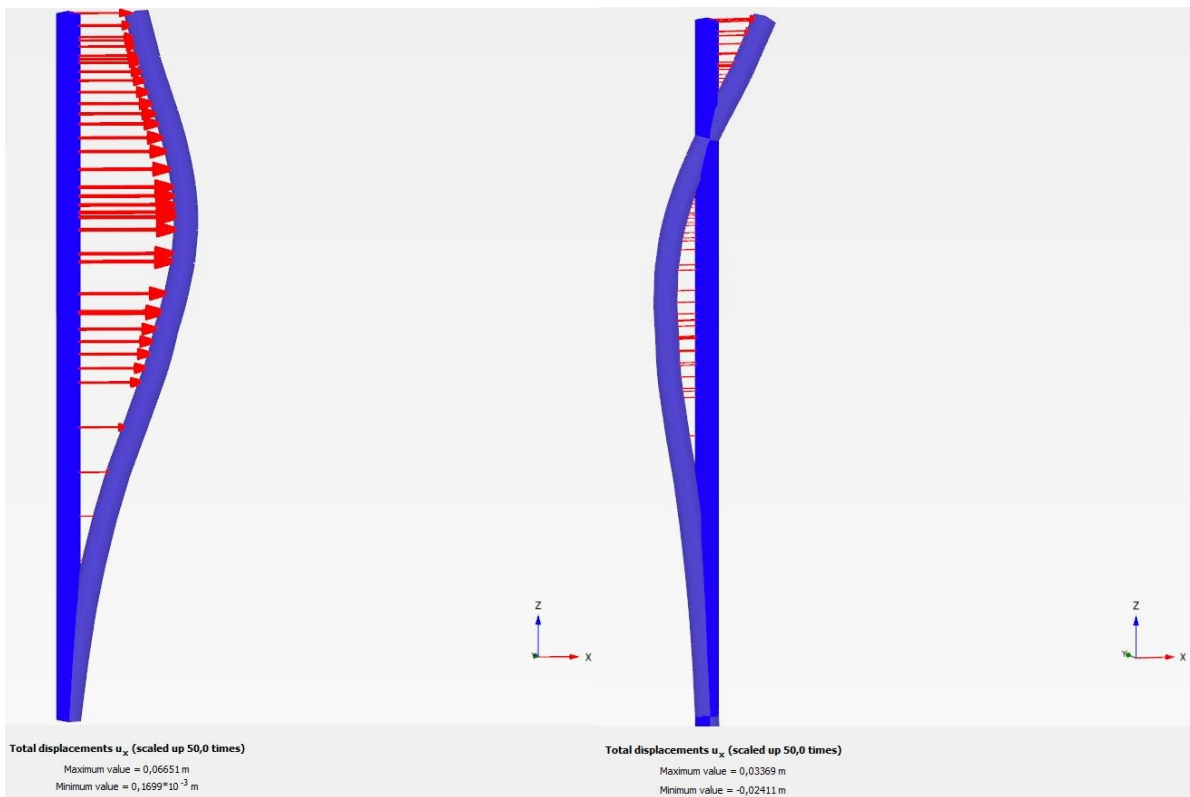


Figure 5-7 Maximum deformation on both sides of excavation pit

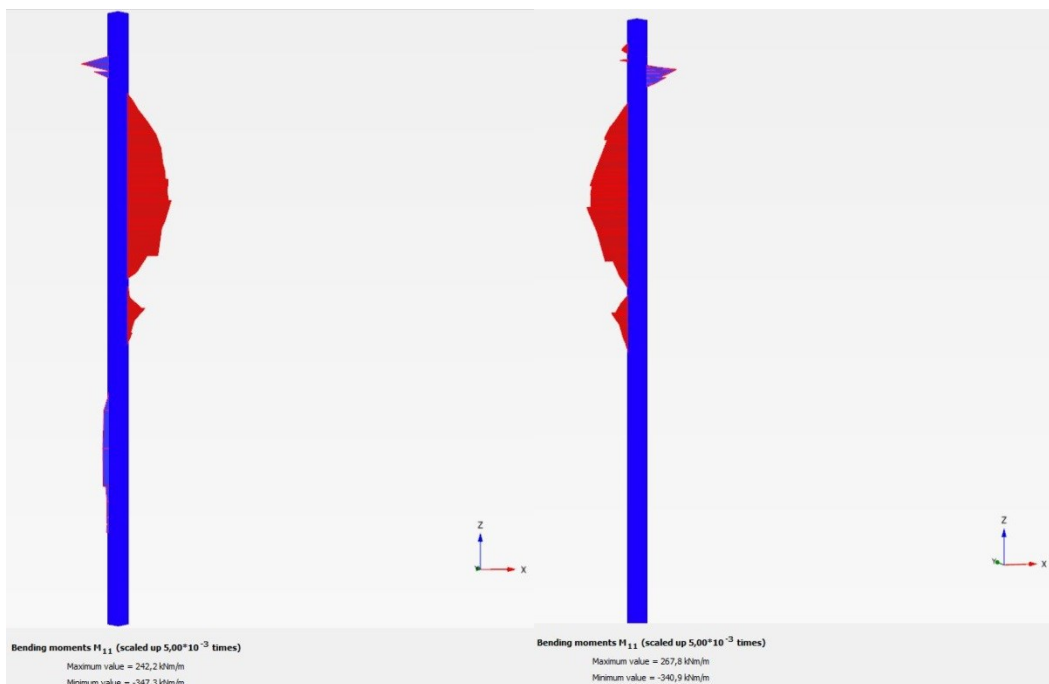


Figure 5-8 Maximum bending moments on both sides of excavation pit

	Displacement (mm)		Bending moment (kNm/m)			
	Left	Right	Left		Right	
			Max	Min	Max	Min
PLAXIS 2D	69,1	34,5	345,1	-153,1	360,0	-124,7
PLAXIS 3D	66,5	33,8	347,3	-242,2	342,6	-296,9

Table 5-2 Comparison of results for PLAXIS 2D and 3D

According to *Table 5-2*, the lateral displacements in PLAXIS 2D and 3D model are very close. The difference can be caused by not enough length and different mesh layout. *Figure 5-9* illustrates the bending moment outline for the sheet pile wall on the left side of the excavation pit. The figure on the left is the front view of the excavation pit from PLAXIS 3D. The one on the right is from PLAXIS 2D. Both figures are on the same scale. It is clear to see that the outline is almost the same below the 1st strut. However, in PLAXIS 2D there are no bending moments above the 1st struts, while in 3D the maximum negative bending moment occurred. And this value is the one that is much higher than 2D in *Table 5-2*.

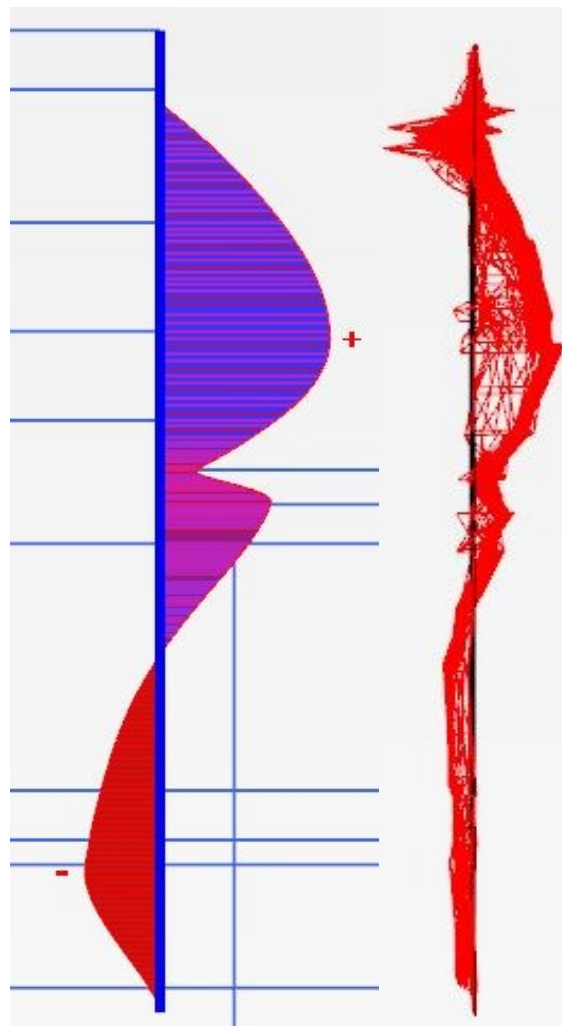


Figure 5-9 Comparison of bending moment contour between PLAXIS 2D (left) and 3D(right)

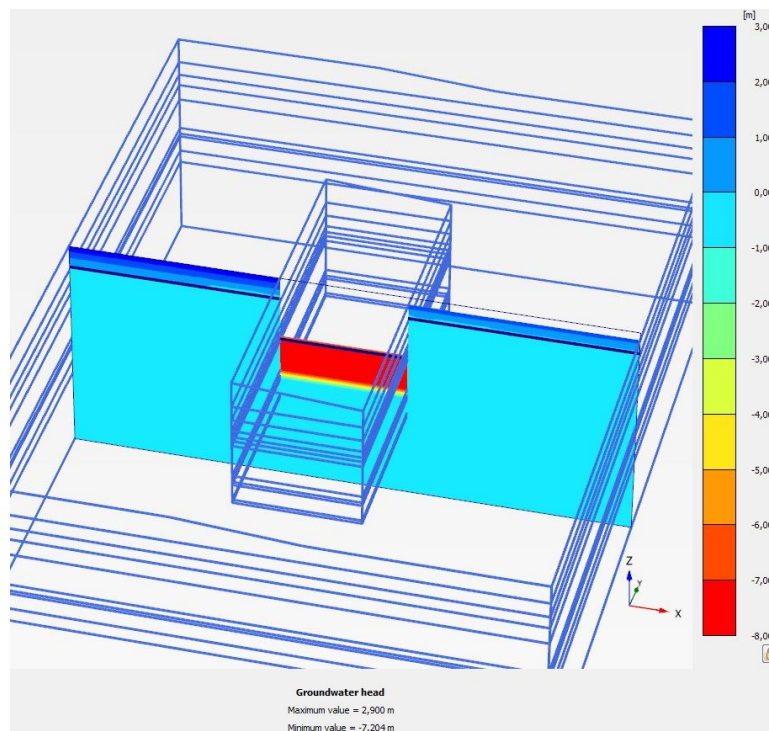


Figure 5-10 Cross-section of water head for the last phase at half of domain

Besides the deformation and inner forces of the retaining structure are checked in PLAXIS output, the stress state and water level are also checked. The water head for the last excavation phase at the half of the excavation zone is displayed in *Figure 5-10*. It is identical to *Figure 4-14*, the water head of last phase in 2D model. This proves that the water level set-up is correct. The influence on the surrounding area is also one of the key investigations for this project. *Figure 5-11* demonstrates the overview of vertical displacement for soil around excavation zone. *Figure 5-12* shows the comparison between 2D and 3D model. According to *Figure 5-12*, the results for vertical movement of soil are almost the same in 2D and 3D models. The difference can be caused by different discretization of the domain.

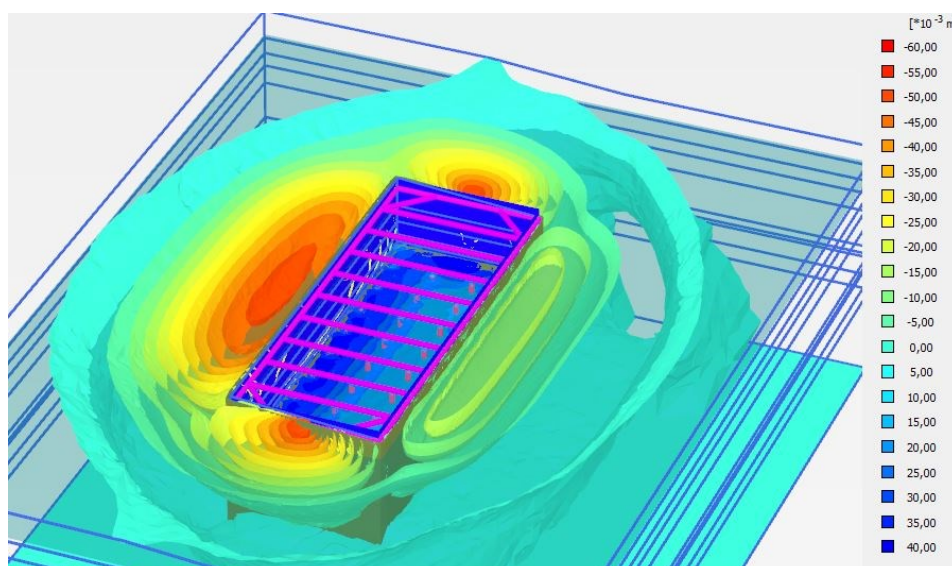
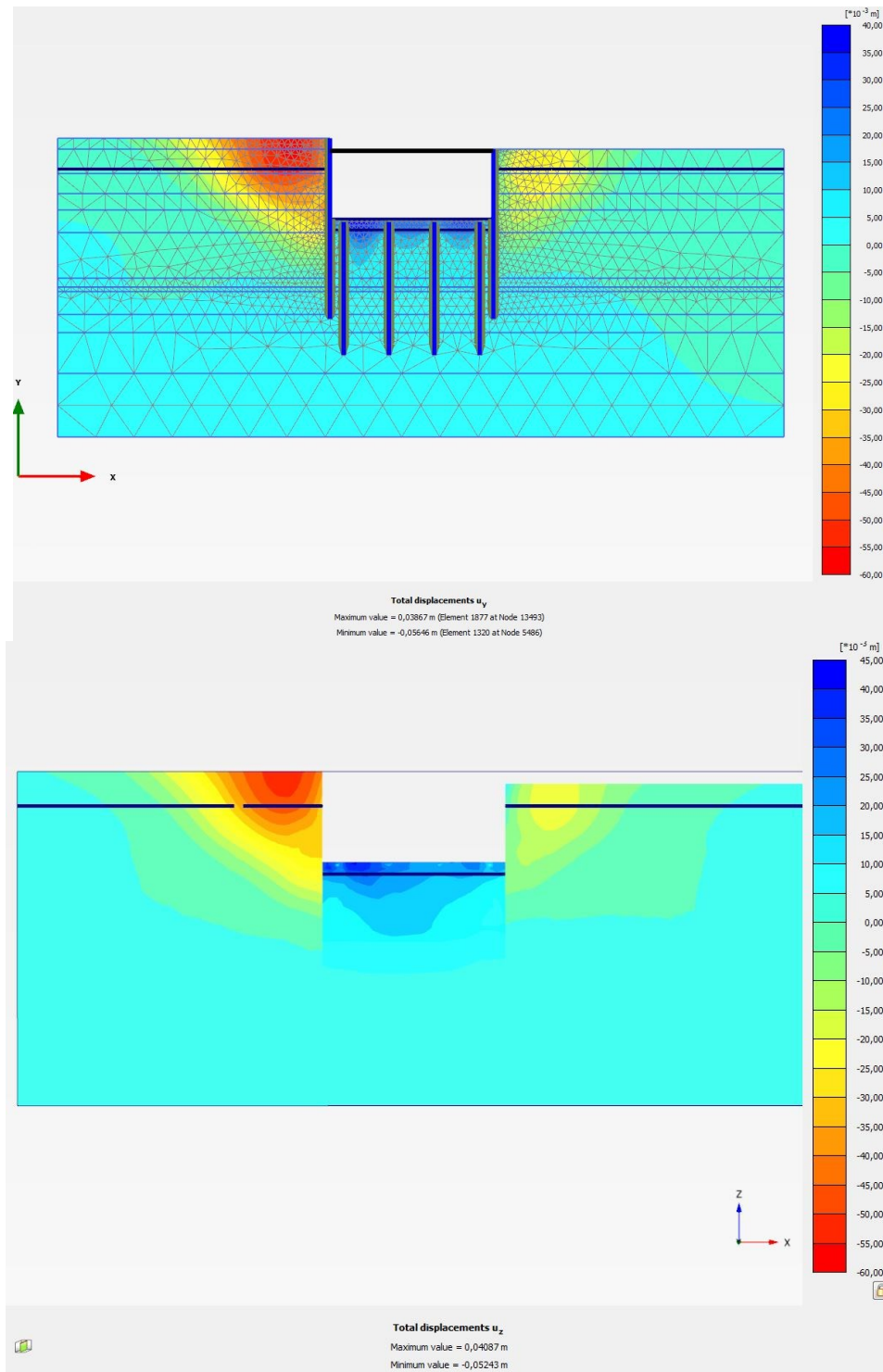


Figure 5-11 Overview of vertical displacement of soil at the last phase



	Maximum value (mm)	Minimum value (mm)
2D	38.7	-56.5
3D	40.9	-52.4

Figure 5-12 Comparison of vertical displacement for soil in 2D (up) and 3D (down) models

The lateral support is also checked and compared between 2D and 3D. The values used for checking lateral support are deformations and normal forces within the struts. Although the struts are modelled as node-to-node anchors instead of beams in 2D, the EA value and L_{space} are set based on material properties used in 3D model. *Table 5-3* shows the normal forces in 1st and 2nd struts in different calculation stages. According to the table, the normal forces in struts correspond with each other in 2D and 3D model. The deformations of the struts are 7mm in both 2D and 3D models.

Calculation stages	2D		3D	
	1st	2nd	1st	2nd
3	607	0	466	0
4	285	1409	286	1363
5	285	1418	288	1372
6	765	0	756	0

Table 5-3 Normal forces within the struts

5.2 Parametric study for 3D staged excavation model

5.2.1 Study on the size of the excavation pit

One of the significant advantages when using 3D finite elements method is the corner effect. In 2D FE model used in this thesis, the model is assumed as infinite long (plane strain). However, the length/width ratio has dramatic influence on the behaviour of the retaining structure. When the pit is not long enough, the maximum displacements and bending moments would be much lower than 2D based calculation, because of the arching of the wall. It is demonstrated in *Figure 5-13*.

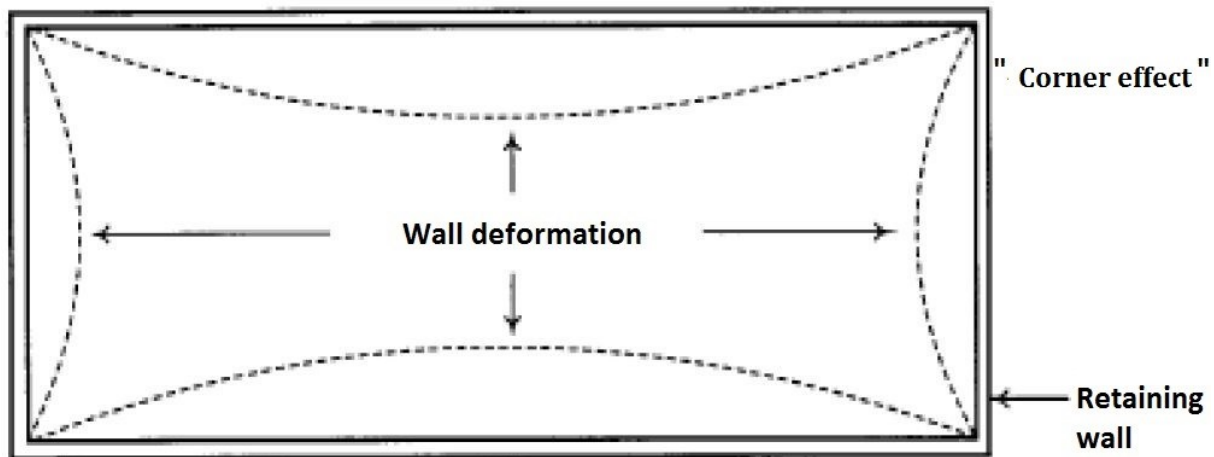


Figure 5-13 Corner effect for 3D modelling

In order to investigate how L/W ratio affects the test results, three sets of test parameters are used: 30m/18m, 50m/18m, and 70m/18m. Since the width is already designed according to the tunnel size, only the length of the pit needs testing. The results of retaining wall displacements and bending moments for different pit length are presented in *Table 5-4*. According to this table, 30m is not long enough that the maximum deflection of sheet pile wall is much below the expectation. The results almost converge when the length is higher than 50m. In reality, for an excavation pit with 18m width, 50m is also a reasonable and often used length. Thus the size chosen for further testing is 50m * 18m. For each model, there is always 30m length of influenced zone around the excavation pit around the excavation zone. The overview of different excavation pit sizes is illustrated in *Figure 5-14*.

	Displacement (mm)		Bending moment (kNm)	
	Left	Right	Left	Right
PLAXIS 2D				
30m	69,1	34,5	345,1	360
50m	55,3	24,6	314,2	384,4
70m	66,5	33,8	347,3	342,6
	67,0	34,2	335,3	345,7

Table 5-4 Comparison of retaining wall displacements and bending moments for different pit length

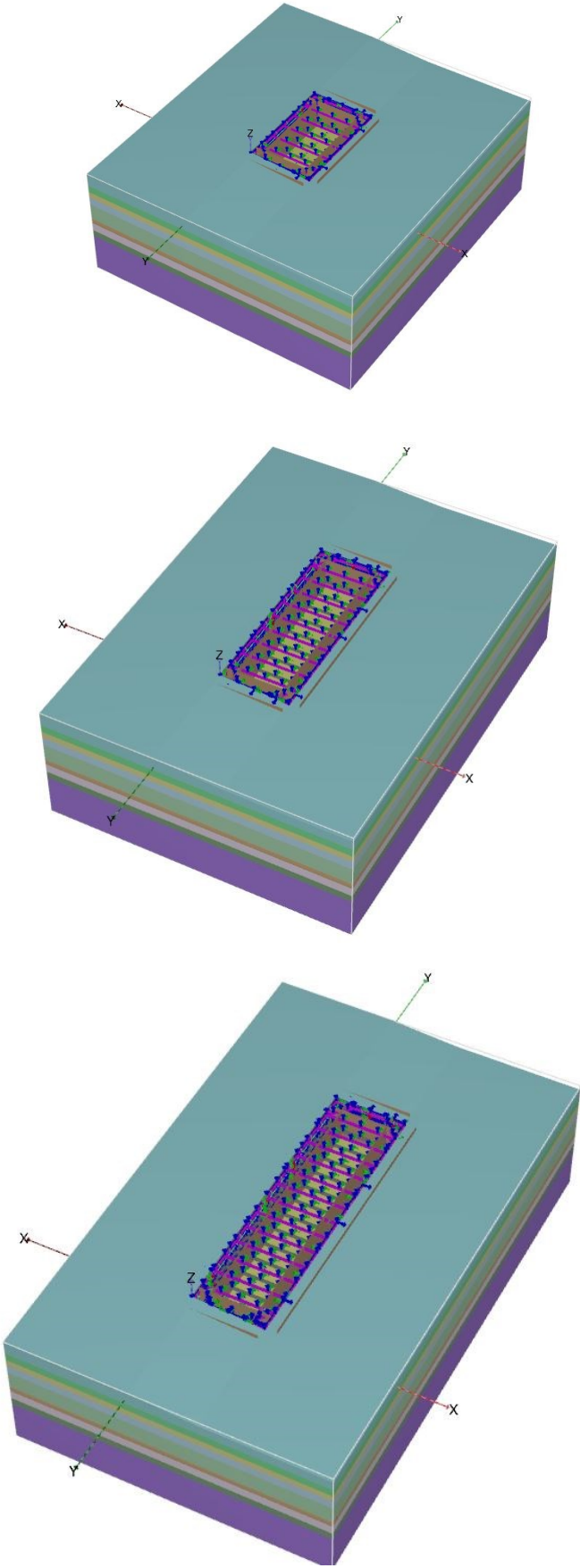


Figure 5-14 Models overview for different testing pit length: 30m, 50m, 70m

5.2.2 Study on the mesh set-up

As mentioned in previous chapters, mesh set-up is one of the key factors in finite element method. The discretization affects the stress distribution in calculations. *Figure 5-15* demonstrates different refinement of mesh set-up from the bottom view of the excavation pit. From left to right, the mesh goes from coarse to medium to refine. The mesh on left gives a quick estimation of the project. But the accuracy is definitely not enough. Since there are places that two piles locate in the same element. And the stress points on the interfaces are way too few to deliver a realistic force distribution analysis. As a result, the forces are concentrated in the limit amount of finite elements, and then lead to higher force than reality.

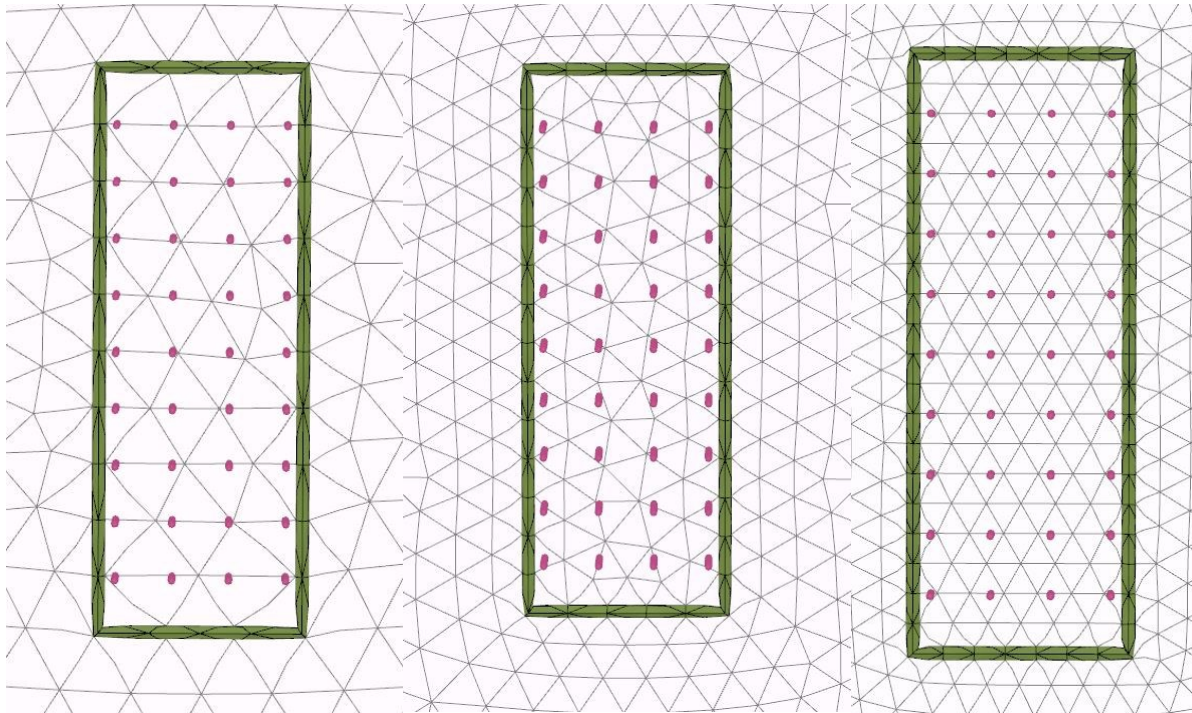


Figure 5-15 Bottom view of the mesh in excavation zone (green area highlights the excavation pit, red dots are piles)

There is a common way to refine the mesh in a specific area in both PLAXIS 2D and 3D, which is creating some surfaces to wrap the area to be investigated. By doing this, the analysts can change the refinement of mesh locally. For this project, it was tested with four surfaces wrapping the whole excavation zone, so that the mesh around retaining walls can be refined. *Figure 5-17* illustrates the surfaces created in the structure view. However, the results changed dramatically, and do not correspond with other models. So this method is not applied to sequential models.

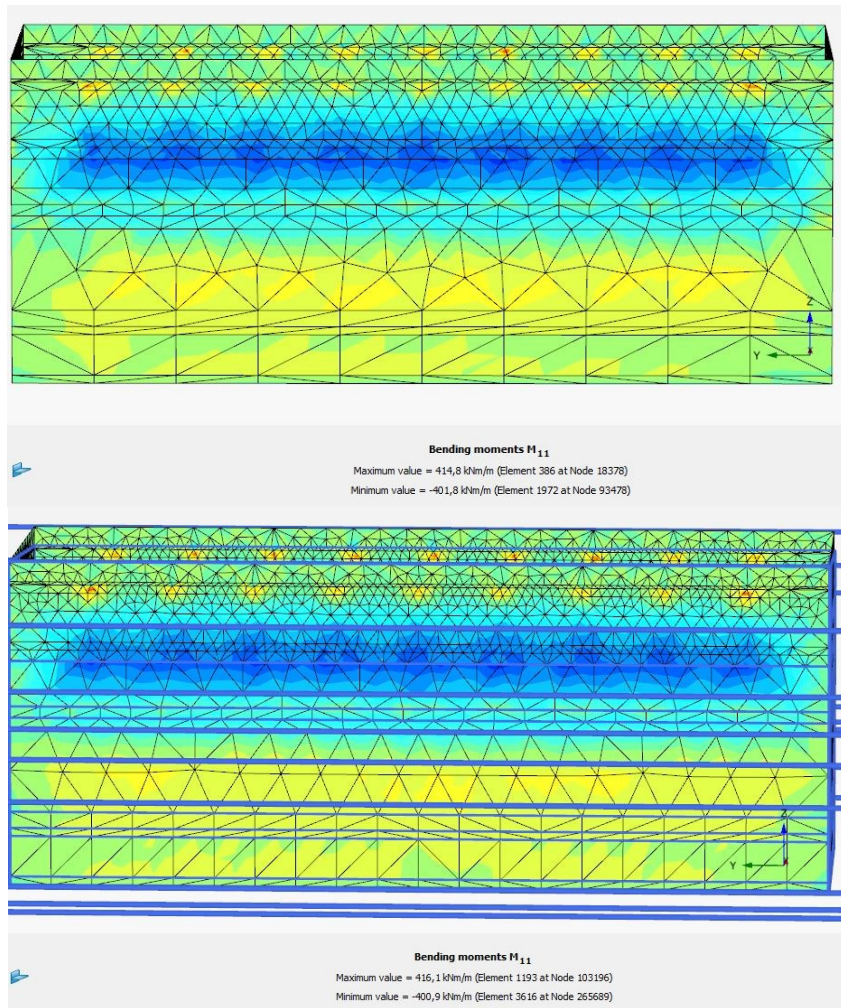


Figure 5-16 Side view of bending moment distribution for different mesh quality

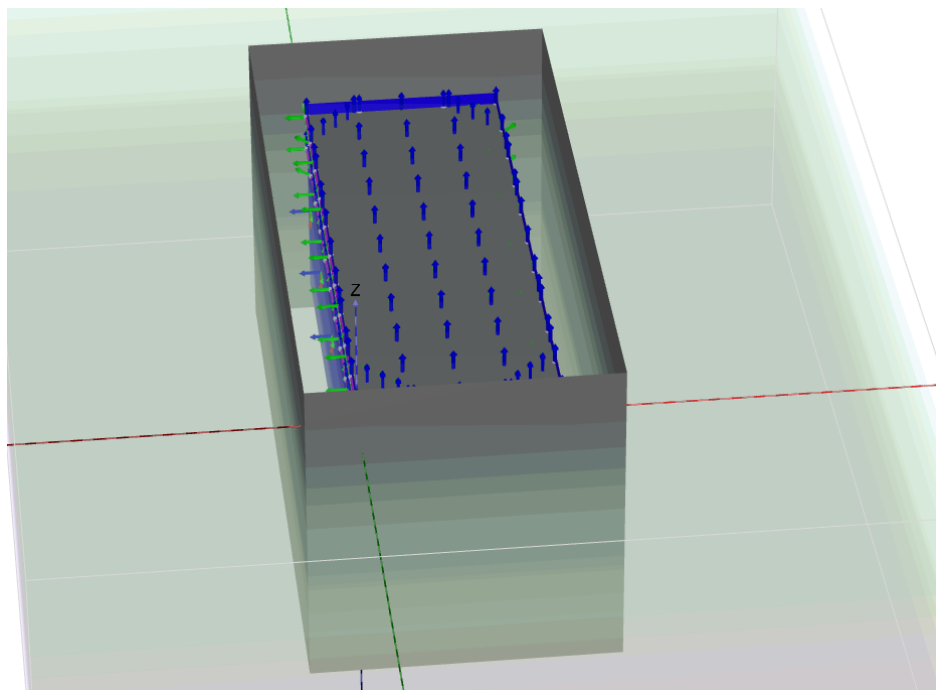


Figure 5-17 Common method to refine mesh locally

5.3 3D sequential excavation model (PLAXIS 3D)

In this chapter, the sequential excavation model is introduced thoroughly and tested with different scenarios so that the set up can be optimized. The model introduced in this chapter is the standard sequential model. In next chapter, variations of testing sequential models and the results will be discussed.

The sequential model is based on the staged excavation model with changes on structure and calculation stages. The materials and mesh set up are the same as staged excavation model.

5.3.1 Sequential structure

The sequential model is achieved by adding surfaces between the construction stages. There are three main stages, namely the 1st struts stage, 2nd struts stage and full excavation stage. The grades of slopes are 2:1. Each excavation step is 5m, which means for every excavation step, the slopes will move forward 5m. To ensure there is enough space to accommodate machinery on the 2nd struts stage, there is always 15m open space at the 2nd struts level. The difference of structure set up is illustrated in *Figure 5-18*.

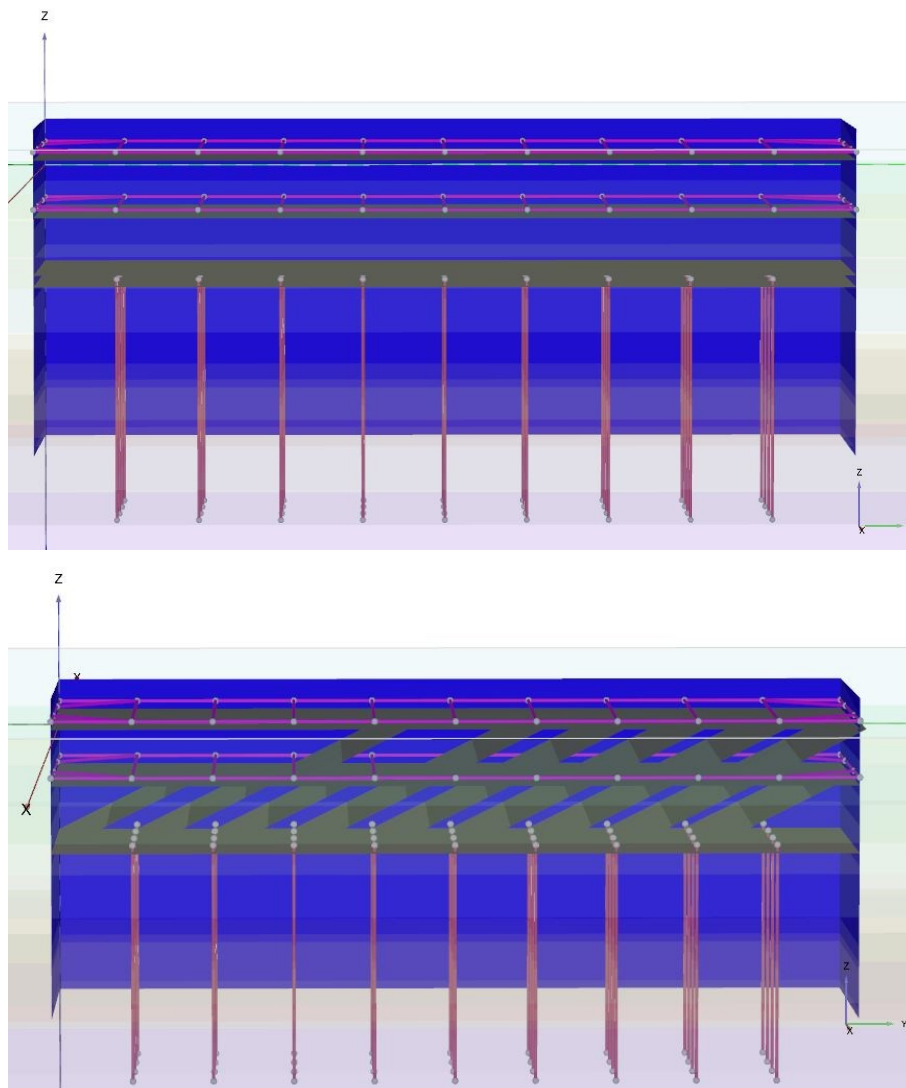


Figure 5-18 Side view for structures of staged excavation model and sequential excavation model

5.3.2 Calculation stages

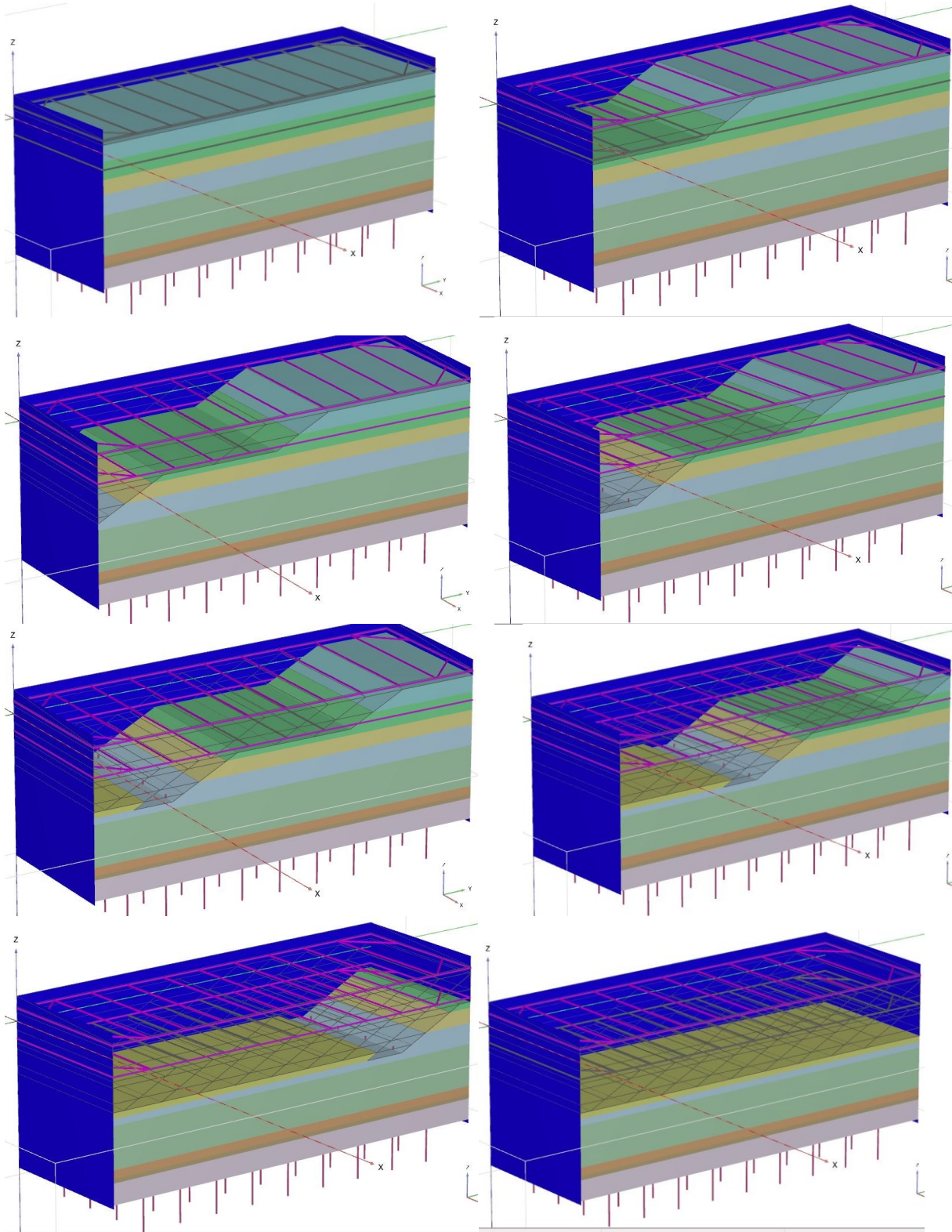


Figure 5-19 Several calculation steps for sequential model

Figure 5-19 demonstrated several calculation steps. This model is built upon the request from the contractor that the 2nd struts shift forward after the concrete floor is constructed in each excavation

step. For each calculation step, the excavation goes forward for 5m. Different excavation steps are further tested and introduced in next Chapter. The whole calculation sequence includes 15 steps instead of 6 steps in staged excavation model. The calculation takes at least 20 hours to finish.

5.3.3 Results

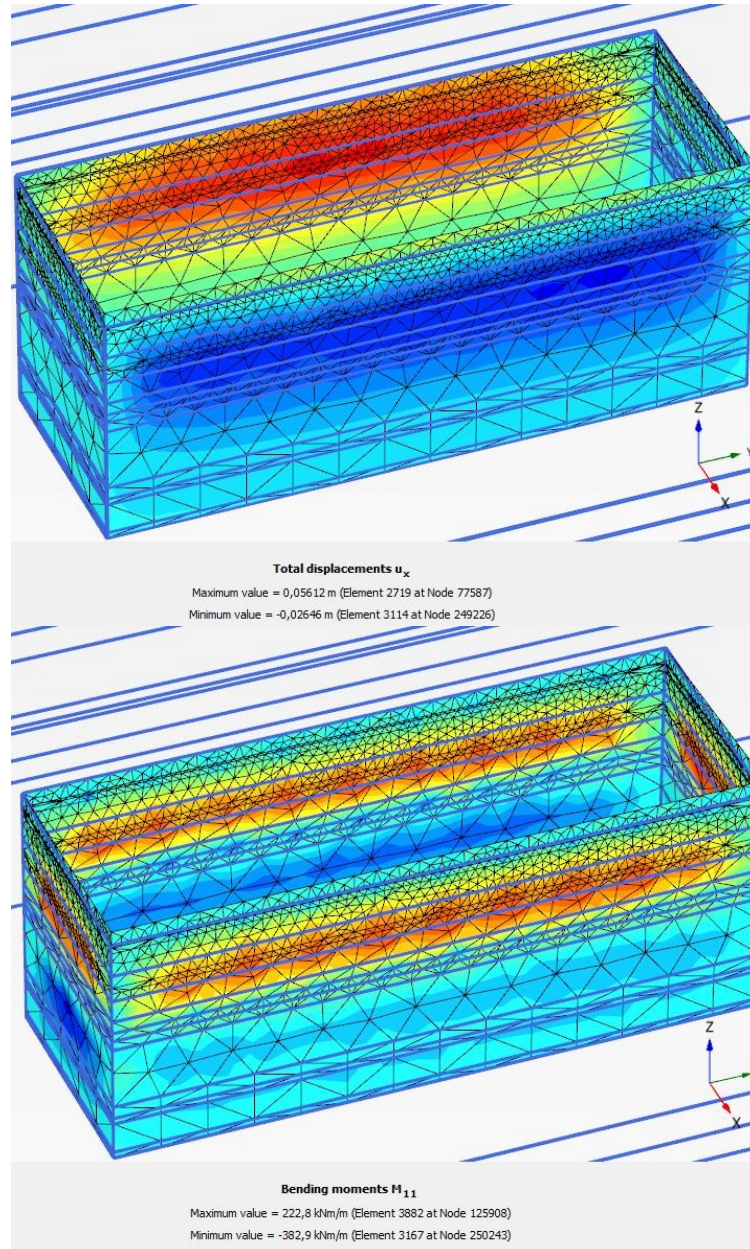


Figure 5-20 Overview of lateral deformation and bending moment for sequential excavation model

Figure 5-20 shows the overview of lateral deformation and bending moment for sequential model, and highlights the maximum and minimum values. The lateral displacement graph is similar to staged excavation model. The bending moment graph shows signs of influence from the sequential model as the distribution have a local trend after each excavation step. As a comparison, the high bending moment area is concentrated in the middle part in staged excavation model.

In order to compare with 2D and 3D staged excavation models, the results from the cross-section at half of the model are presented *Figure 5-21*.

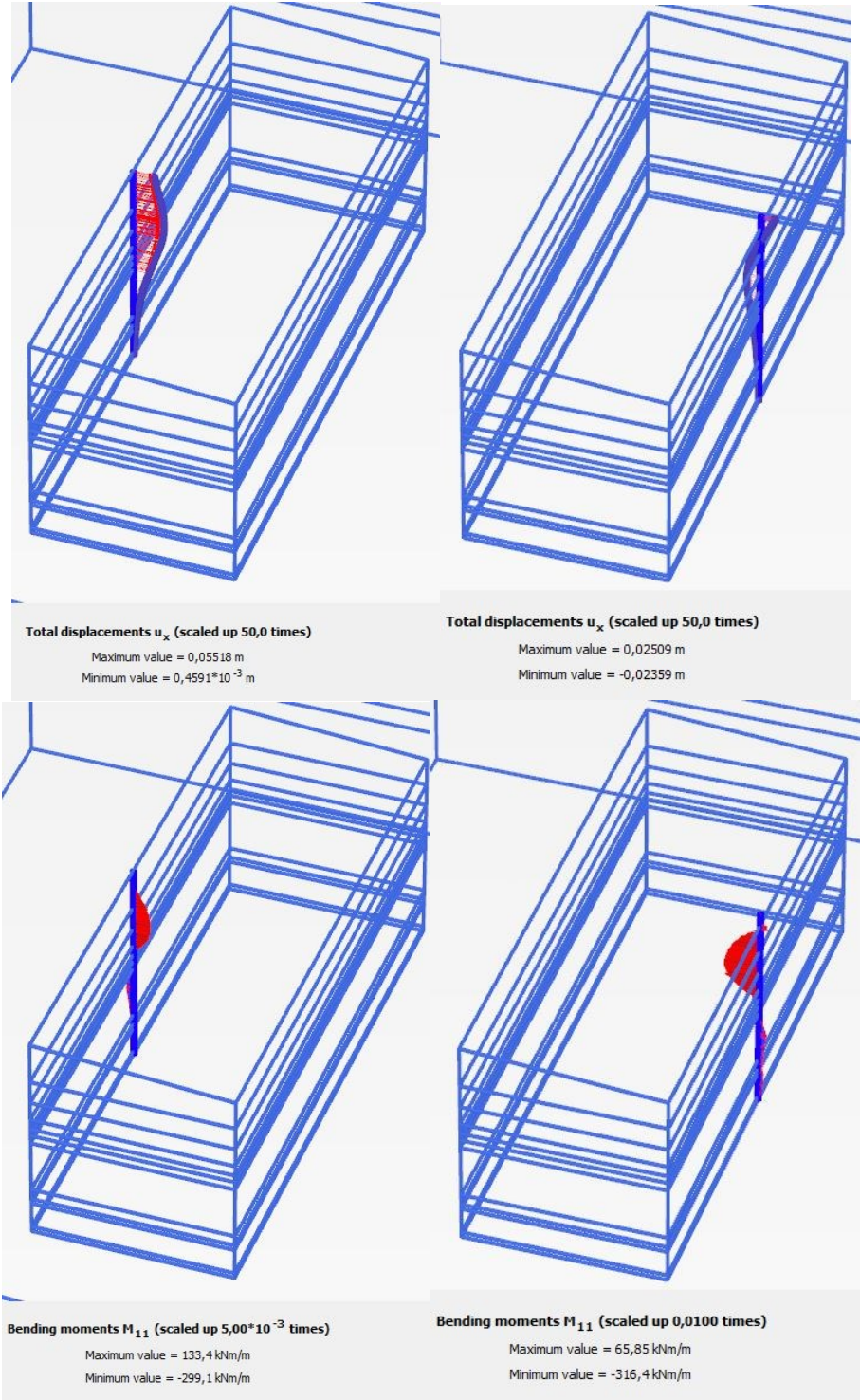


Figure 5-21 Maximum deformation and bending moment on both sides of excavation pit

	Displacement (mm)		Bending moment (kNm/m)			
	Left	Right	Left		Right	
			Max	Min	Max	Min
PLAXIS 2D	69,1	34,5	345,1	-153,1	360,0	-124,7
3D staged	66,0	32,7	353,9	-199,9	349,0	-205,3
3D sequential	55,2	25,1	299,1	-133	316,4	-65,85

Table 5-5 Comparison of displacement and bending moment among different models

Table 5-5 is concluded based on previous chapter and the results in Figure 5-21. It is clear that the displacement and bending moment dropped significantly. Especially the for the lateral displacement, by applying sequential excavation model, the deformation of the sheet pile wall decreased by almost 20%. This can be very beneficial for excavation done in settlement sensitive areas, for instance city centre with old buildings and busy traffic. And this is further confirmed by the settlement graph displayed in Figure 5-22.

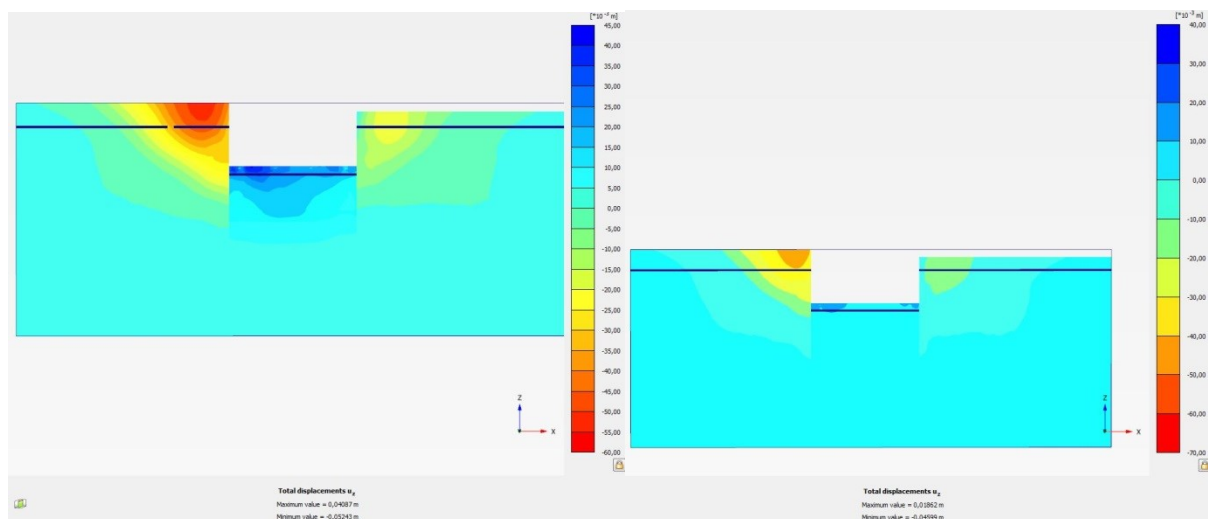


Figure 5-22 Comparison of vertical movement of soil

	Maximum value (mm)	Minimum value (mm)
2D	38.7	-56.5
3D staged excavation	40.9	-52.4
3D sequential excavation	18.6	-46.0

Table 5-6 Comparison of vertical movement of soil

According to Figure 5-22 and Table 5-6, the sequential model not only lowered the settlement behind the sheet pile wall. More importantly, the heave within the excavation pit is now less than half of what was calculated in either 2D or 3D staged excavation model. This is probably because that the concrete floor is constructed after each excavation step in sequential model, while in staged models, the vertical balance that the concrete floor provides is added after the excavation of the whole pit.

This chapter is focus on the comparison between sequential model and the staged excavation model. Detailed results for each excavation step in sequential model will be presented and compared against different sequential model in next chapter.

5.4. Conclusion on 3D modelling

In comparison with 2D numerical modelling, the most influential factors are the geometry and mesh set-up. The engineering theories applied are the same in 2D and 3D modelling. The differences in results are most likely to be caused by the geometry of the investigating domain, namely the corner effect in 3D modelling. The deflections of sheet pile wall are limited in the corners. If the length/width ratio of the excavation zone was not big enough, the deflection of the sheet pile wall would not be fully developed. Besides, the rotation and deformation of corners could not be modelled in 2D models. However, for this graduation project, because there are no field data to verify the modelling results, the size chosen for excavation zone was to be more comparable between 2D and 3D modelling. Thus the whole domain became more plain strain, the corner effect was limited. In general, the domain size for this project limited the advantages of 3D modelling.

The meshing is another key factor in finite element method as explained in literature review. The difference in meshing between PLAXIS 2D and 3D was explained in Section 3.3. As it was shown in Section 5.2.2, the parametric study on the mesh set-up, the results especially the distribution of forces in sheet pile wall varied due to different mesh set-up. In short, coarse mesh leads to forces distributed to limited number of nodes, some nodes receive extra force than the actual condition. This of course is the problem for all FEM models. But for 3D FEM models, the degree of refinement of mesh is essential. Because the time required for calculation is very long, the sequential excavation model presented in this chapter for instance, might need more than 20 hours for calculation depending on the capacity of the computer. The balance between time (cost) and output relies on the experience of analyst and the requirements from certain project.

The necessity of applying sequential excavation method is worth debating according to the test results in this chapter. On one hand the deflection of sheet pile wall was reduced by 20%, the settlement and the heave at the bottom of excavation pit were also reduced significantly. On the other hand, the deflection of sheet pile wall and settlement from the normal staged excavation models were well within the range of acceptance, but the improvement was not as striking as expected. The excavation is almost 10 metre on one side, but the difference of deflection results is only 1.5 cm. The difference is almost negligible in practice. Besides, the execution of sequential excavation method is way more expensive than normal open excavation, especially the small excavation step used in this sequential FEM model (5 metre).

For the Spaarndammertunnel project in particular, the 3D FEM model is useful to determine the size of excavation pit and detailed design on struts and wailing beams, in order to save the cost and increase safety. The preliminary design was carefully adjusted and tested, since the deformations of sheet pile wall and surrounding soil were acceptable. This results in less advantage of using sequential excavation model. According to the size of disturbed zone and the distance between the nearby construction and this tunnel, the sequential excavation method is not preferable for this project.

6. Optimization for sequential excavation model

6.1. Test on lateral support

6.1.1. Model introduction

The sequential model presented in Chapter 5 is based on the construction plan from the contractor. The 2nd struts are shifting with the excavation step, which is more budget beneficial and more risky design. In staged excavation models, the concrete floor stage has the lateral support from the concrete floor as well as all the struts on 2nd strut stage. As a comparison, the sequential model in Chapter 5, the second to last stage only has two struts for lateral support. This is illustrated in *Figure 6-1*. In order to get a better comparison between staged excavation model and sequential excavation model, a more reserved model is created.

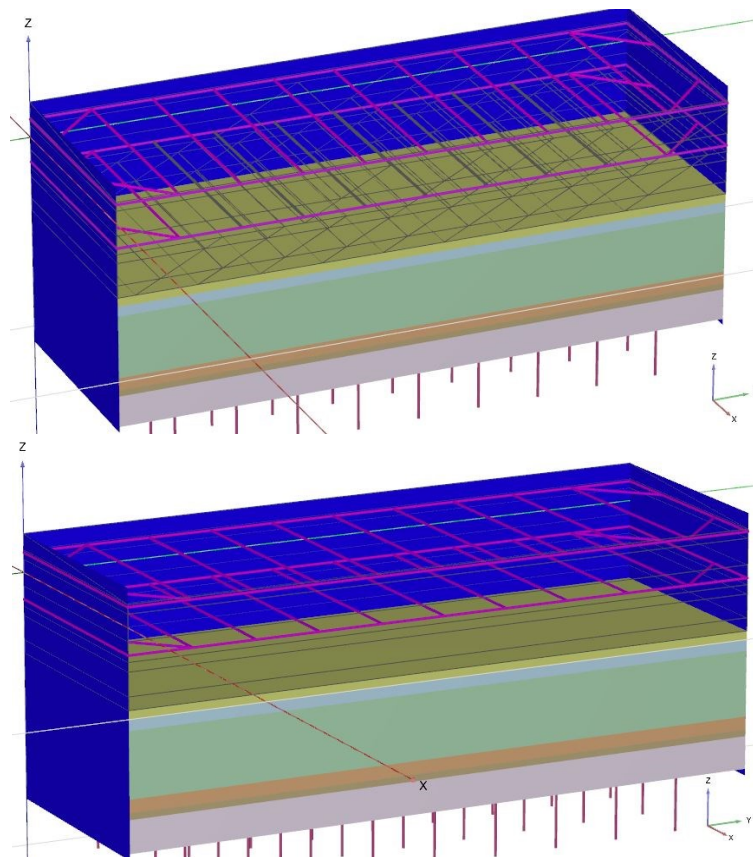


Figure 6-1 Comparison of construction stage in sequential model and staged excavation model

6.1.2. Model set-up

The soil profile, structures, mesh set up and water conditions are the same as the sequential excavation model in Chapter 5. One thing differs is the calculation stage. Instead of shifting the struts together with the excavation step, the 2nd struts are activated step by step and remain activated until the last stage. Then the 2nd struts are deactivated in the last stage.

This sequential model is comparable to both staged excavation model and the sequential model in Chapter 5. All the calculation steps in staged model are included in this model. And the calculation

steps in both sequential models are identical, so that the deformation and bending moment are comparable in each single calculation stage.

6.1.3. Test results

In this section, the test results for this sequential model will be presented with comparison to sequential model introduced in Chapter 5 as well as the staged excavation model. The model introduced in Chapter 5 will be named as “Sequential V1”, which is the model that the 2nd struts are shifted together with excavation steps. The model introduced in Section 6.1 is named as “Sequential V2”.

The results for maximum lateral displacements of sheet pile wall are compared in *Table 6-1* and *Figure 6-2*. The results are taken from the left side of the mid-point of the excavation zone. As it has the largest deformation and directly influenced by the struts. Since the staged excavation model does not have the detailed excavation process, the graph has a linear relationship from stage 2 to stage 13.

In general, both sequential models decreased the maximum lateral deformation for almost 20%. The set-up of stage 14 and 15 in staged model and sequential V2 are the same, thus both result in a sudden change of lateral deformation from stage 14 to stage 15, when all 2nd struts are removed. As for sequential V1, the sudden change of deformation happened from stage 11 to 12, when struts are shifted forward. After stage 12, the lateral deformation remains constant as the excavation proceeds.

According to *Table 6-1* and *Figure 6-2*, the biggest difference in model sequential V1 and V2 is the timing of shifting or removing 2nd struts. This causes the difference of maximum lateral deformation in different calculation stages. But the final results are very close.

Maximum lateral deformation on Left side (mm)			
	Sequential V1	Sequential V2	Staged excavation
0	0,0	0,0	0
1	5,1	5,8	2,7
2	21,7	23,4	21,7
3	22,2	23,9	33,8
4	24,9	25,6	56,5
5	31,0	30,9	56,5
6	33,3	31,9	66,5
7	36,1	32,9	
8	38,2	34,4	
9	43,0	39,3	
10	43,6	39,7	
11	46,5	42,3	
12	54,1	42,5	
13	55,0	42,6	
14	55,2	42,6	
15	55,2	52,3	

Table 6-1 Maximum lateral displacements of the sheet pile wall at mid-point

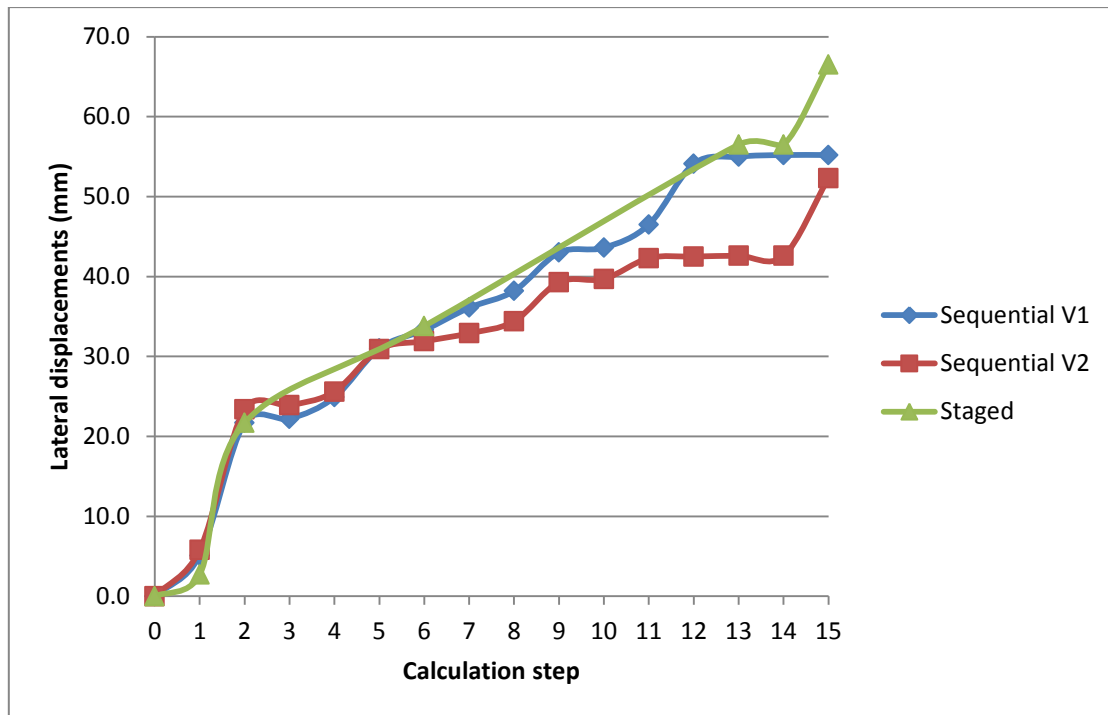


Figure 6-2 Maximum lateral displacements of the sheet pile wall at mid-point

The results for maximum bending moments at the left mid-point are shown in Table 6-2 and Figure 6-3. The sequential models also result in lower maximum bending moments compared to stage excavation model, especially the maximum bending moment on the negative side. The sequential model V2 comes with lower bending moments compared to V1 for most calculation stages. Like the lateral deformation curve, it also has a sudden change when 2nd struts are removed.

	Maximum bending moment on Left side (kNm/m)					
	Sequential V1		Sequential V2		Staged excavation	
	Max	Min	Max	Min	Max	Min
0	0,0	0,0	0,0	0,0	0,0	0,0
1	0,2	-7,2	1,4	-9,2	1,3	-2,0
2	33,5	-30,0	34,2	-25,6	31,3	-27,6
3	36,2	-35,5	37,4	-40,1	177,3	-133,0
4	93,9	-59,3	86,4	-98,9	330,1	-235,8
5	163,5	-92,2	149,0	-119,4	333,2	-237,7
6	179,2	-100,0	164,6	-114,5	343,9	-239,3
7	201,0	-108,4	151,3	-111,1		
8	214,5	-106,9	187,3	-100,8		
9	274,1	-149,1	256,6	-115,7		
10	255,9	-132,2	234,0	-103,1		
11	257,0	-132,3	230,6	-103,0		
12	294,0	-132,8	230,3	-102,7		
13	297,7	-133,2	230,0	-102,5		
14	298,5	-133,3	230,0	-102,5		
15	299,1	-133,4	275,3	-108,0		

Table 6-2 Maximum bending moments of the sheet pile wall at mid-point

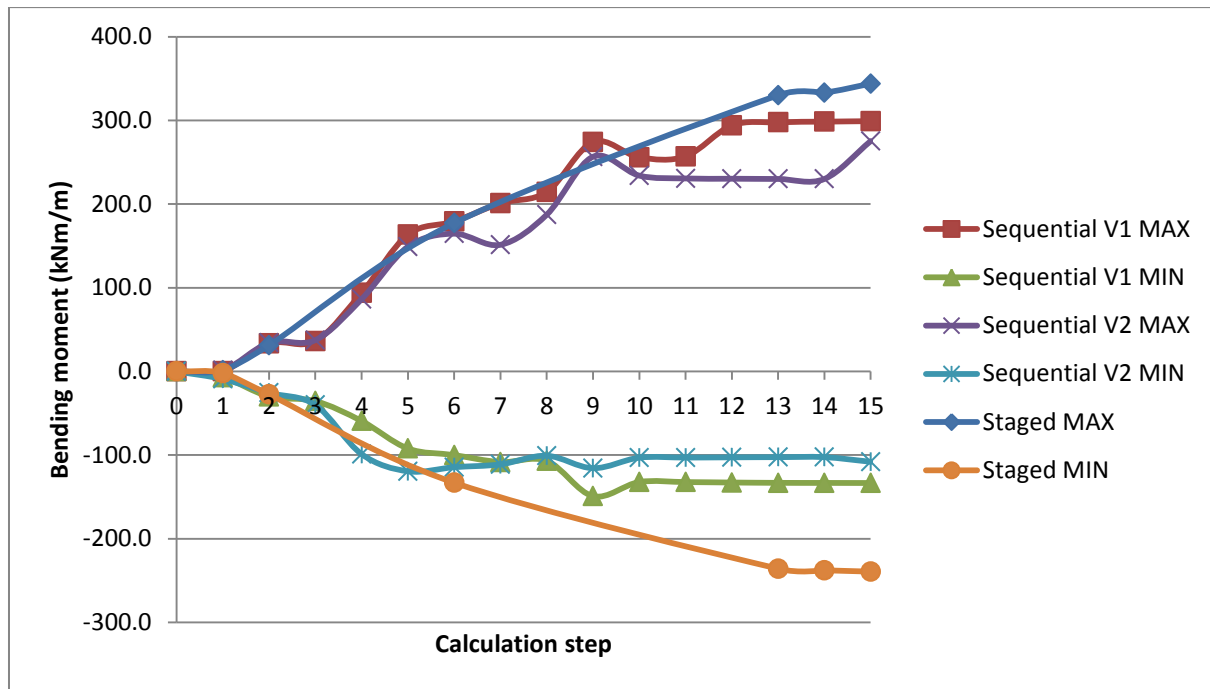


Figure 6-3 Maximum bending moments of the sheet pile wall at mid-point

Based on the analysis above, both sequential model result in lower lateral deformation and bending moment. The sequential V2 provides more optimistic results compared to V1. But the differences between two sequential models are not very significant. Considering the maximum bending moment the retaining structure can handle and budget saving, sequential V1 model is more favourable for real excavation process.

6.2. Test on excavation step

6.2.1. Model introduction

The excavation steps used in both sequential models introduced in last section were 5 metres. This is a conservative design, which leads to more calculation steps and more calculation time. Like the test on the size of the excavation pit in Section 5.2.1, the length of each excavation step needs testing to optimize the sequential models.

6.2.2. Model set up

The excavation steps tested are 5m, 10m, 15m, 20m and 25m. All test models use the same set up for soil profile, structure, mesh and water conditions. The only difference is the surfaces added to simulate each single excavation step and the number of calculation steps.

6.2.3. Test results

Due to the different excavation steps, the distribution of the lateral displacements and bending moments of the sheet pile wall changed dramatically. *Figure 6-4* highlights the lateral displacements of the sheet pile wall on the left bank when the excavation step is 25m. It is clear to see that the maximum lateral deformation take place near the 1/3 area from the start of the sequential excavation. Thus instead of using the results from the half of the sheet pile wall as previous chapters, the results from the whole retaining wall will be recorded and compared.

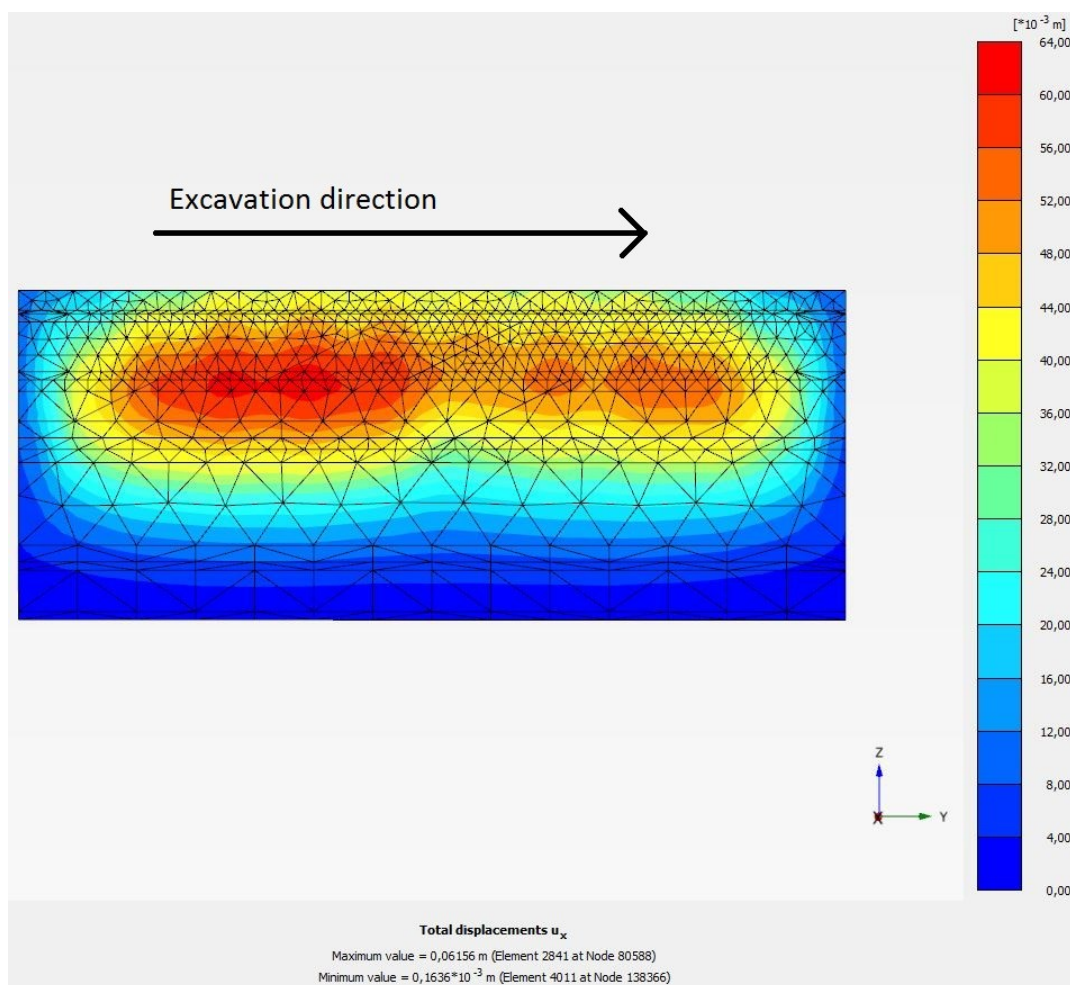


Figure 6-4 the plot for lateral displacements for 25m excavation step

Plaxis 3D has a function called result smoothing. It is designed to reduce the numerical noise resulting from the extrapolation of the results obtained in stress points to nodes. The function is available for plots and tables. The result of this function is more continuous plots. Without the results smoothing, there are some nodes result in very high stress distribution. The use of this function relies on the engineering experience. For this project, the smoothing function only affects the bending moment distribution. Both smoothing and raw results for the maximum bending moments will be presented and compared.

Maximum displacements (mm)						
	5m	10m	15m	20m	25m	Staged
0	0,0	0,0	0,0	0,0	0,0	0,0
1	5,1	5,1	5,0	5,1	5,0	2,7
2	21,7	21,8	23,4	23,4	23,4	21,7
3	22,2	21,8	31,5	31,4	31,4	34,9
4	24,9	30,0	35,1	35,0	32,9	59,2
5	31,0	31,5	49,7	52,3	52,5	59,3
6	33,3	41,3	50,6	52,9	53,1	67,6
7	36,1	51,3	57,5	60,0	53,1	
8	38,2	53,8	59,3	60,3	61,6	
9	43,0	55,1	59,7	60,7		
10	43,6	55,2				
11	46,5	55,5				
12	54,1					
13	55,0					
14	55,2					
15	55,2					

Table 6-3 Maximum lateral displacements on left side of the excavation pit

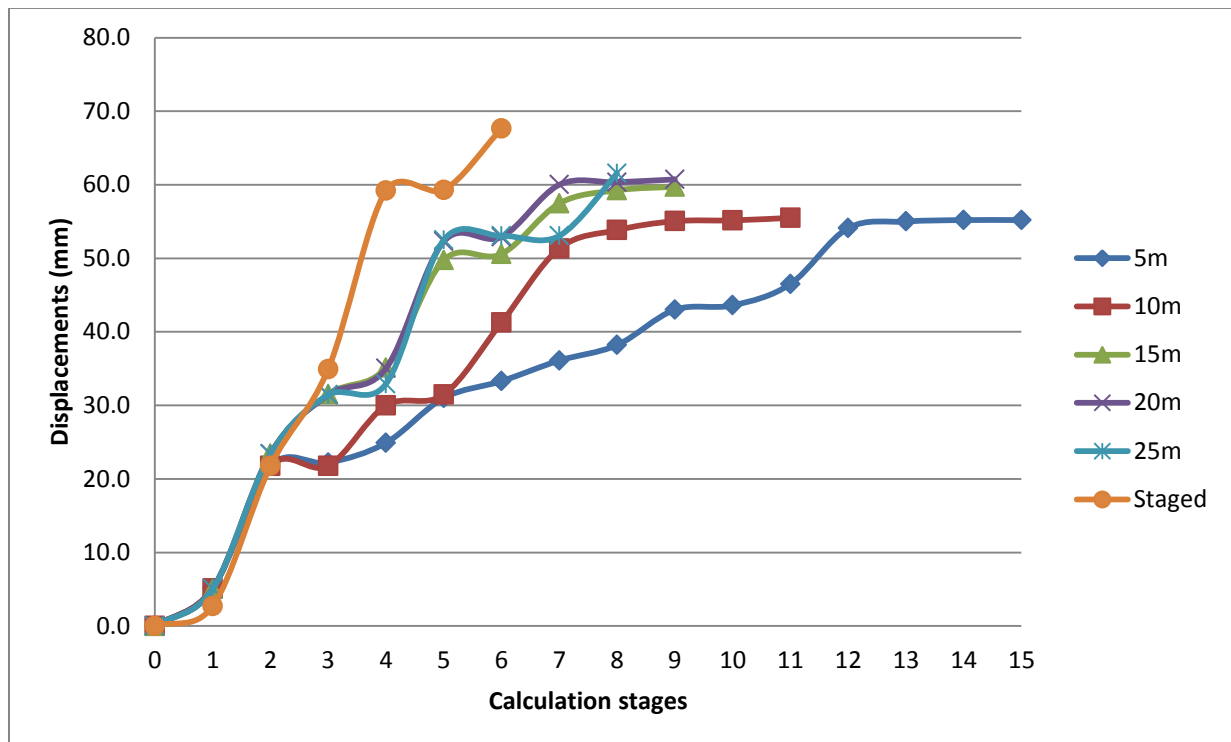


Figure 6-5 Maximum lateral displacements on left side of the excavation pit

Table 6-3 shows the results of the maximum lateral displacements for each calculation step. The results are taken from the sheet pile wall on left bank of the excavation pit. The small excavation step, 5m for instance, requires more calculation steps and calculation time. While the large excavation step results in higher lateral displacements. Figure 6-5 clearly shows comparison of the results for the maximum lateral displacements. Because of the slop used for excavation steps, for 15m excavation model, instead of 4 excavation steps(15m, 30m, 45m, 50m), only 3 steps (15m, 30m, 50m) were used. Both 15m and 20m models have 9 calculation stages. The maximum excavation step possible in this model is the same as the staged excavation model, which has an excavation step of 50m.

Table 6-4 and Figure 6-7 show the results for maximum bending moments from each calculation step after smoothing function. Table 6-5 and Figure 6-8 present the maximum bending moments from each calculation step without using smoothing function. In general, shorter excavation step result in more calculation steps and less bending moments. Especially for negative maximum bending moments without using smoothing function, long excavation step leads to more than 150% of bending moments.

According to Figure 6-6, the biggest differences for using smoothing functions are the bending moments at the 1st struts. This can be cause by the size and properties of the lateral support system. The dimensions and physical properties are not clearly stated in preliminary design report. The capacity of bending moments for AZ 26-700 varies from 624 to 1118kNm/m, depending on the grade of steel used (Table 2-5). Some models result in bending moments higher than 700kNm/m is not preferable in real construction. Thus the parameters for struts and wailing beam can be further optimized. By comparing the results before and after smoothing, it is also clear that the results from short excavation step model (5m, 10m) are less affected by the smoothing function. This means more uniform and accurate results.

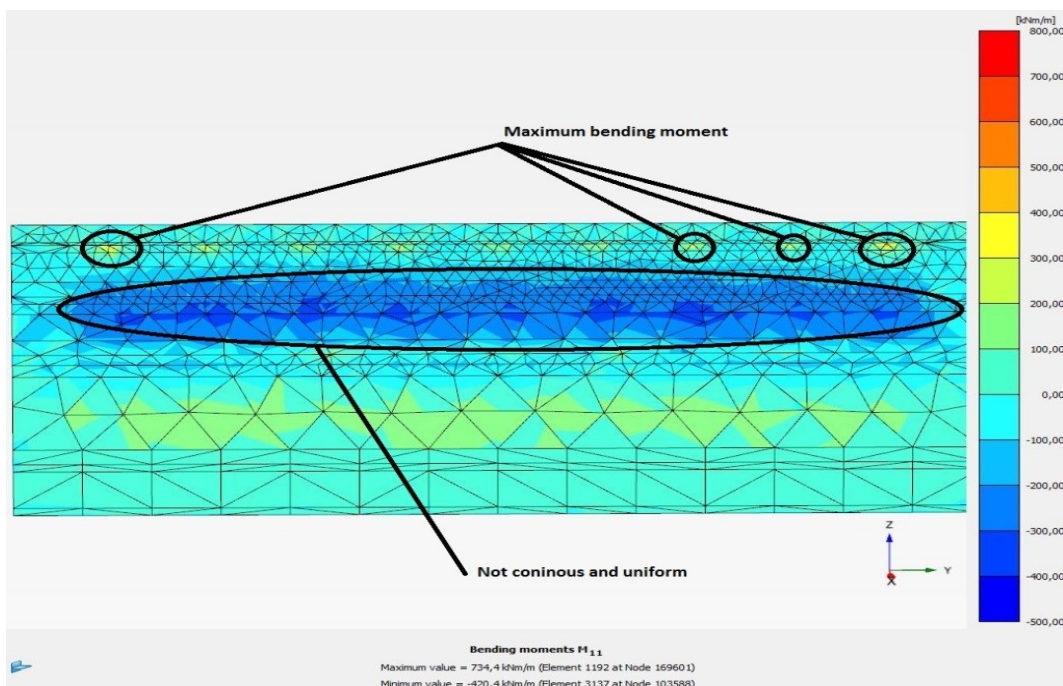


Figure 6-6 Bending moments distribution without using smoothing function for 15m model

Maximum Bending moments (kNm/m)												
	5m		10m		15m		20m		25m		Staged	
	Max	Min	Max	Min								
0	0	0	0	0	0	0	0	0	0	0	0	0
1	3,3	-7,8	3,3	-7,9	3,2	-7,1	3,1	-7,6	3,1	-7,2	1,6	-2,2
2	50,1	-36,4	55,8	-39,8	47,0	-38,3	47,3	-47,4	46,1	-36,8	44,4	-33,5
3	175,1	-183,6	187,5	-183,6	192,3	-182,6	188,2	-182,5	182,3	-186,9	195,7	-210,3
4	206,2	-157,5	217,9	-158,0	220,0	-156,1	216,1	-156,0	203,8	-156,4	411,2	-384,1
5	278,5	-208,4	368,3	-298,8	390,9	-330,9	401,1	-353,1	389,8	-361,9	415,5	-387,2
6	295,8	-209,7	369,8	-294,0	395,0	-340,2	405,9	-383,2	394,7	-448,9	379,5	-379,0
7	296,4	-211,8	371,8	-300,2	395,5	-353,8	406,6	-385,4	394,7	-451,1		
8	295,9	-212,2	372,3	-300,7	396,0	-341,2	407,3	-363,9	363,6	-327,3		
9	336,3	-217,0	372,2	-345,0	386,6	-311,3	377,3	-316,6				
10	346,1	-218,5	372,3	-350,2								
11	342,5	-188,3	369,4	-320,3								
12	347,4	-191,7										
13	349,1	-324,8										
14	361,9	-330,9										
15	362,6	-192,6										

Table 6-4 Bending moments results after smoothing function

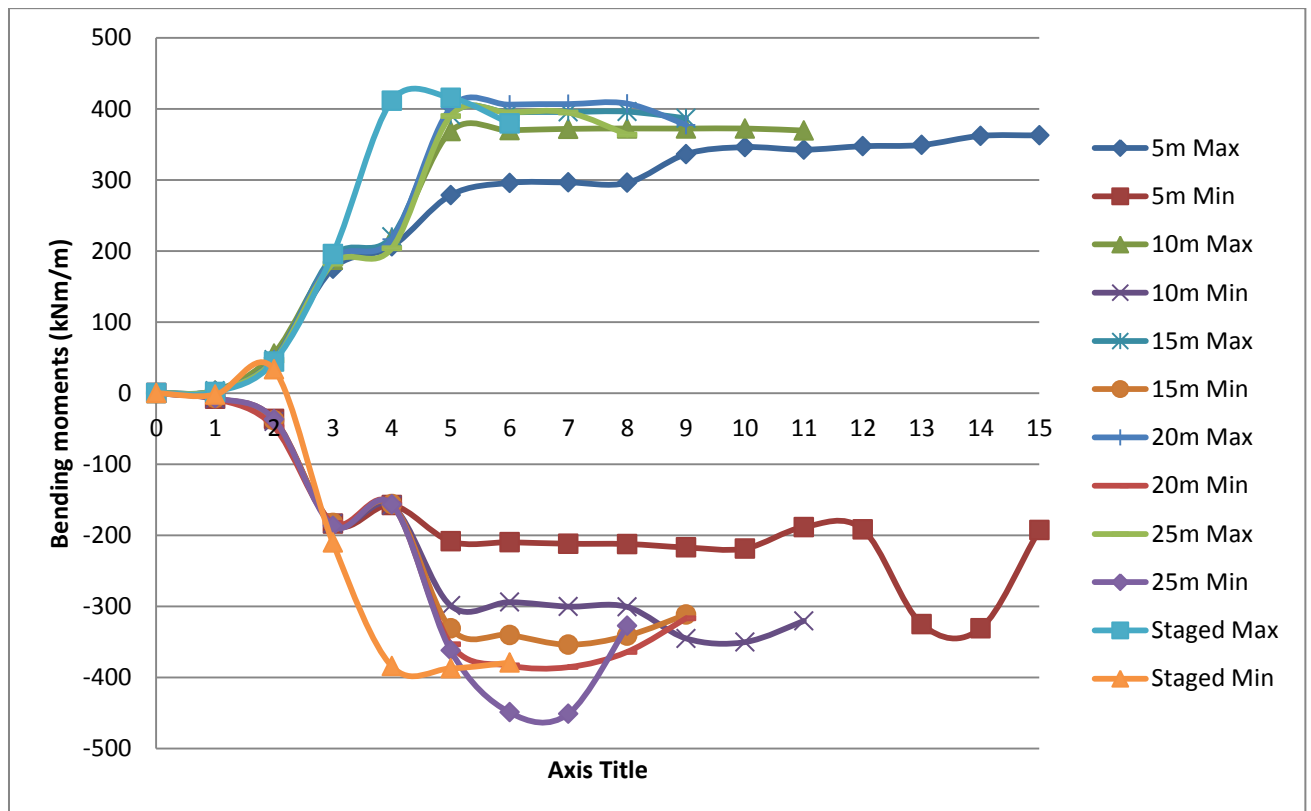


Figure 6-7 Bending moments results after smoothing function

Maximum Bending moments (kNm/m)												
	5m		10m		15m		20m		25m		Staged	
	Max	Min	Max	Min								
0	0	0	0	0	0	0	0	0	0	0	0	0
1	5,1	-8,4	5,1	-8,2	5,0	-7,8	4,9	-8,0	4,9	-7,9	2,8	-2,5
2	59,4	-59,9	61,5	-60,6	72,1	-64,5	70,6	-64,0	73,2	-60,3	68,2	-61,7
3	235,4	-306,6	237,6	-306,6	241,1	-305,4	240,4	-305,4	239,1	-305,0	248,8	-426,7
4	260,2	-265,6	263,2	-266,5	266,4	-264,7	265,2	-264,6	262,4	-264,4	467,1	-615,3
5	328,2	-299,6	368,3	-414,9	390,9	-469,7	417,3	-486,3	397,7	-498,3	472,2	-619,0
6	347,0	-302,4	369,8	-420,2	402,6	-542,6	410,8	-583,6	397,8	-739,2	438,3	-767,5
7	347,2	-306,8	412,3	-430,5	412,3	-657,8	429,9	-584,4	400,8	-742,7		
8	347,0	-318,1	415,5	-431,4	413,6	-668,0	431,4	-529,0	421,7	-569,5		
9	356,4	-364,5	415,6	-520,4	420,4	-734,4	439,6	-524,6				
10	358,5	-368,8	415,6	-529,0								
11	359,4	-236,8	413,6	-510,6								
12	361,0	-240,6										
13	366,7	-438,4										
14	373,4	-447,0										
15	379,9	-241,1										

Table 6-5 Bending moments results without smoothing

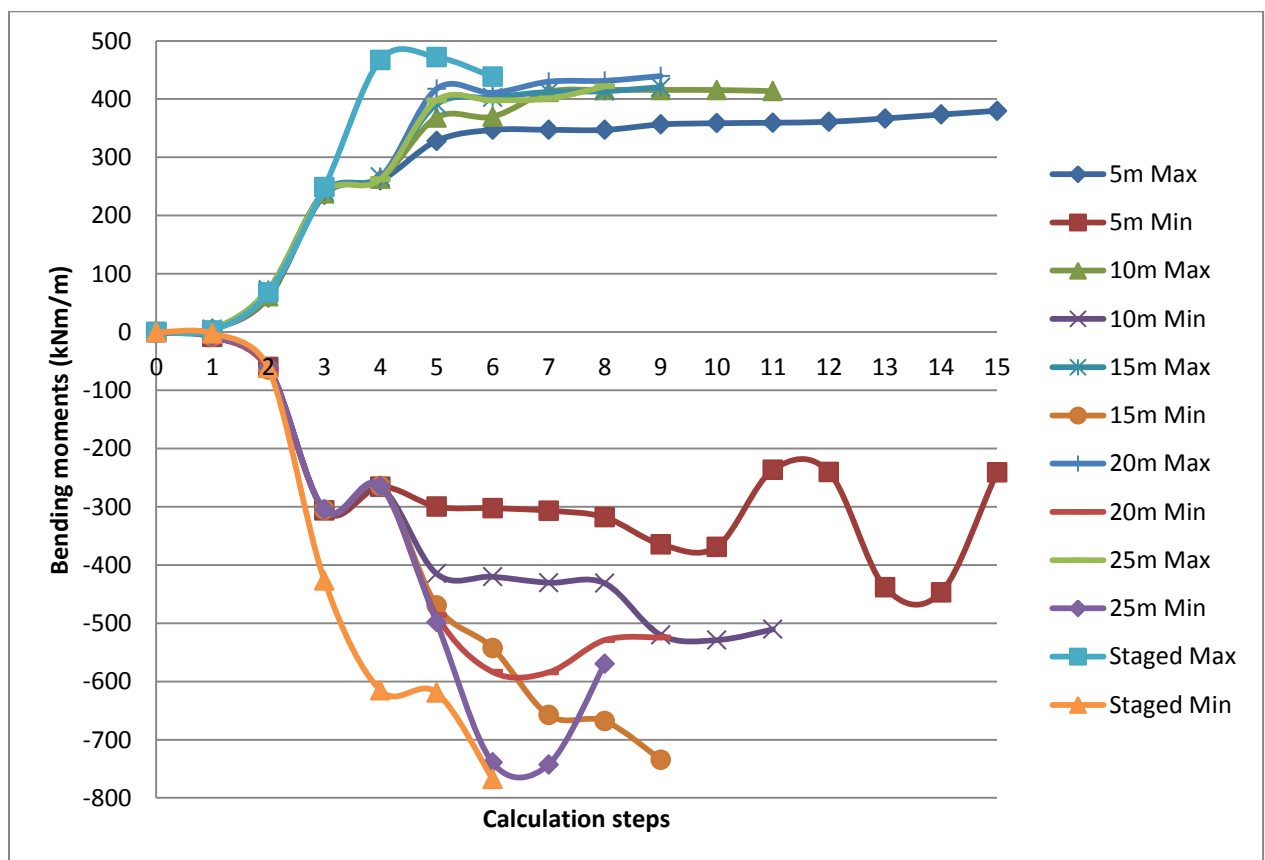


Figure 6-8 Bending moments results without smoothing

6.3. Test on sequential set up

6.3.1. Model introduction

For this particular project, the excavators are placed at the bottom of the excavation pit. And the whole sequential excavation goes from one side to the other. But in real constructions, it can also be done by excavating from top. In order to maximize the corner effect in 3D modelling, a test model is created that the excavation is done in the centre to two sides. The structure of the test model is illustrated in Figure 6-9.

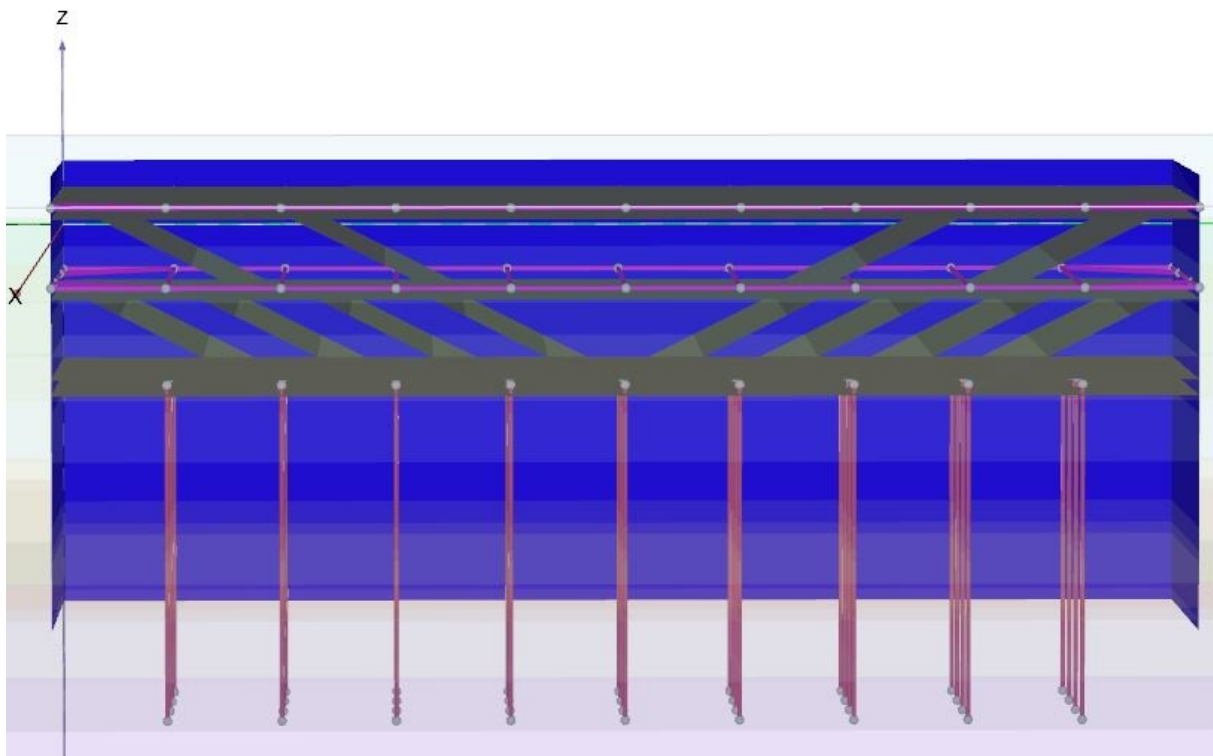


Figure 6-9 Structure of test sequential model

6.3.2. Model set-up

The first two steps are the same as previous models, namely install the sheet pile wall and pile foundation, and excavate to the 1st struts level. The sequential excavation starts with the excavation of a 15m long platform on the 2nd struts level. And the excavation continues towards both ends with 5m excavation step. There are 10 calculation stages in total. The execution requires similar time to 10m sequential model in real life. But because of the complexity of calculation for excavation towards two directions, the calculation of this model is more than the 10m sequential model.

Similar to previous sequential models, the concrete floor is constructed one phase after the excavation is done. The 2nd struts are removed after the concrete floor is constructed.

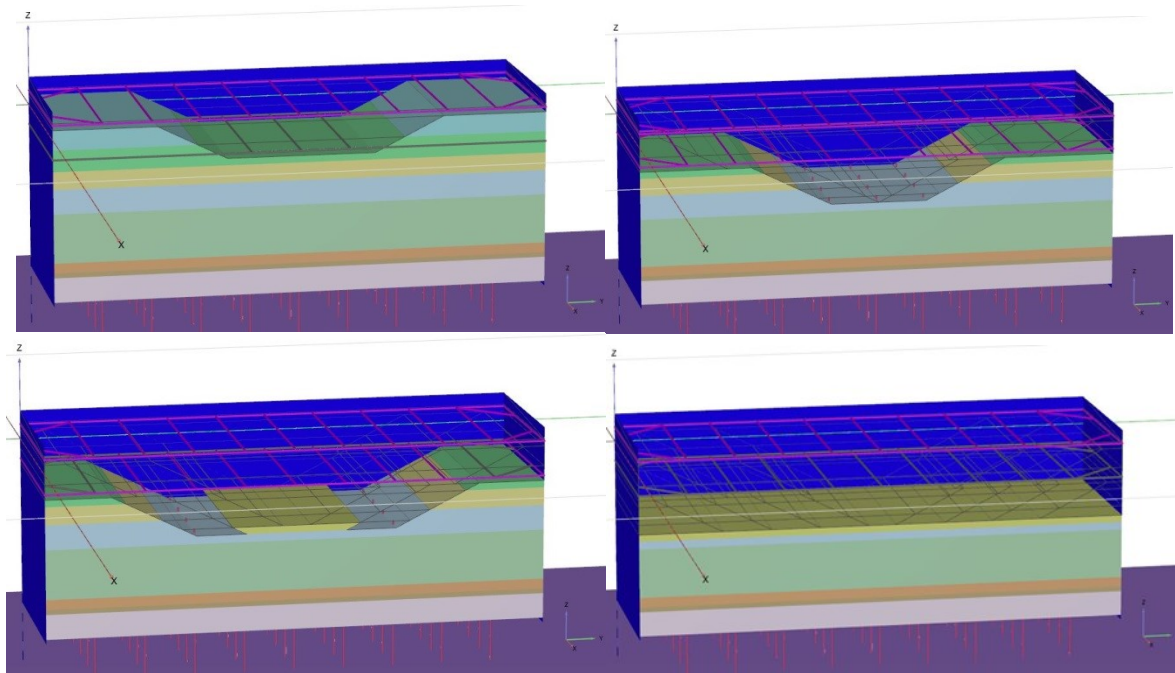


Figure 6-10 Calculation sequence for the test sequential model

6.3.3. Test results

Figure 6-11 and Figure 6-12 demonstrate the deflection of the sheet pile wall on left side of the excavation pit. Figure 6-11 shows the deflection distribution at the last phase. As it is shown in the figure, the maximum lateral deformation is right in the centre of the sheet pile wall. And well distributed over the length. However, by comparing the maximum lateral displacements against sequential models with excavation step of 10m, 15m and 20m, the test model does not have advantages in terms of minimize the deflection. The 10m sequential model needs similar excavation time to test model, but results in lower deflection. The 15m and 20m models result in similar deflection to the test model, but requires much less calculation and construction time.

Figure 6-14 shows the comparison of maximum bending moment for each calculation step. With the smoothing function switched on, the test model results in slightly lower maximum bending moment. But without the smoothing function, for certain calculation stages, the bending moment in the test model is ridiculously high.

Figure 6-15 illustrates the distribution of bending moment for the test model at calculation step 6, when it results in more than 1000kNm/m. According to the figure, the very high bending moment comes from the concentration of stress at the point where the 2nd strut locates. This can be caused by numerical noise.

In general, excavation from the centre to both ends does not have particular advantages in terms of reducing the calculation and construction time, deflection and bending moment of the sheet pile wall.

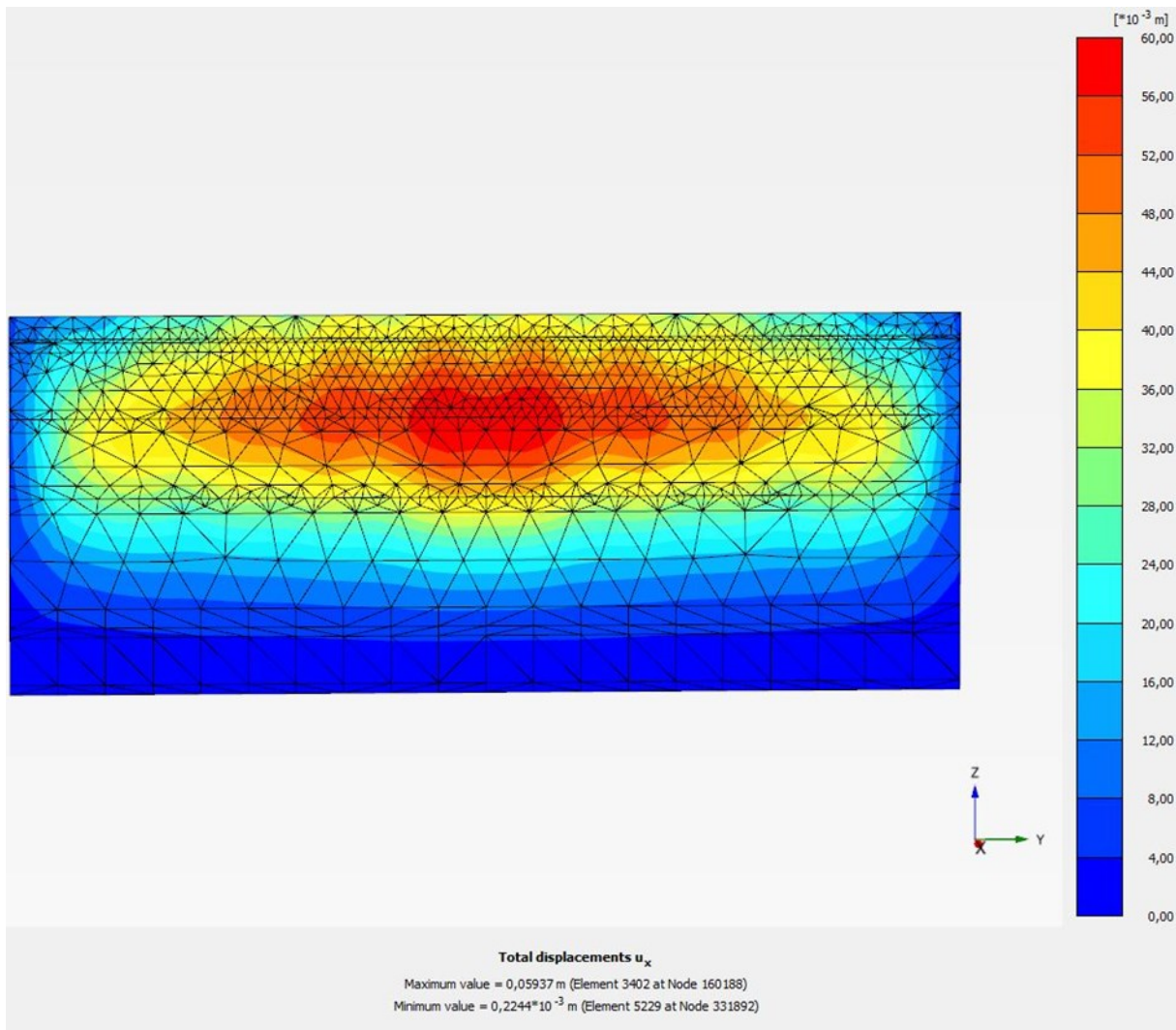


Figure 6-11 The lateral displacements distribution for the sheet pile wall on left side

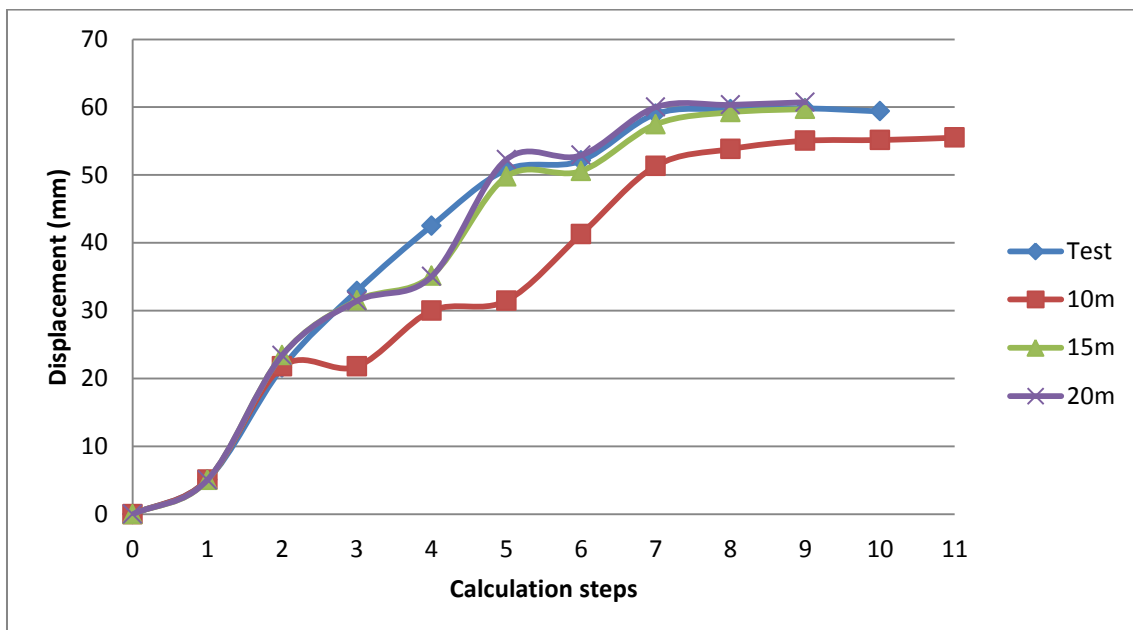


Figure 6-12 Lateral displacements for test sequential model

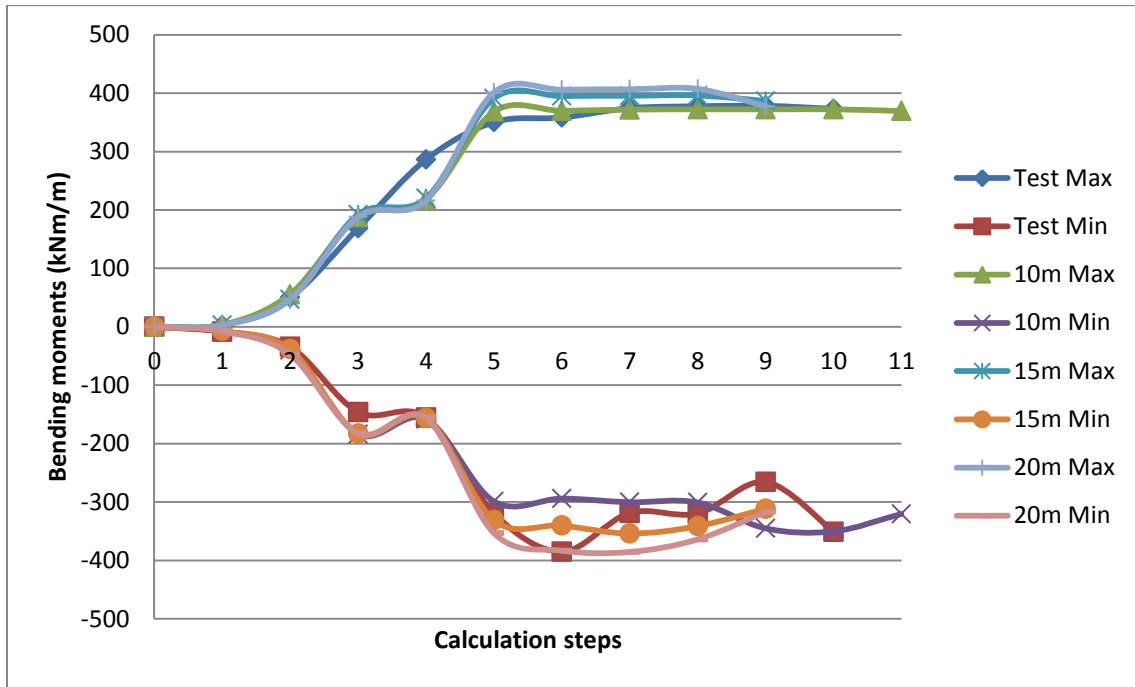


Figure 6-13 Comparison of maximum bending moments with smoothing function

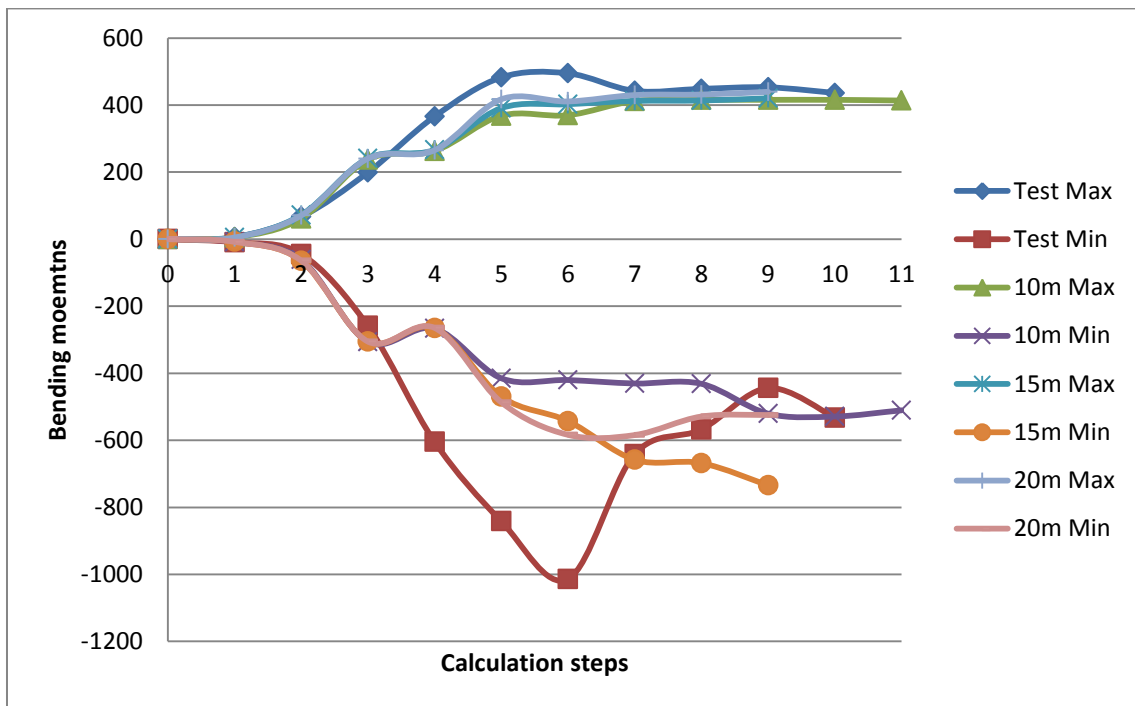


Figure 6-14 Comparison of maximum bending moments without smoothing function

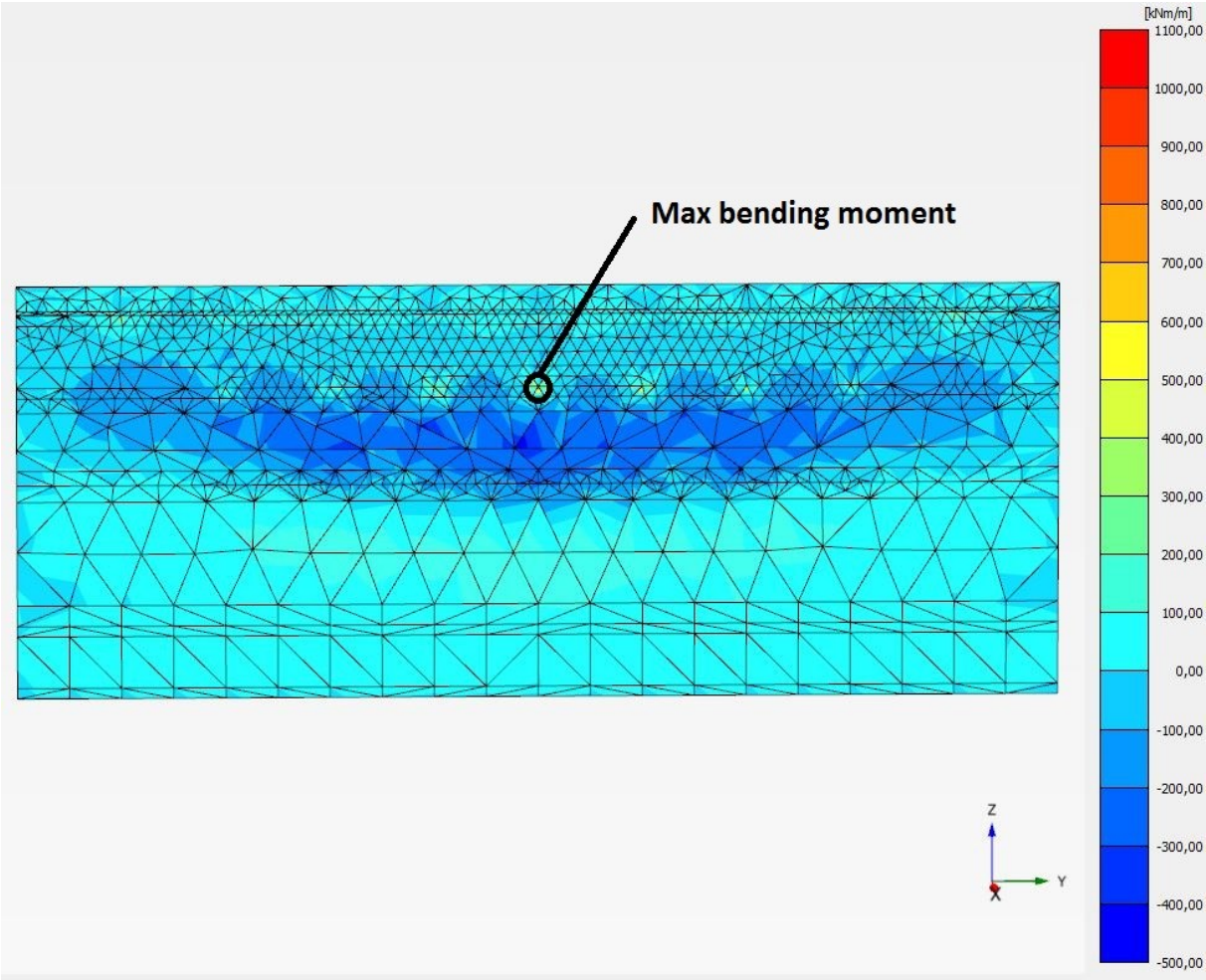


Figure 6-15 Bending moments of test model at calculation stage6

6.4. Conclusion of testing for sequential excavation

As it was stated in Section 5.4, the conclusion of 3D modelling, the sequential model made was not preferable, due to limited advantage in reducing the deformations and high cost in execution. The intention of this chapter was to investigate the optimization of sequential excavation model, so that the sequential model is more favourable.

Several different scenarios were tested including different struts set-up, excavation step and excavation directions. The main focus was the excavation step, since the most difficult part of execution of sequential model was the small excavation step used in the first sequential excavation model. The excavation step tested ranged from 5metre to 25metre. However, the results were less impressive as the number of test operated. The results from normal staged excavation model and the sequential model with 5metre excavation model set the boundaries for all results. In general, longer excavation step result in less calculation time and higher deflection. Ultimately, the whole soil layer was taken at once as the staged excavation model simulated. Unfortunately the range between the two boundaries was very small in terms of real project. Therefore, all models with different length of excavation steps were as unprofitable as the sequential excavation model presented in Chapter 5.

Due to the same reason, the results from other tested model with different struts set-up and excavation direction were also in the narrow range of results. It is hard to distinguish the real difference in different test method. Thus it is hard to draw a real conclusion that how the sequential excavation method would benefits from these optimizations.

Based on the test experience presented in this Chapter, it is advised to apply the sequential excavation model when it is really needed. For instance, the results from normal staged excavation model were acceptable. Thus the potential of improving the results is low, the advantage of applying sequential model is low. Further testing on 3D FEM sequential excavation method is still recommended as how different excavation plan influence the final results remains unclear.

7. Conclusions and recommendations

7.1 Introduction

Three dimension finite elements method is still a rather new method that rarely applied in geo-engineering design. The analytical method and 2D numerical methods provide a decent accuracy of estimation for retaining structure and require a lot less time to operate, compared to 3D FEM model. However, whether the plain strain or axisymmetric approach applied in 2D model, it is simplified or even idealized conditions. When it comes to the problem that geometry matters, it is hard or even impossible to analyse in 2D solutions. For instance, the 3D FEM models presented in this thesis, a lot of parametric studies for the geometry are tested. The test results show that the dimension of excavation pit may have great influence over the response of the sheet pile wall. The sequential model is impossible to model in 2D due to multi cross-sections.

In this chapter, the comparison between 2D and 3D models, and the various results from 3D sequential models are concluded; the advantages and disadvantages for applying sequential excavation method in both numerical model and real construction are specified; the recommendations for future research are highlighted.

7.2 Conclusions of modelling

The whole graduation project contains fair amount of numerical calculations and analysis regarding the excavation and retaining structure of the Spaarndammertunnel. The soil profile and parameters were collected from in situ soil investigation. The parameters were also compared with the database of Amsterdam North-South metro line. The structural design and material properties were implemented into numerical models based on the preliminary design of the Spaarndammertunnel project.

The soil and building material parameters were tested and verified in two different common geo-technical software, D-Sheet piling and PLAXIS 2D. These two numerical programmes approach the excavation process with two different theories. The results from two different programs corresponded with each other. The difference was mainly caused by the normal force in the struts, as D-Sheet piling is not able to handle an asymmetrical domain automatically.

The same soil and building material parameters were later used in 3D FEM models. The 3D staged excavation model uses the same calculation set-ups as 2D model. Parametric studies regarding the size of the excavation pit and the mesh set-up for 3D models are done. The results show that when the excavation zone is longer than 50 metres, the domain can be considered as plain strain situation. The calculation results for the deflection and bending moments of sheet pile wall, the settlement around the pit and the deformation and force within struts were at the same level in both 2D and 3D staged excavation models. The refinement of the mesh plays important role affection the calculation time and results accuracy.

Based on the modelling experience in this project, the main differences between 2D and 3D FEM models are the geometry and mesh set-up. The result varies due to the change of section length in 3D model, even if the cross-section remains the same. Due to the size of the domain, there are way more nodes and stress points in 3D models than 2D. As it is introduced in Chapter 3, the

discretization of domain is different in PLAXIS 2D and 3D. If the mesh is not properly set up, it causes some nodes receiving very high stresses during the calculations. The meshing of 3D model for this project may be the reason causing unexpected high bending moments where the 1st struts locate.

- What are the conditions that worth applying 3D modelling, and how the project can benefit from 3D modelling?

It is worth applying 3D FEM model if the domain is hard to approach for 2D or the optimization of domain size needs to be done. According to this specific project, when the length of the excavation section is shorter than 2.5 times of the width, the project can benefit from the corner effect in 3D models. The deflection and bending moments in sheet pile wall, and the settlement of the surrounding area are reduced.

7.3 Advantages and disadvantages of sequential excavation model

Judging by the results from normal 2D/3D models and 3D sequential model, the major benefit of using sequential excavation is to minimize the settlement of the surrounding area. The settlement and affecting area in sequential model is significantly lower compared to normal staged excavation model. But in terms of optimizing the retaining structure performance, the advantage of using sequential excavation is not that convincing. This can be caused by the rather simple excavation domain shape and the low range of optimization for sheet pile wall design. Since the deflections and bending moments for sheet pile wall were already optimized in the original design, the potential of decreasing the deflections and bending moments are low. Apart from the design, the geometry of the excavation zone is also chosen with the values that is easy to be compared with 2D models. For instance, if the length of the excavation pit is 30m instead of 50m, as it is shown in section 4.2.2, the deflections and bending moments are a lot lower due to the corner effect in 3D modelling. But the size and the shape of current excavation pit make it possible to be modelled by plain strain approach. The benefit of applying 3D modelling thus is limited.

Meanwhile applying 3D modelling and 3D sequential modelling for excavation also means high cost. The modelling itself requires a lot more time for calculation and engineering experience to analyse the results. For this particular project, the 2D PLAXIS model takes around 2 hours for calculation, while the 3D model requires 1-2 hours per calculation stage. For example the sequential model with 5m excavation step with 15 calculation stages takes around 25 hours to finish calculation.

As a matter of fact, the sequential excavation with small excavation step is hard to perform in reality. The extreme case tested in numerical models is the one with 5m excavation step, which means the excavation goes forward 5m per day. Since the concrete floor constructed on the bottom of the building pit requires time to dry out. Moreover, it also costs time for shifting the excavator and equipment for pouring concrete floor. Thus the sequential excavation will inevitably result in high building cost.

- How Spaarndammertunnel project can benefit from sequential excavation model?

To summarise, the disadvantages of 3D sequential excavation model for this project outweigh the advantages. The 3D sequential model requires too much time to calculate, but the benefits gained from sequential model are not very significant. The execution of the sequential excavation with small excavation step is not favourable in real construction as well. But for some projects locate in city

centre and the surroundings are really sensitive to settlement, it is useful to apply the sequential excavation to minimize the influenced zone due to excavation.

7.4 Recommendations for future research

- Verification with field test

One of the aspects that this graduation project really lacks is the verification from monitoring data. The sequential model is promising as it reduces the deflection and bending moments for retaining walls. But the calculation results only come from the PLAXIS 3D software. There are many aspects affect the test result in numerical modelling, especially 3D FEM modelling. The discretisation of the domain, for instance, can greatly influence the stress distribution. So the first recommendation for further research is the comparison between numerical model and data collected from real construction. The verification from the monitoring data can greatly help to improve the modelling.

- Test with complex excavation domain

Based on the research done in this project and experience learned from other 3D FEM models, the advantage of applying 3D FEM modelling would be more significant when the construction and excavation domain is more complex. Thus the corner effect would contribute more in the results for modelling. As it is illustrated in *Figure 7-1*, the excavation zone with reflex angle would be very hard to simulate for 2D modelling. This can cause more problems for projects using anchors as lateral support, since multiple anchors are pulling the soil in different directions. However, the excavation zone in this project is a simple rectangular shape. When the length of the excavation pit reaches a certain value, the problem becomes more like plain strain situation, which is the same in 2D PLAXIS.

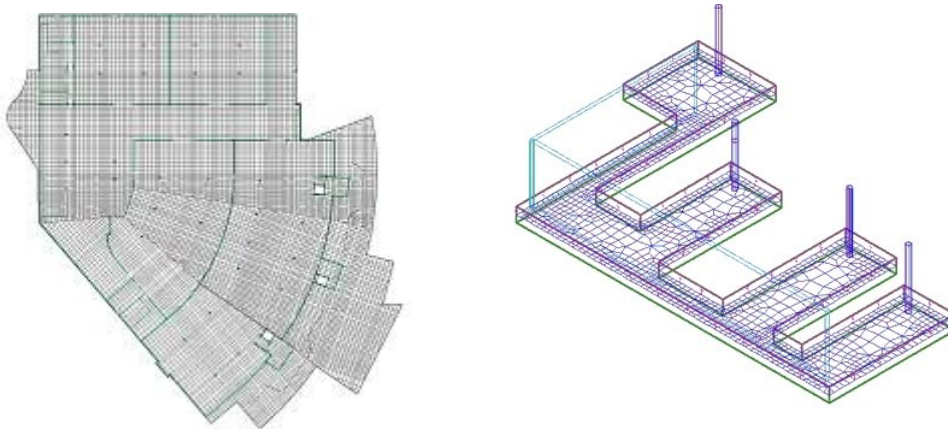


Figure 7-1 Example of more complex excavation zone

- Test for the lateral support set-up

According to the test results in Chapter 4, 5 and 6, the lateral support in the models can be further optimized. Especially for the bending moments in sheet pile walls, the places where the high struts locate result in very high values. Whether it is because of the parameters used for struts and wailing beam or the numerical noise, is not yet clear in this project. There are some researches done for the struts and wailing beam in PLAXIS models, investigating the proper setting and the comparison between numerical modelling and real case. But the results are not clear and definite. Some

parameters used in this graduation research are adopted from suggestions given in other master thesis. Unfortunately the results in this project are not as positive as the original article suggested.

- Test for the mesh set-up

Last but not least, the meshing as mentioned many times in this thesis does influence the test results notably. For PLAXIS, the mesh is generated semi-automatically. It would be useful to investigate how the mesh set up affect the final results in 3D modelling. The difference between the mesh set up in 2D mesh and 3D, and how it influence the difference in results. When a sophisticated excavation domain is applied, proper mesh set up would help remarkably.

Bibliography

Bartels (2014) – Spaarndammertunnel Amsterdam project introduction. Available at <http://www.bartels-global.com/projects/spaarndammertunnel-amsterdam>.

Biot, M.A (1937) – Bending of an Infinite Beam on an Elastic Foundation. *Journal of Applied Mechanics*, Volume4, Pages A1-A7.

Blum, H. (1931) – *Einspannungsverhältnisse bei Bohlwerken*. W. Ernst & Sohn. Berlin.

Boussinesq,J. (1885) – Discussed in *Theory of Elasticity*, McGraw-Hill, N.Y. (1970) Page 398-402.

Caquot,A. and Kerisel,J. (1048) – *Tables for the Calculation of Passive Pressure, Active Pressure, and Bearing Capacity of Foundations*, Gauthier-Villars, Paris.

Coulomb, C. A. (1776) – *Essai sur une application des regles des maximis et minimis a quelques problemesde statique relatifs, a la architecture*. *Mem. Acad. Roy. Div. Sav.*, vol. 7, Page 343–387.

CUR 166 – *Damwandconstructies*, 4th edition

Day, R. A. & Potts, D. M. (1993) – “Modelling sheet pile retaining walls”. *Computers and Geotechnics*, 15, Page 125- 143.

Delattre,L (2001) – A century of design methods for retaining walls, The French point of view. *Bulletin Des Laboratoires des ponts et chaussées* (2003), Page 31-51

Eurocode 7 (BS EN 1997-1:2004). “Geotechnical design - Part 1: General rules.” *Computers and Geotechnics*, 15, 125- 143.

Han, S.M.; Benaroya, B.;Wei,T., (1999) – Dynamics of Transversely Vibrating Beams using four Engineering Theories. *Journal of Sound and Vibratations*, Volume 225(5), Page935 – 988

Jaky J., (1948) – *Pressure in soils*, 2nd ICSMFE, London, Vol. 1, Page 103-107.

Kim, D. et al., (2010) – *Geotechnical Design Based on CPT and PMT*. Purdue University. Available at Purdue e-Pubs. Page 56 – 67.

Lunne, T., and Andersen, K.H., (2007). Soft clay shear strength parameters for deep water geotechnical design. *Proceedings 6th International Conference, Society for Underwater Technology, Offshore Site Investigation and Geomechanics*, London, Page 151-176.

Lunne, T., Eidsmoen, T., Gillespie, D., and Howland, J.D., (1986). Laboratory and field evaluation on cone penetrometers. *Proceedings of ASCE Specialty Conference in Situ’86: Use of In Situ Tests in Geotechnical Engineering*. Blacksburg, ASCE, GSP 6 Page 714-729

Lunne, T., Robertson, P.K., and Powell, J.J.M., (1997). *Cone penetration testing in geotechnical practice*. Blackie Academic, EF Spon/Routledge Publ., New York, 1997, Page 312 .

Obrazud. R, (2010) – On the use of Hardening soil model. Numerics in geotechnics and structures, 25 YEARS ZSOIL&STRUCTURES. 30-31 August 2010. Lausanne

Ou, C.Y, (2006) – Deep Excavation: Theory and Practice. CRC Press. Page 91 – 120.

Ou, C.Y; Chiou,D.C.; Wu, T.S, (1993) – Three-dimensional finite element analysis of deep excavations. Journal of Geotechnical Engineering, Volume 122(5), Pages 337-345.

PLAXIS, (2011) – PLAXIS 2D Material models manual. <http://www.plaxis.nl/files/files/2D2011-3-Material-Models.pdf>. P193 – P194.

PLAXIS, (2013) – Plaxis 3D Reference Manual.

Potts,D., and Zdravkovic, L., (1999) – Finite Element Analysis in Geotechnical Engineering. Thomas Telford Limited

Rankine, W., (1857) – On the stability of loose earth. Philosophical Transactions of the Royal Society of London, Vol. 147.

Rémai,Z, (2012) – Correlation of undrained shear strength and CPT resistance. Periodica Polytechnic Civil Engineering 57/1 (2013) Page 39 – 44.

Robertson, P.K and Cabal, K.L (2012) – Guide to Cone Penetration Testing for Geotechnical Engineering. 5th Edition. www.cpt-robertson.com.

Rowe, P. W. (1955) – “A theoretical and experimental analysis of sheet-pile walls”. ICE Proceedings. Part I, Vol. I.

Terzaghi, K. (1943) – Theoretical soil mechanics. New York: John Wiley & Sons.

USS (1975) – “Steel Sheet Piling Design Manual”. United States Steel.

Verruijt, A. (2012) – Soil Mechanics. Available at <http://geo.verruijt.net/>.

Appendix A – CPT data and derivation of soil parameters

1. Soil investigation and CPT correlations

The soil investigation for the Spaarndammertunnel includes 84 CPTs and 8 bore holes. The CPT data provides the information for the soil identification, estimation of geotechnical parameters and direct evaluation of pile bearing capacity (Robertson et al., 2012).

2. CPT correlation and soil parameters

The main part of the soil investigation for Spaarndammertunnel is the CPT data. In order to get the soil parameters, certain correlations are needed. However, some empirical correlations represent more or less local correlations, and are not always applicable to different types of soil (Robertson et al., 2012)

The undrained shear strength S_u is one of the most important design parameters in clay soils, can be derived from CPT data by applying certain correlations. The general equation for estimating S_u is:

$$S_u = \frac{q_t - \sigma_v}{N_k} \quad (3)$$

Where N_k is the cone factor, q_t is the cone resistance and σ_v is total overburden stress. Typically N_k varies from 10 to 18, with 14 as an average for S_u (ave).

Some researchers claim the cone factor N_k is influenced by a plasticity index I_p , and suggest correlations between N_k and I_p (Lunne et al. 1976, Baligh et al. 1980, Lunne and Kleven 1981, Aas et al. 1986, and Rochelle et al. 1988) However, the results from Aas et al. (1986) show increasing trends of cone factor with plasticity index, while Lunne et al. (1976) and Baligh et al. (1980) show decreasing trends. Thus the trend of cone factors N_k are not consistent and based on localized soil data. It is evident that there is not a clear and reliable correlation between cone factor N_k and I_p so far (Daehyeon Kim. et al., 2010).

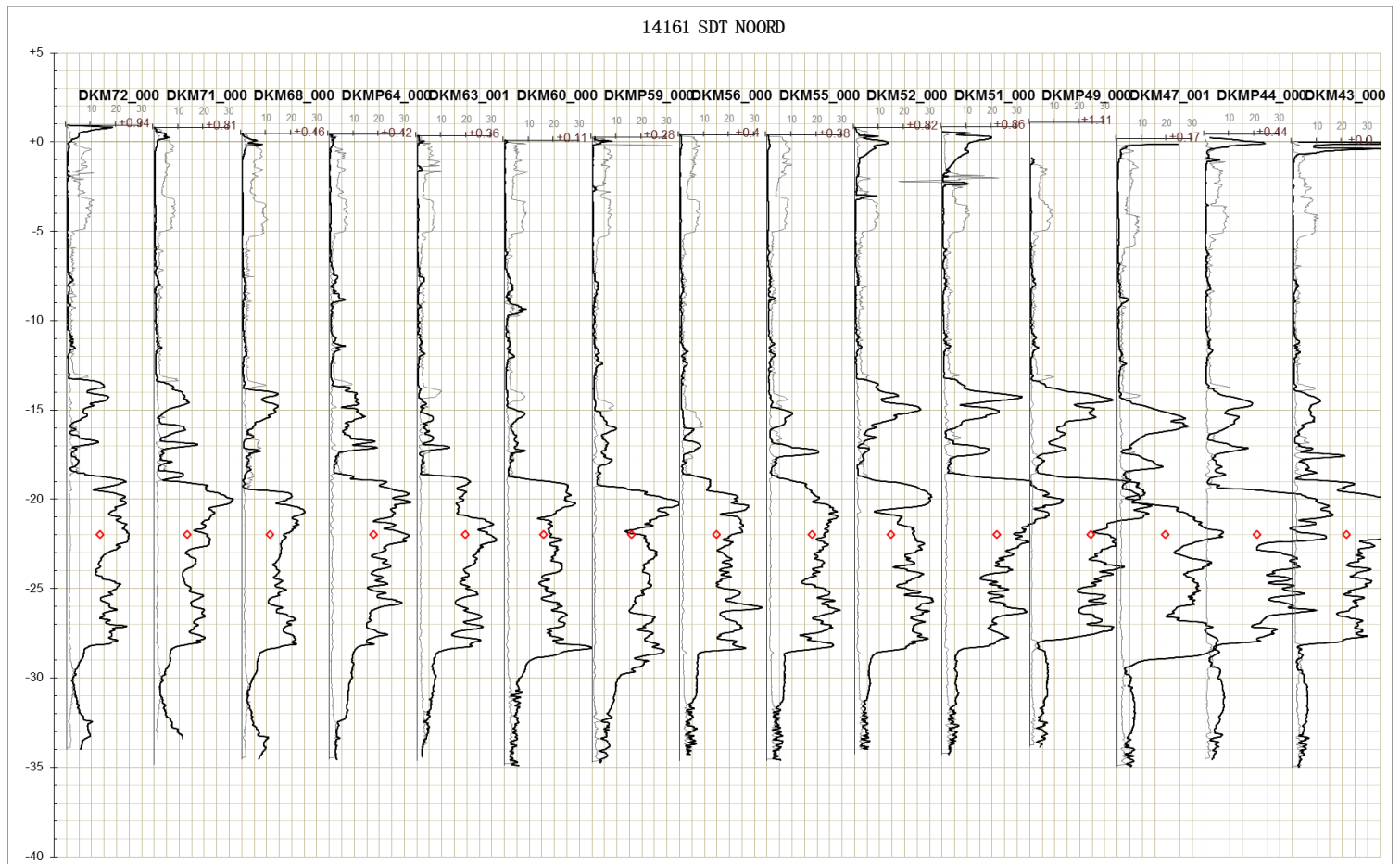
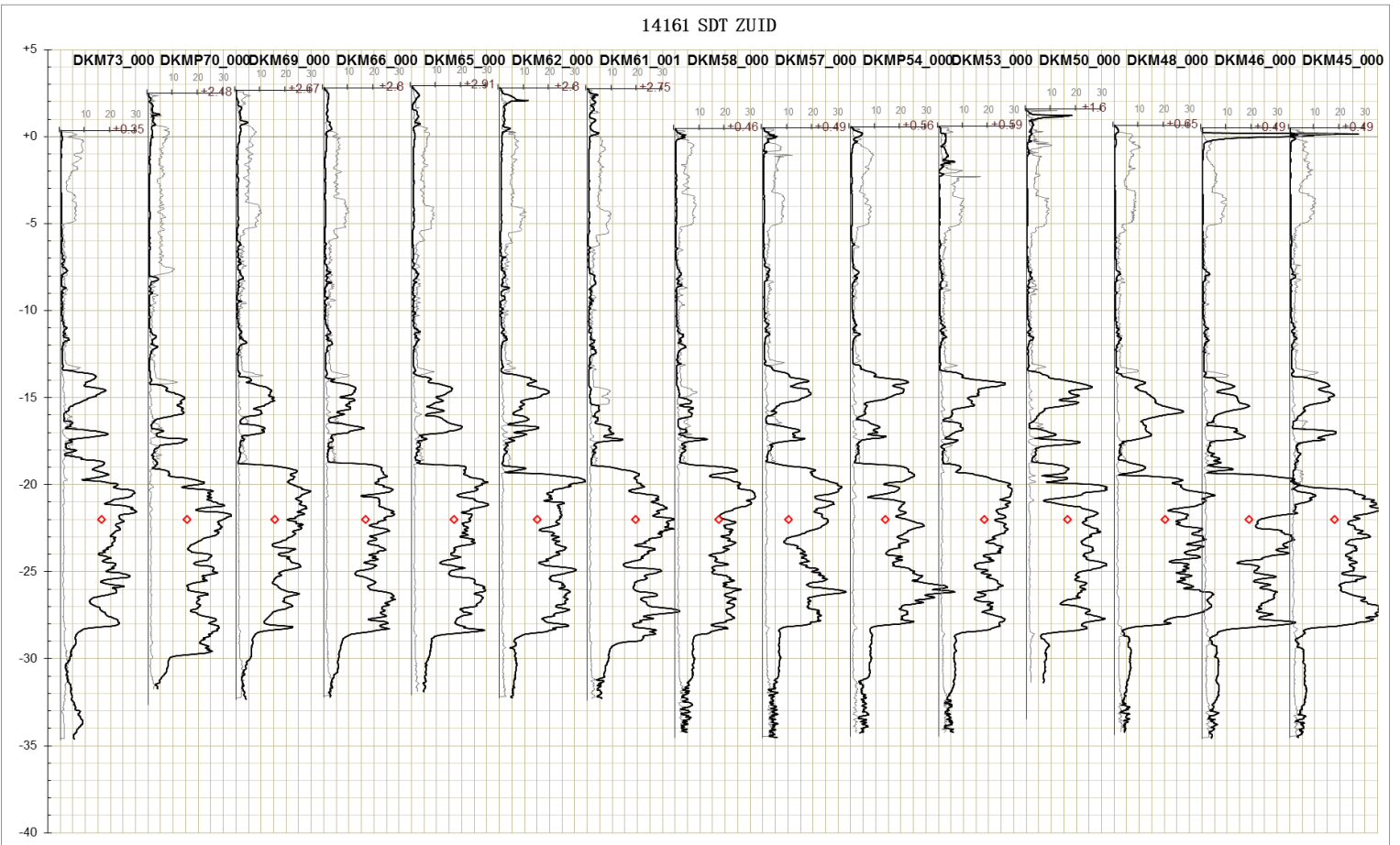
Daehyeon Kim et al., (2010) suggested, the cone factor is influenced by soil type, penetration rate during the CPT, and test methods for undrained shear strength.

P. K. Robertson et al. (2012) stated N_{kt} tends to increase with increasing plasticity and decrease with increasing soil sensitivity. Lunne et al., 1997 showed that N_{kt} varies with normalized pore pressure parameter, B_q , where N_{kt} decreases as B_q increases. In sensitive fine-grained soil, $B_q \sim 1.0$, N_{kt} can be as low as 6.

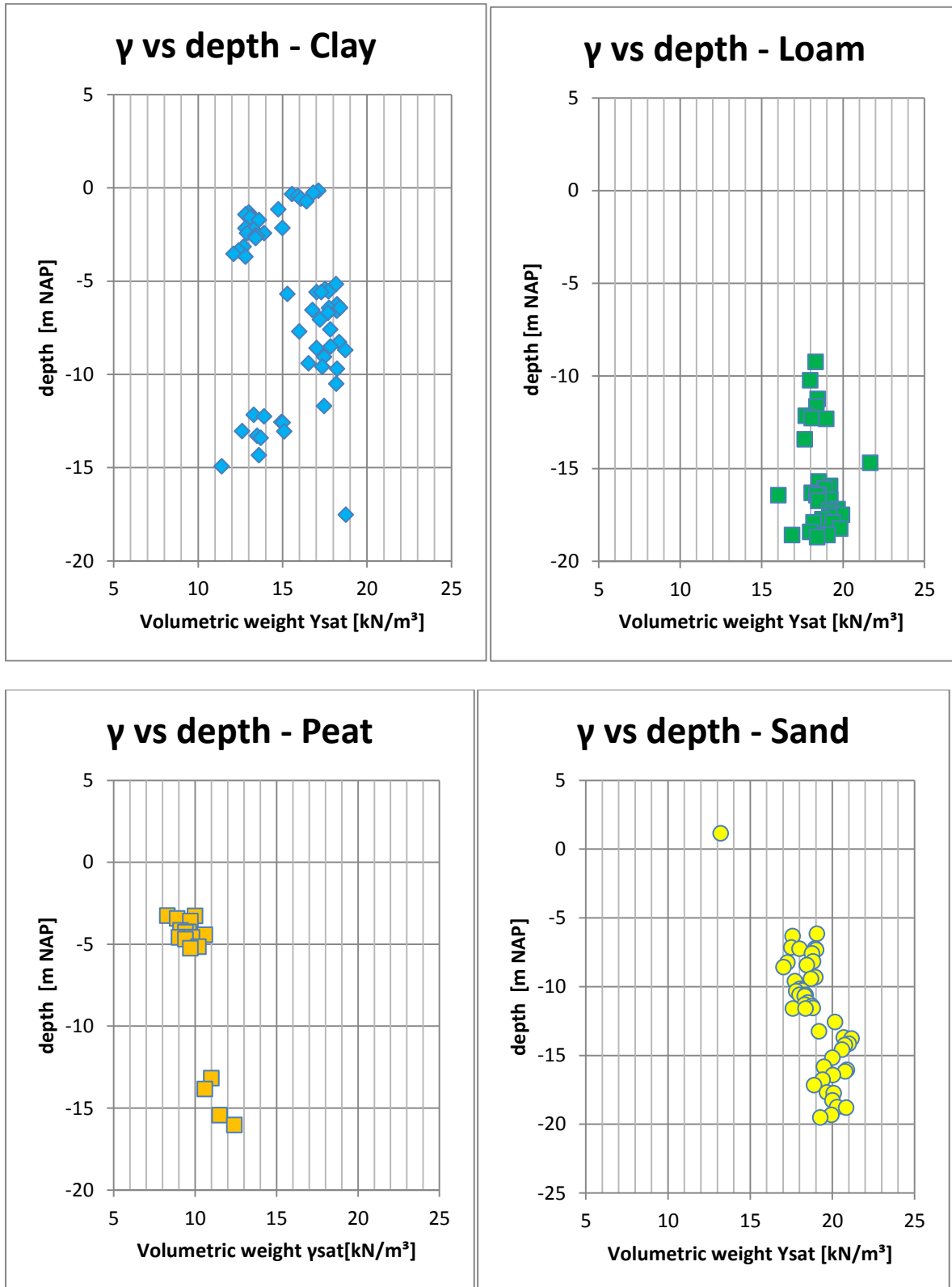
Zsolt Rémai (2012) also stated that the use of soil parameters (e.g. plasticity index, overconsolidation ratio, pore pressure coefficient of CPT) dependent cone factor to improve the accuracy does not result in reliable correlations for soft Holocene clay. But a reliable correlation was found between cone factor $N_{\Delta u}$ and the CPTu pore pressure coefficient B_q . Using a B_q dependent cone factor $N_{\Delta u}$ increases the reliability of the calculation (Rafal Obrazud, 2010).

As a conclusion, there is no certain correlation for CPT data that can be applied universally. The correlation is depended on local engineering experience and vast number of soil test. As for this project, the number of lab soil test is limited. And certain local correlation cannot be derived. Moreover, deriving a local correlation is not the main topic in this thesis. However, the location of the tunnel is close to the Amsterdam North-South metro line, where extended soil investigation has been performed. And the company CRUX Engineering BV also has a lot of experience for geotechnical engineering in Amsterdam. Thus soil parameters are derived from CPT data, and based on the Amsterdam North-South metro line database, and previous engineering experience from CRUX Engineering.

3. CPT results



4. Volumetric weight of different soil layers



Appendix B – Analytical method for retaining structure design

1. Lateral stresses in soil

Lateral earth pressure is the pressure that soil exerts in the horizontal direction. The lateral earth pressure is important because it affects the consolidation behaviour and strength of the soil and because it is considered in the design of geotechnical engineering structures such as retaining walls, basements, tunnels, deep foundations and braced excavations.

The coefficient of lateral earth pressure, K , is defined as the ratio of the horizontal effective stress, σ'_h , to the vertical effective stress, σ'_v . The effective stress is the inter-granular stress calculated by subtracting the pore pressure from the total stress as described in soil mechanics. K for a particular soil deposit is a function of the soil properties and the stress history.

Suppose friction does not exist between the retaining wall and the soil. When the retaining wall is not allowed to move, the stresses below the ground surface are under elastic equilibrium with no shear stresses. The lateral earth pressure at rest of a horizontal layered soil mass can be estimated with:

$$\sigma'_h = K_0 * \sigma'_v \quad (4)$$

In which σ'_h is the horizontal effective stress, σ'_v is the vertical effective stress and K_0 is the lateral earth pressure coefficient at rest.

The total lateral stress is

$$\sigma_h = \sigma'_h + u \quad (5)$$

In which u is pore water pressure, the sum of the static water pressure and excess pore water pressure.

The lateral earth pressure coefficient at rest K_0 , can be measured by a dilatometer test (DMT) or a borehole pressuremeter test (PMT). But these tests are rather expensive to perform. Empirical methods are developed to estimate the value of K_0 .

For cohesionless soil, K_0 can be estimated by Jaky's (1944) equation:

$$K_0 = 1 - \sin \phi' \quad (6)$$

In which ϕ' is the effective internal angle of friction.

When cohesionless soils are in the unloading or preconsolidated states (i.e. overconsolidated), K_0 can be expressed by the following equation (Alpan 1967; Schmidt 1967):

$$K_{0,OC} = K_{0,NC} * (OCR)^\alpha \quad (7)$$

In which $K_{0,OC}$ is the coefficient of lateral earth pressure at rest of overconsolidated soils with overconsolidation ratio, OCR; $K_{0,NC}$ is the coefficient of lateral earth pressure at rest of a normally consolidated soil; α is empirical coefficient, $\alpha \approx \sin \varphi'$.

In general, Eq (4) provides accurate enough results for normally consolidated soil. For over consolidated clay, no matter cohesive or not, the results from Eq (5) are not satisfactory. The complexity of the formation process of over consolidated clay is one of the main reasons. The best way to determine the K_0 value is to carry out in situ test.

2. Rankine earth pressure theory

Rankine's theory, developed in 1857 by William John Macquorn Rankine, is a theory of lateral earth pressure in conditions of failure in front of and in back of a retaining wall on the basis of the concept of plastic equilibrium. The possible stresses in a soil are limited by the Mohr-Coulomb failure criterion.

Rankine's Theory assumes that failure will occur when the maximum principal stress at any point reaches a value equal to the tensile stress in a simple tension specimen at failure. This theory does not take into account the effect of the other two principal stresses. Rankine's theory is satisfactory for brittle materials, and not applicable to ductile materials. This theory is also called the Maximum Stress Theory. This theory, which considers the soil to be in a state of plastic equilibrium, makes the assumptions that the soil is homogeneous, isotropic and has internal friction. The pressure exerted by soil against the wall is referred to as active pressure. The resistance offered by the soil to an object pushing against it is referred to as "passive pressure". Rankine's theory is applicable to incompressible soils. The Rankine theory assumes a frictionless soil-wall interface and a vertical wall (no wall slope).

The parameters of soil strength on both side of retaining wall are c and ϕ . Suppose there is no friction between the retaining wall and adjacent soil, the earth pressure coefficient of soil on both sides are K_0 before the retaining wall moves. The Rankine theory is demonstrated in [Figure 0-1](#).

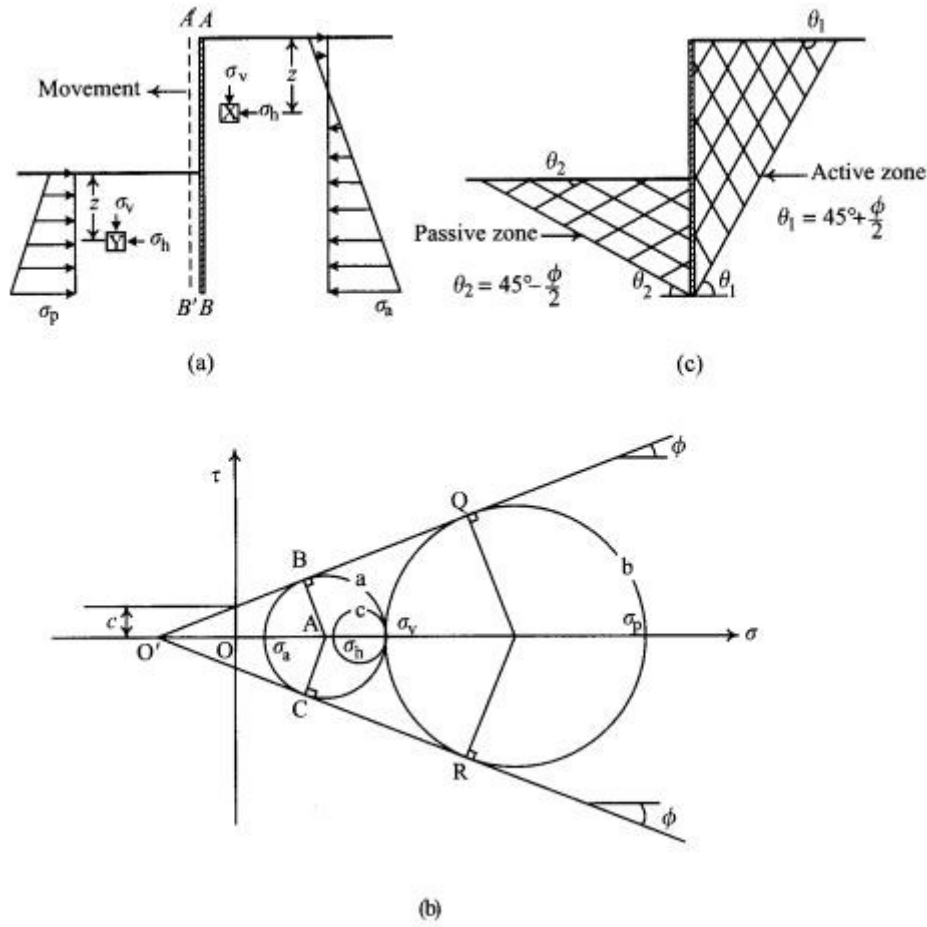


Figure 0-1 Rankine's earth pressure theory (Source: Ou.C.Y, 2006)

The figure A in Figure 0-1 shows that the earth pressure on the back of the retaining wall causes the wall to shift from position AB to A'B'. The horizontal stress then decreased while the vertical stress remains the same. The Mohr's circle shown in figure B grows larger and intersects with the failure envelope at a certain point. The pressure induces this kind of failure is called active earth pressure.

$$\sin \phi = \frac{AB}{AO'} = \frac{AB}{OO' + OA} = \frac{(\sigma_v - \sigma_a) / 2}{c * \cot \phi + (\sigma_v + \sigma_a) / 2}$$

Thus the soil pressure on the active side can be expressed by:

$$\sigma_a = \sigma_v \frac{1 - \sin \phi}{1 + \sin \phi} - 2c \frac{\cos \phi}{1 + \sin \phi} = \sigma_v * K_a - 2c * \sqrt{K_a} \tag{8}$$

In which K_a is the Rankine's coefficient of lateral active earth pressure.

$$K_a = \tan^2(45^\circ - \frac{\phi}{2})$$

The soil pressure on the passive side is expressed by:

$$\sigma_p = \sigma_v \tan^2\left(45^\circ + \frac{\phi}{2}\right) + 2c \tan\left(45^\circ + \frac{\phi}{2}\right) = \sigma_v * K_p + 2c * \sqrt{K_p} \tag{9}$$

In which K_p is the Rankine’s coefficient of lateral active earth pressure.

$$K_p = \tan^2\left(45^\circ + \frac{\phi}{2}\right)$$

Rankine’s earth pressure theory applies, originally, only to problem under specific conditions: vertical and smooth wall backs, homogeneous soil, level grounds, and no surcharge. Real excavation problems, however, are seldom that pure and simple. Some modifications are necessary when applying the theory to practical cases.

3. Coulomb earth pressure theory

Long before the analysis of Rankine the French scientist Coulomb presented a theory on limiting states of stress in soils. The theory enables to determine the stresses on a retaining structure for the cases of active and passive earth pressure. The method is based upon the assumption that the soil fails along straight slip planes. (Verruijt) And the soil in back of the retaining wall is homogeneous and cohesionless, the wedge between the wall and the failure surface is rigid material, and the weight of the wedge, the reaction of the soil and the reaction of the wall are in equilibrium.(Ou CJ)

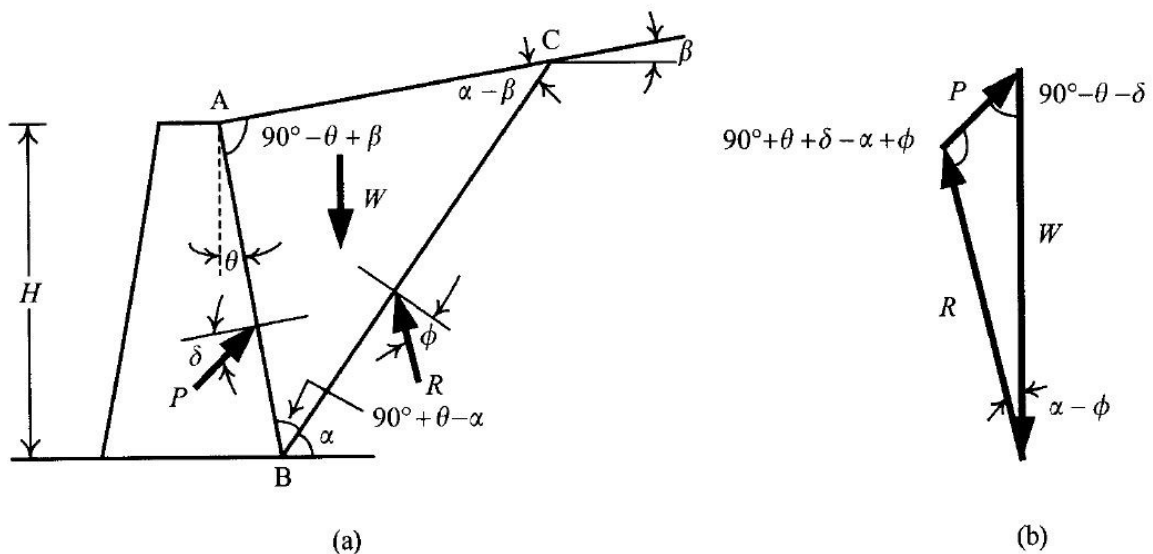


Figure 0-2 Coulomb's active earth pressure (source OU,C.Y 2006)

In **Figure 0-2**, the height of the retaining wall is represented by H , the angle of friction for the soil is ϕ , and the angle of friction between the wall and soil is δ . BC is the assumed failure plane that intersects with the horizontal plane at an angle of α . The **Figure 0-2** (b) demonstrates the force equilibrium by the reaction of the wall against the wedge (P), the reaction of soil against the wedge[®] and the weight of soil (W). Thus the following equation can be derived.

$$\frac{W}{\sin(90^\circ + \theta + \delta - \alpha + \phi)} = \frac{P}{\sin(\alpha - \phi)} \tag{10}$$

$$P = \frac{W \sin(\alpha - \phi)}{\sin(90^\circ + \theta + \delta - \alpha + \phi)} = \frac{1}{2} \gamma H^2 \left[\frac{\cos(\theta - \alpha) \cos(\theta - \beta) \sin(\alpha - \phi)}{\cos^2 \theta \sin(\alpha - \beta) \sin(90^\circ + \theta + \delta - \alpha + \phi)} \right] \tag{11}$$

In which γ is unit weight of soil, parameters $\gamma, \phi, \theta, \delta, \beta, H$ are constants, α is a variable since BC is one of the assumed failure planes. P varies with α . Thus the minimum active pressure P_a can be calculated by:

$$\frac{dP}{d\alpha} = 0$$

$$P_a = \frac{1}{2} \gamma H^2 K_a \tag{12}$$

$$K_a = \frac{\cos^2(\phi - \theta)}{\cos^2 \theta \cos(\delta + \theta) \left[1 + \sqrt{\frac{\sin(\delta + \theta) \sin(\phi - \beta)}{\cos(\delta + \theta) \cos(\phi - \beta)}} \right]^2} \tag{13}$$

In which K_a is Coulomb's coefficient of active earth pressure. When $\theta = 0, \beta = 0$ and $\delta = 0$, $K_a = \tan^2(45^\circ - \frac{\phi}{2})$, which corresponds to Rankine's.

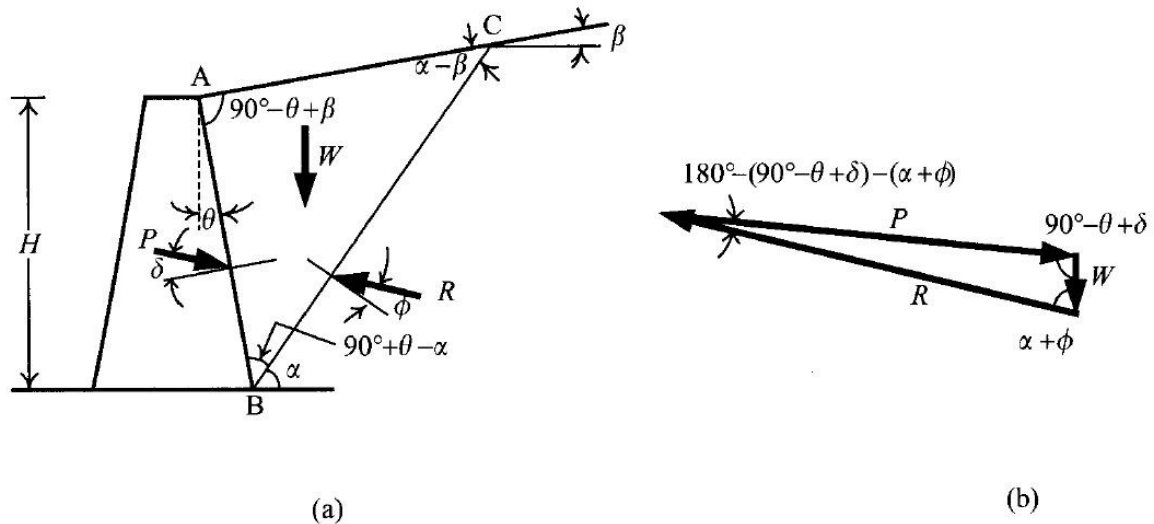


Figure 0-3 Coulomb's passive earth pressure (source OU,C.Y 2006)

The Figure 0-3 illustrates the passive soil failure in back of the retaining wall that is pushed away by an external force. BC is an assumed failure surface. The passive earth pressure (P_p) can express by:

$$P_p = \frac{1}{2} \gamma H^2 K_p \tag{14}$$

$$K_p = \frac{\cos^2(\phi + \theta)}{\cos^2 \theta \cos(\delta - \theta) \left[1 + \sqrt{\frac{\sin(\phi + \delta) \sin(\phi + \beta)}{\cos(\delta - \theta) \cos(\beta - \delta)}} \right]^2} \quad (15)$$

In which K_p is Coulomb's coefficient of passive earth pressure. When $\theta = 0, \beta = 0$ and $\delta = 0$, $K_p = \tan^2(45^\circ + \frac{\phi}{2})$ which corresponds to Rankine's as well.

The Coulomb's method can be extended to more general cases, for instance, when the soil surface is a slope instead of flat surface, and the soil may carry a surface load. There are three essential steps when applying Coulomb's earth pressure theory:

- Selection of plausible failure mechanism
- Determination of forces on failure surface
- Use equilibrium equations to determine the maximum thrust

4. Other earth pressure theories

There are some later theories introduce more advanced and sophisticated method to analyse the lateral earth pressure. For instance in 1948, Albert Caquot (1881–1976) and Jean Kerisel (1908–2005) developed an advanced theory that modified Muller-Breslau's equations to account for a non-planar rupture surface. They used a logarithmic spiral to represent the rupture surface instead. This modification is extremely important for passive earth pressure where there is soil-wall friction (Wiki). But these theories are way too complicated to calculate by hand. Instead, tables and computers are used when applying these advanced theories.

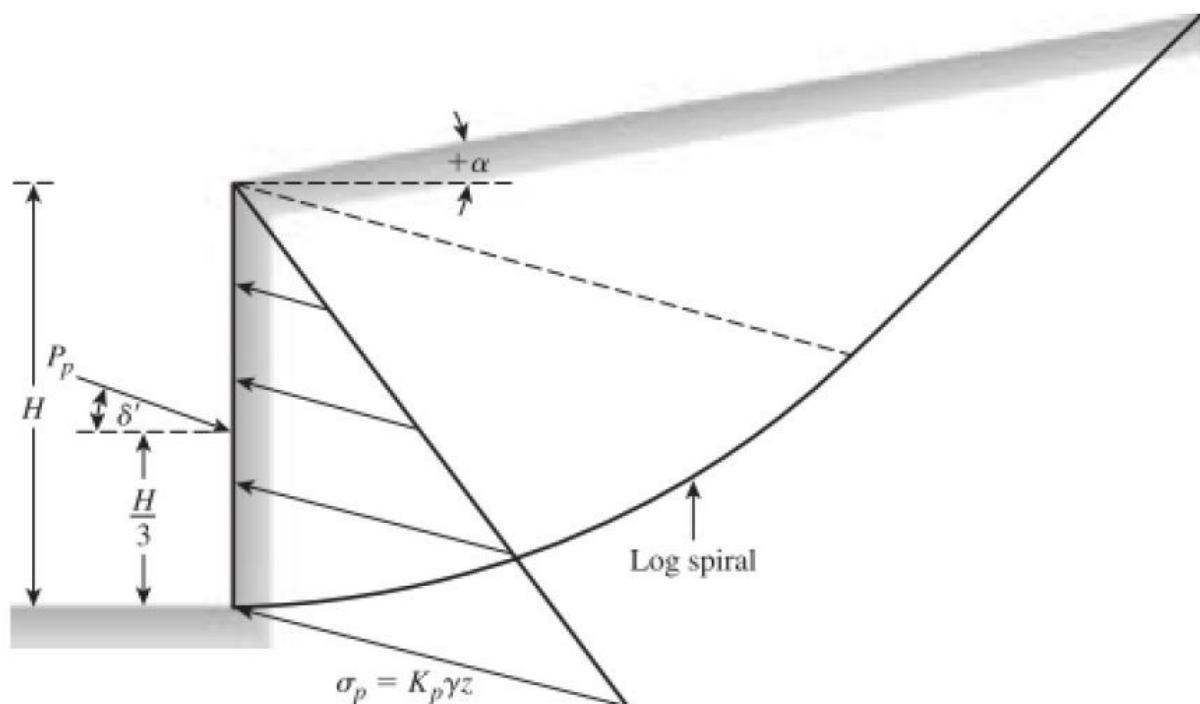


Figure 0-4 Illustration of curved slip failure surface based on Caquot and Kerisel solution of K_0 for a vertical retaining wall and inclined backfill (source figure: Das, B.M.; 2007a)

5. Sheet pile wall design

For soft soil with limited space, an effective way to retain the soil is to install a vertical wall consists of long thin elements. These sheet pile walls are normally made of steel, vinyl or wood. Compared to traditional gravity and cantilevered retaining walls, the sheet pile wall is easy to install in tight space, re-usable and provides high resistance to driving stresses. It is a flexible structure, in which bending moment develops due to the lateral earth pressure. The deformation and the bending moment are the two most important indexes that the sheet pile wall design has to take into account. The sheet pile wall material needs to be chosen accordingly to the maximum bending moment developed, so that the design is cost efficient and safe. And the deflection of the sheet pile wall directly affects the soil settlement behind the retaining structure. For projects locate in city centre or near roads, the soil settlement would be an important factor.

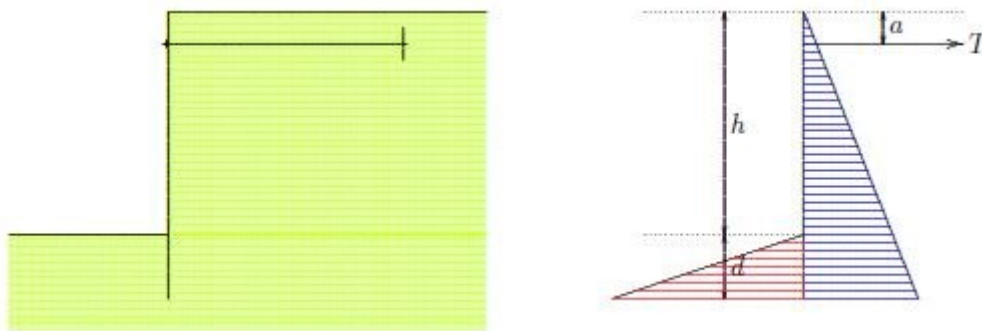


Figure 0-5 cross-section and assumed stress distribution of an anchored sheet pile wall (source: Verruijt, 2007)

The cross-section and assumed stress distribution for an anchored sheet pile wall is illustrated in Figure 0-5. The basic idea of sheet pile wall is that the soil pressure behind the sheet pile wall (on the right side of the sheet pile wall in the figure) causes the sheet pile wall to deform towards left. Thus the soil behind the retaining wall become close to active state. The deformation of the sheet pile wall then initiate the passive stresses to develop on the left of the sheet pile wall. To achieve the equilibrium state, with sufficient length of passive zone can be developed, the embedment of the sheet pile wall needs to deep enough. By adding anchors tie the back of the sheet pile wall to the right, or struts between two parallel walls, the balance can be achieved without very large displacement of the wall.

According to the theory elaborated above, the minimum length (depth of embedment) should be determined first. For an anchored sheet pile wall, the equilibrium of moment at the anchor point can be estimated by:

$$\left(\frac{d}{h}\right)^2 = \frac{2K_a}{3K_p} \left(1 + \frac{d}{h}\right)^2 \frac{1 + (d/h) - \frac{3}{2}(a/h)}{1 + \frac{2}{3}(d/h) - (a/h)} \quad (16)$$

In which, h is the excavation depth, d is the depth of embedment, a is the depth of anchor point, K_a and K_p are coefficient of active and passive earth pressure respectively. Equation (16) can be solved iteratively with an initial estimate of d/h . And the magnitude of the anchor force can be determined from the horizontal force equilibrium.

$$T = \frac{1}{2} K_a \gamma (h + d)^2 - \frac{1}{2} K_p \gamma d^2 \quad (17)$$

In which, T is the anchor force, γ is the volumetric weight of the soil.

Note that this is only a simple demonstration for the principle of how the sheet pile wall length, anchor point and anchor force are determined. In this approximation, the soil is assumed to be homogeneous dry sand with no pore pressure taken into consideration. In case of pore pressures presence, the vertical stresses and pore pressures should be determined first. Then the vertical effective stress can be calculated according to different vertical total stress and pore pressure. The horizontal effective stress can be derived by using appropriate value of K_a or K_p . There are several methods for retaining structure developed in the last century as illustrated in [Figure 0-6](#). The left side of the diagram shows serviceability limit state analysis methods (from right to left (1): classical methods, (2): subgrade reaction method, (3): finite element method (*) and (4): empirical methods) and the right side of the diagram (5) shows ultimate limit state analysis methods. The most widely known and applied theory for analytical estimation, Blum's method, will be introduced in next section.

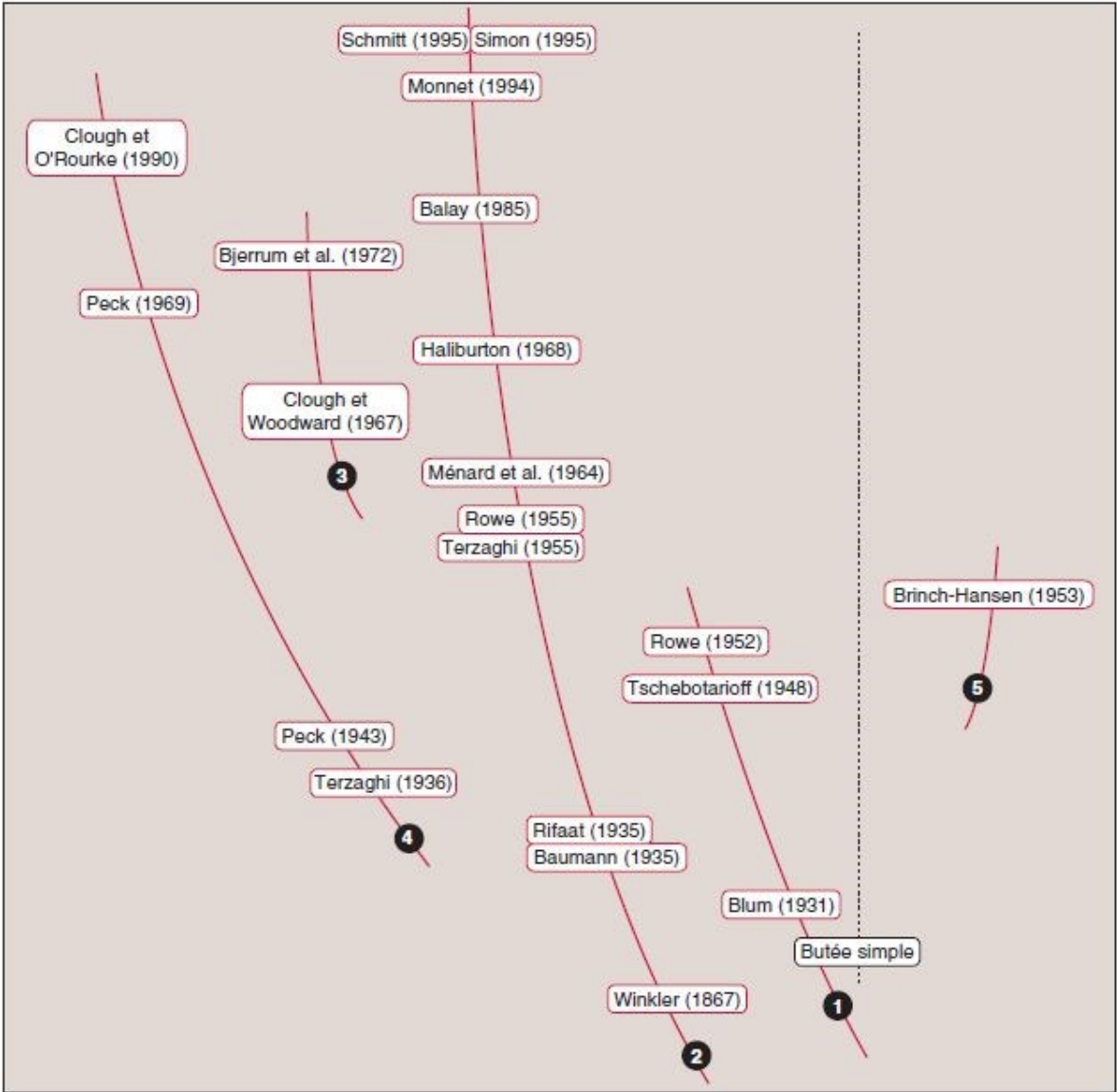


Figure 0-6 major directions and principal stages in the development of retaining walls design methods. (source: Delattre, L 2001)

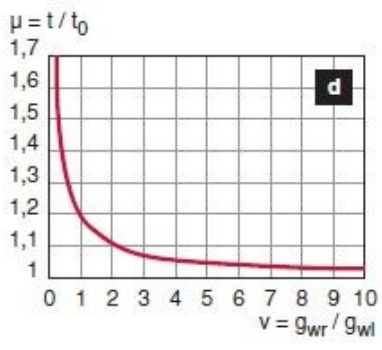
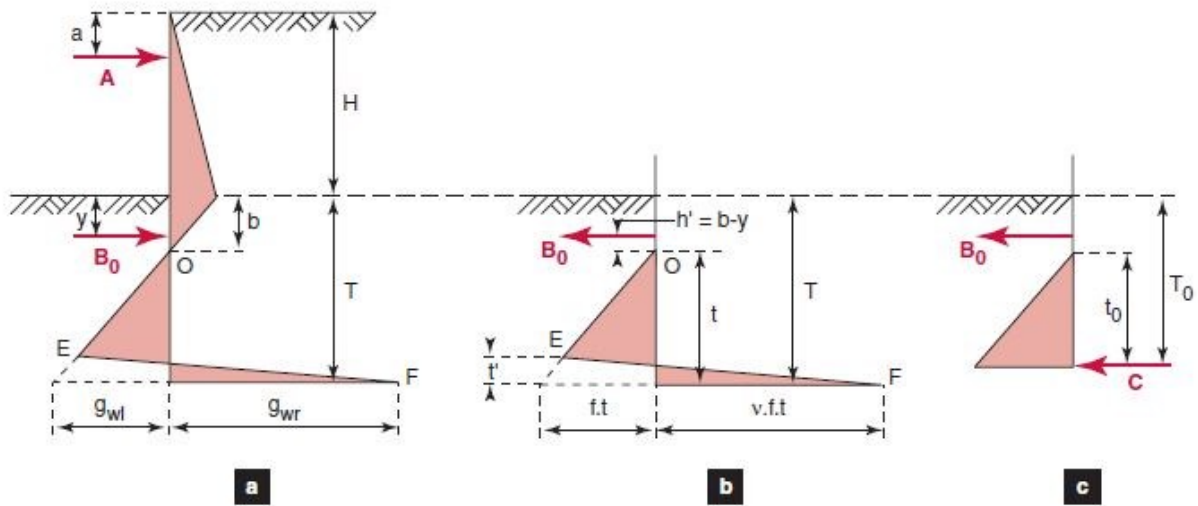
6. Blum’s method

The general procedure of how minimum depth of the sheet pile wall is introduced in section 2.3.1.7, the deformation and bending moment in the wall should be analysed afterwards to secure safety. Certain analytical method was developed by Blum in 1931. In the case of a retaining wall anchored by a row of tiebacks near its top, Blum analysed, for different depths of embedment, the distributions of the pressures acting on the structure, the bending moments and the horizontal deflection of the structure. His analysis was essentially qualitative and based on the interdependence of the distributions (the deflection of the retaining wall has points of inflexion where the moment is zero, as does the plot of moments where the pressure is zero and the mobilized pressure is related to the lateral deflection of the wall). This analysis allowed Blum to observe that those structures with a short embedded depth will simply be supported by the soil and that increasing the embedment depth mobilizes fixity in the soil.

Among all the possible configurations, Blum considered that the best compromise with regard to the fixity of the retaining wall is obtained for embedment such that the tangent to the deflected wall at its toe passes through the anchorage point. Greater embedment depths do not lead to a significant increase in the fixity of the wall, while smaller embedment depths result in a reduction in the fixity moment.

The problem thus posed can be solved graphically, but the process is nevertheless relatively long. To simplify computation, Blum stated that in the case of an embedded retaining wall, the point at which the bending moment is equal to zero is fairly close to the point at which the resultant pressure is zero. He therefore proposed that for computation the bending moment should be considered to be zero at the point of zero pressure (the so-called “approximate loading” of the “equivalent beam”, Fig. 7b). In view of the small difference that is observed between the position of the point where the bending moment is zero and the point of zero resultant pressure, it is assumed that no significant error is introduced into the estimation of the maximum bending moment and the support reaction.

In addition, with the aim of simplifying calculation of the embedment depth, Blum proposed that the distribution of resultant passive pressures acting on the fixed portion of the wall should be modelled by a single force, applied to the wall’s axis of rotation (Fig. 7c). A comparison between the embedment depth obtained with this “idealized loading” method that obtained with the “approximate loading” method shows that the ratio between them depends simply on the mobilization of the resultant of passive pressure acting behind the wall whose ratio to active pressure acting in front of the wall, is denoted by n^* (Fig. 7d). This led Blum to propose the “idealized” load solution increased by a factor of 20% as the design value for embedment depth. (Delattre,L)

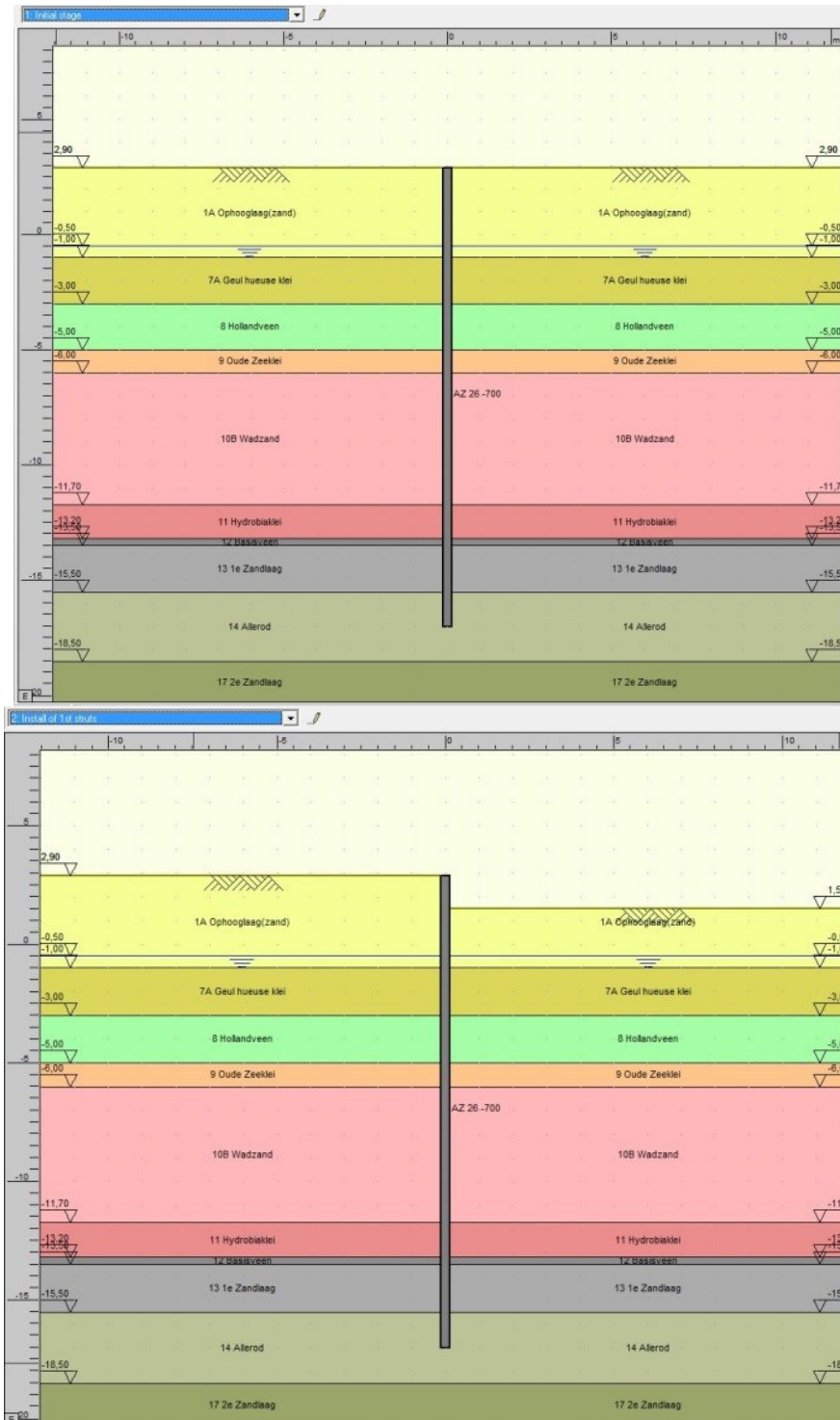


- H: free height of the wall
- T: embedment depth
- t: "net" embedded depth
- y: level of point where the moment is zero
- b: level of point with zero resultant pressure
- a: upper support reaction
- B_0 : shear stress at the point where the moment of zero
- A: upper support reaction
- C: resultant of active pressure acting behind the wall and active pressure acting in front of the wall
- g_{wl} : net passive pressure at foot of screen
- g_{wr} : net resultant of active pressure acting behind the wall and active pressure acting in front of the wall divided by the net embedment depth
- f: net passive pressure passive pressure at toe of wall
- v: net resultant of active pressure acting behind the wall and active pressure acting in front of the wall divided by the net passive pressure

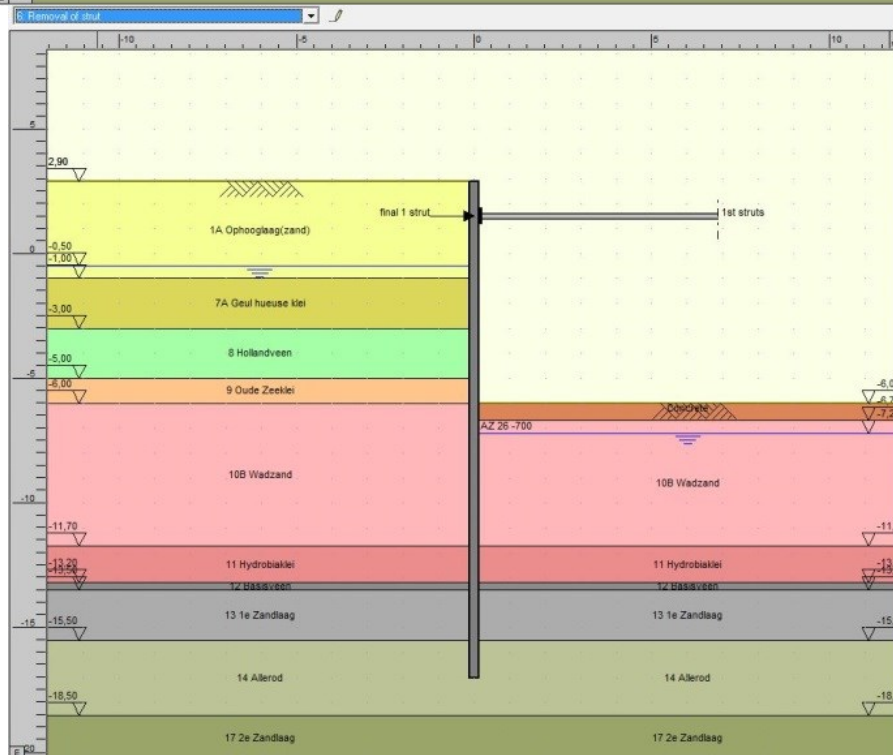
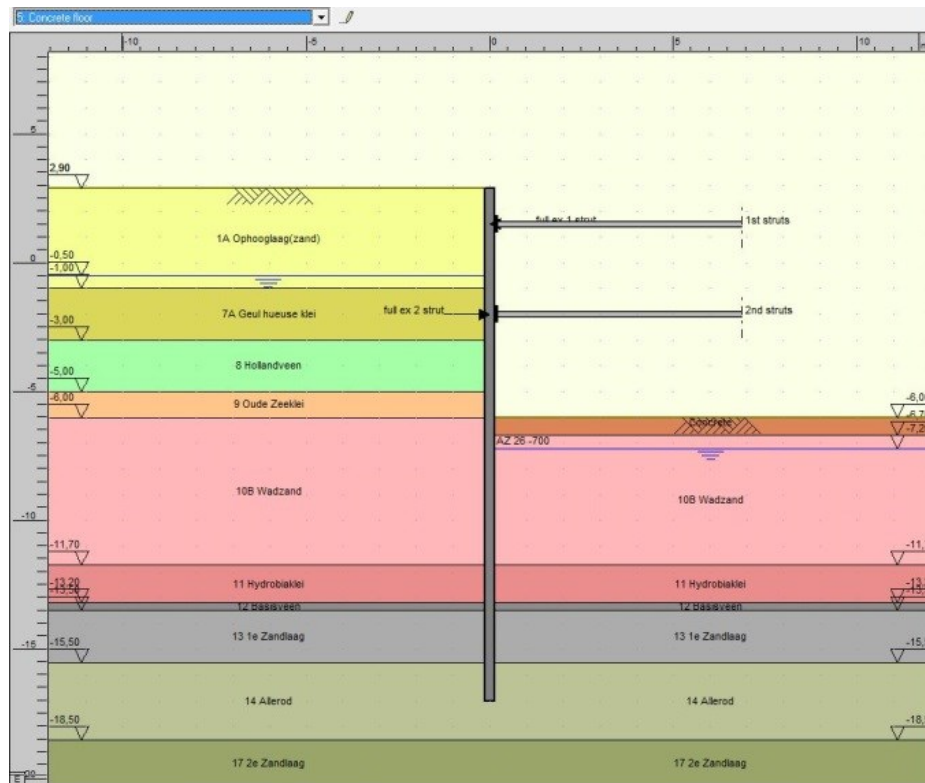
Figure 0-7 Blum's method for the anchored sheet piles design

Appendix C

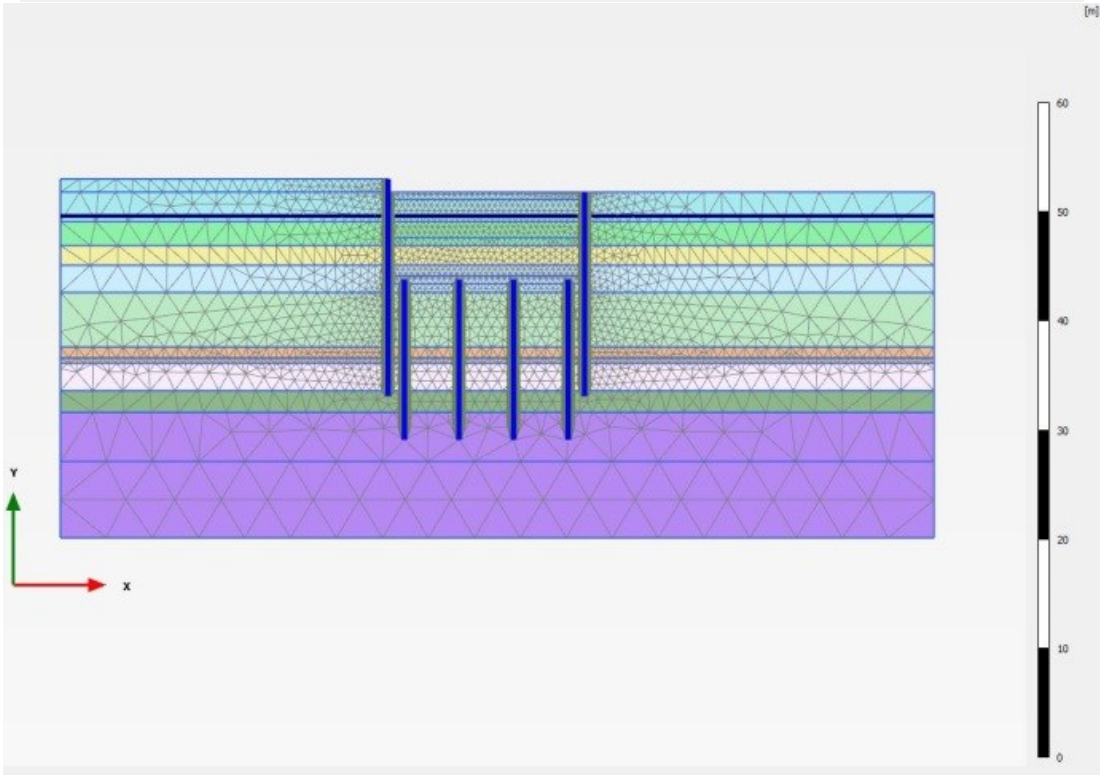
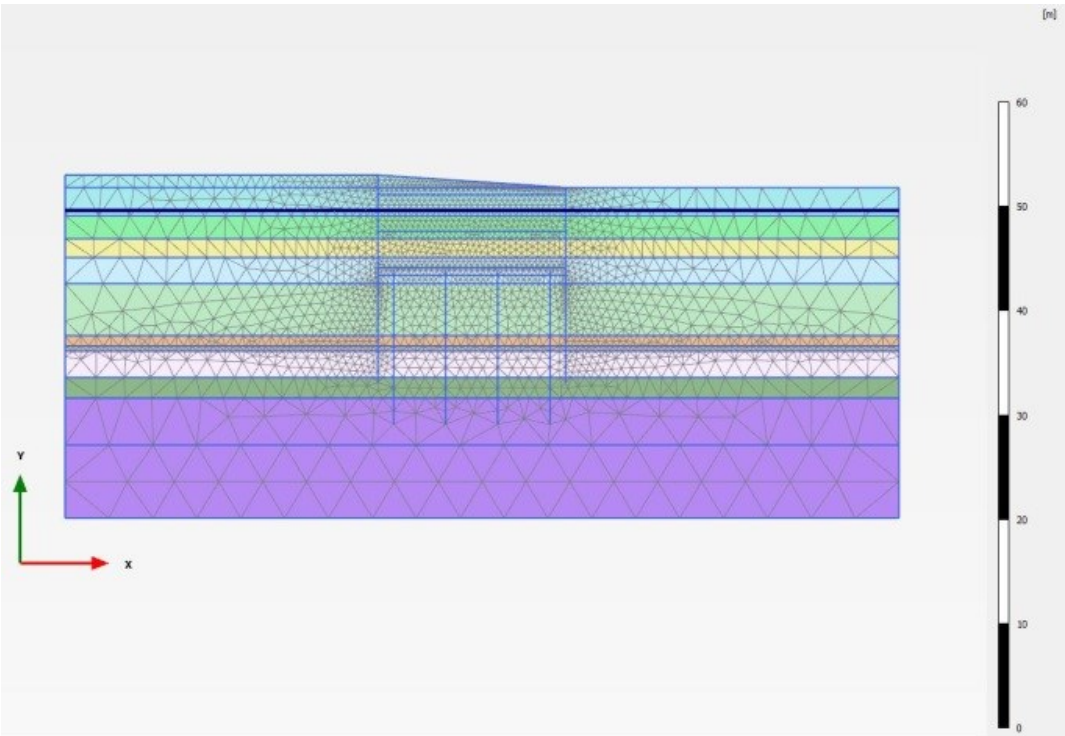
1. Calculation steps for D-Sheet piling

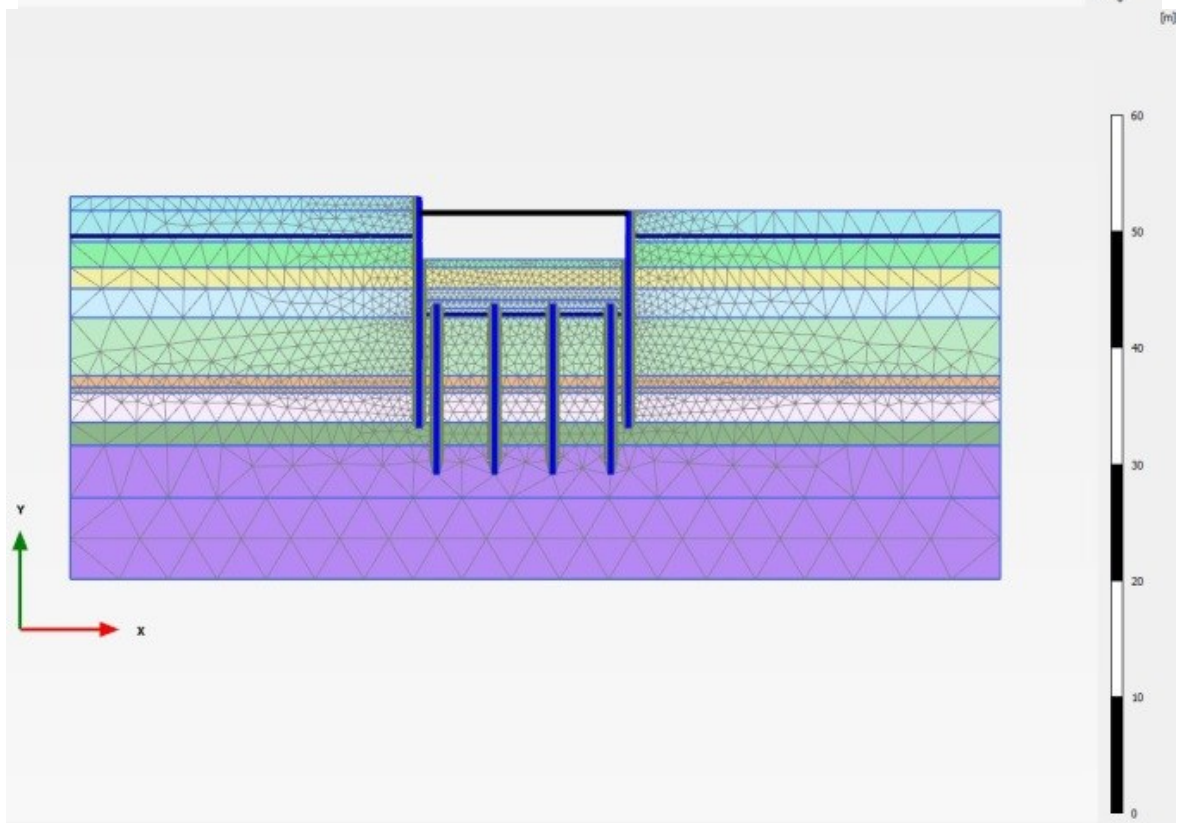
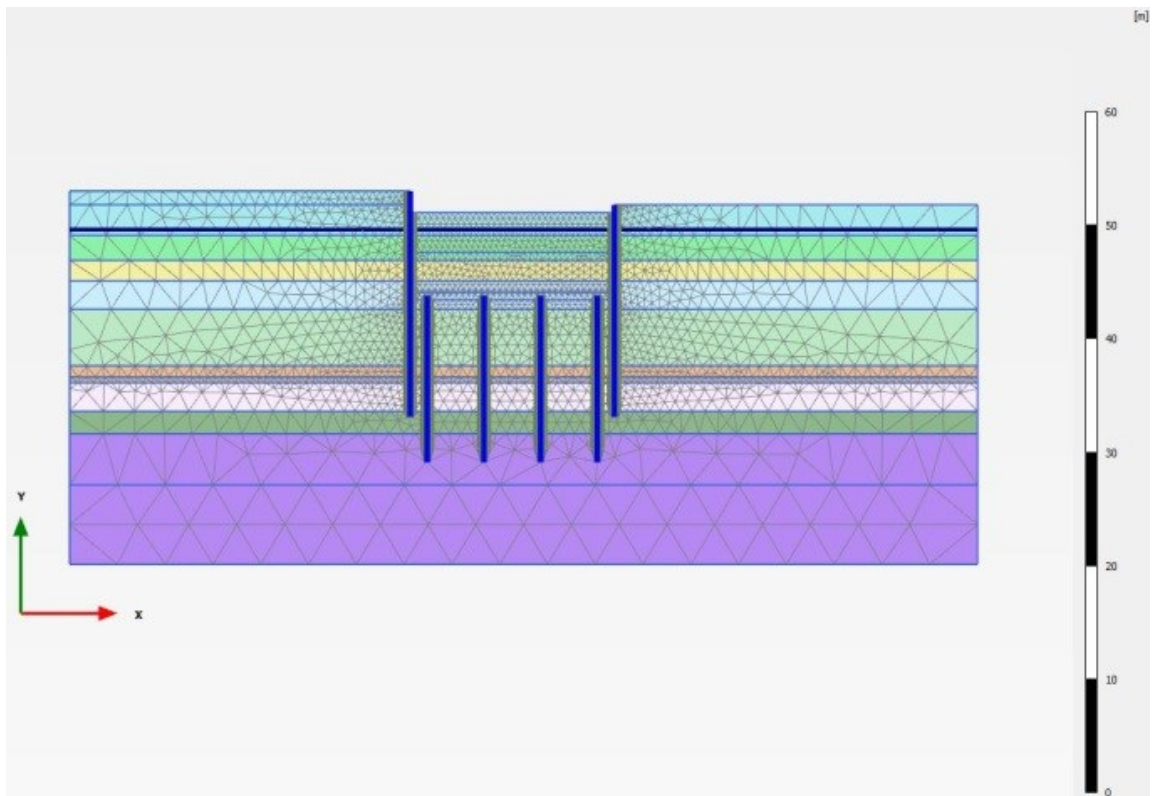


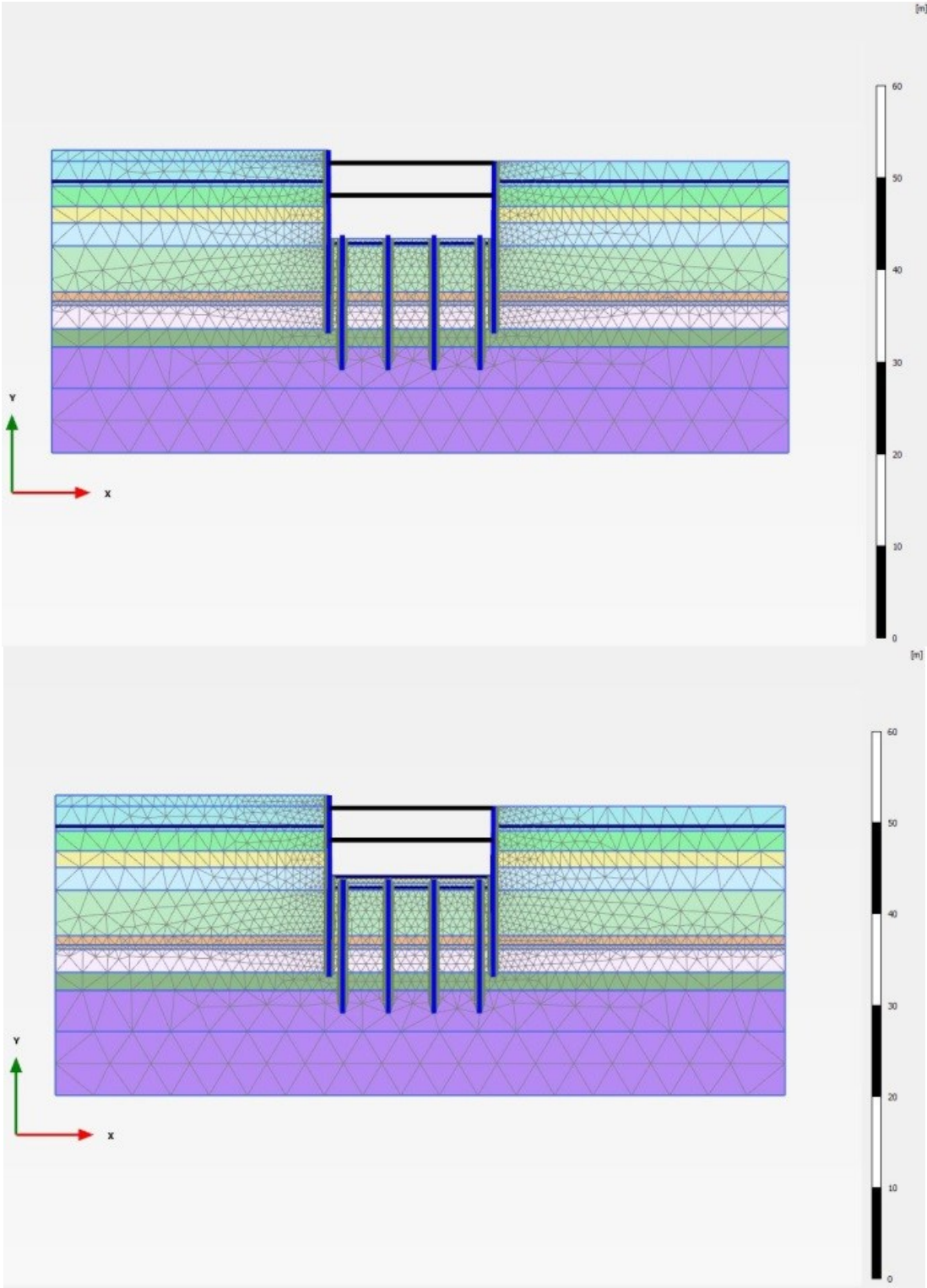


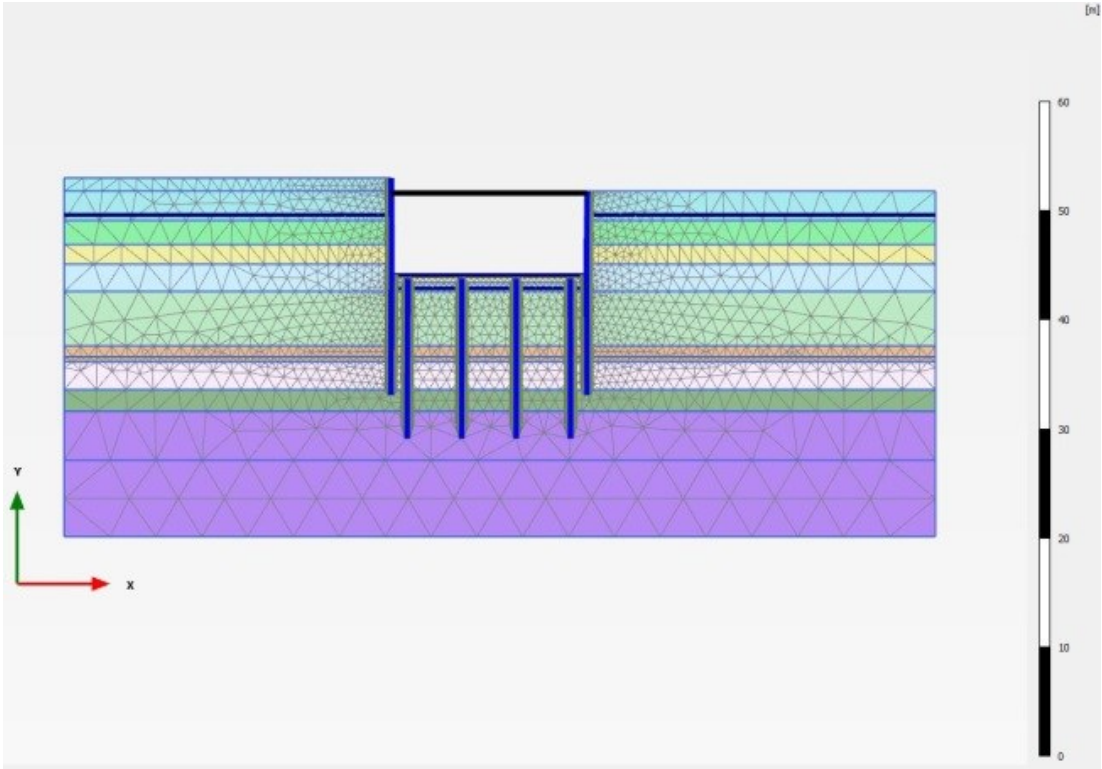


2. Calculation steps for PLAXIS 2D









3. Calculation steps for 3D staged excavation model in PLAXIS 3D

